

Aus der I. Medizinischen Klinik (Institut für Kardiologie, Angiologie,
Pneumologie, Hämostaseologie und internistische Intensivmedizin)
der Medizinischen Fakultät Mannheim
(Direktor: Prof. Dr. med. Daniel Dürschmied)

Roles of Endothelial Dysfunction in the Pathogenesis of Takotsubo Syndrome

Inauguraldissertation
zur Erlangung des Dr. sc. hum
der
Medizinischen Fakultät Mannheim
der Ruprecht-Karls-Universität
zu
Heidelberg

vorgelegt von
Xuehui Fan
aus
Shandong, China
2023

Dekan: Prof. Dr. med. Sergij Goerd

Referent: Prof. Dr. med. Ibrahim Akin

CONTENTS

1	ABBREVIATIONS	1
2	INTRODUCTION.....	6
2.1	Takotsubo Syndrome.....	6
2.2	The pathophysiological mechanism of TTS.....	9
2.3	Endothelial dysfunction in TTS.....	11
2.4	Endothelial-cardiomyocyte interactions in cardiac remodeling and vascular regeneration.....	13
2.5	Roles of exosomes and microRNAs for communication between endothelial cells and cardiomyocytes.....	14
2.6	Ion channel functions in endothelial cells and cardiomyocytes.....	17
2.7	The application of human induced pluripotent stem cell-derived cardiomyocytes in TTS.....	19
3	MATERIALS AND METHODS	22
3.1	Ethics Statement.....	22
3.2	Materials and reagents.....	22
3.3	Methods	32
3.3.1	Study design.....	32
3.3.2	HCMECs culture.....	34
3.3.3	Differentiation and culture of hiPSCs.....	35
3.3.4	Real-time quantitative PCR.....	36
3.3.5	Levels of ET-1 and NO.....	37
3.3.6	Tube formation assay.....	37
3.3.7	Enzyme-linked immunosorbent assay (ELISA) for Ang II.....	37
3.3.8	Apoptosis assay	38
3.3.9	Measurement of ROS.....	38
3.3.10	Measurement of the mitochondrial membrane potential (MMP)	38
3.3.11	ATP detection	39

3.3.12	Detection of intracellular calcium transients.....	39
3.3.13	Isolation and quantification of exosomes.....	40
3.3.14	Confirmation of exosomes by flow cytometry.....	40
3.3.15	Exosome labeling for myocyte uptake assessments.....	41
3.3.16	Immunofluorescence staining.....	41
3.3.17	Dual-Luciferase assay.....	42
3.3.18	Single-cell contraction measurement.....	45
3.3.19	Electrophysiological recording in single cell.....	45
3.3.20	Western blot.....	47
3.3.21	Statistics.....	48
4	RESULTS.....	49
	Part I. Catecholamine could induce endothelial dysfunction via Ang II, SK4 channel and ROS signaling.....	49
4.1	Catecholamine-induced changes of ET-1 and NO release in HCMECs contained roles of Ang II and SK channels.....	49
4.2	SK4 channels contributed to Ang II-effects on endothelial cell functions.....	51
4.3	Ang II could regulate membrane potential and SK4 channel function in HCMECs.....	56
4.4	Ang II reduced SK4 channel current via promoting ROS production.....	58
4.5	Protein kinase A contributed to the effect of Ang II on SK4 channel.....	60
	Part II. Catecholamine could induce cardiac ion channel dysfunction through endothelial cell secreted exosomes	61
4.6	Isolation and characterization of exosomes derived from HCMECs.....	61
4.7	Exosomes secreted by endothelial cells can be taken up by hiPSC-CMs.....	62
4.8	Endothelial cell-derived exosomes changed arrhythmic events induced by epinephrine in hiPSC-CMs.....	63

4.9	Exosomes contributed to action potential changes induced by epinephrine.....	64
4.10	The ionic mechanisms of action potential changes induced by Epi and exosomes.....	66
4.11	miR-126-3p was involved in the effects of endothelial exosomes.....	74
4.12	Exosomes secreted by endothelial cells overexpressing miR-126-3p increased arrhythmia-like events of hiPSC-CMs.....	78
4.13	The endothelial exosome overexpressing miR-126-3p affected ion channel expression in hiPSC-CMs.....	81
4.14	RGS3 is targeted by miR-126-3p in hiPSC-CMs.....	83
5	DISCUSSION.....	86
5.1	Novelty of the study.....	86
5.2	Roles and mechanisms of Ang II/SK4 related endothelial dysfunction in the pathogenesis of TTS.....	87
5.3	Roles and mechanism of endothelial exosomes in the pathogenesis of TTS.....	91
5.4	Study limitations.....	97
5.5	Conclusions.....	97
6	SUMMARY.....	98
7	REFERENCES	101
8	LIST OF FIGURES AND TABLES	116
8.1	List of figures.....	116
8.2	List of tables.....	117
9	CURRICULUM VITAE.....	119
10	ACKNOWLEDGEMENT	122

1 ABBREVIATIONS

TTS: Takotsubo syndrome

LV: Left ventricular

CAD: Coronary artery disease

TTC: Takotsubo cardiomyopathy

AMI: Acute myocardial infarction

NSM: Neurogenic stunned myocardium

NE: Norepinephrine

Epi: Epinephrine

SAH: Subarachnoid hemorrhage

BNP: Brain natriuretic peptide

AF: Atrial fibrillation

LVOTO: Left ventricular outflow tract obstruction

SAM: Systolic anterior motion

STEMI: ST-segment elevation myocardial infarction

NSTEMI: Non-STEMI

β -AR: β -adrenoceptor

ROS: Reactive oxygen species

NO: Nitric oxide

FMD: Flow-mediated dilation

CBF: Coronary blood flow

PAT: Peripheral arterial tonometry

VWF: Von Willebrand factor

PAI-1: Plasminogen activator inhibitor-1

Ang II: Angiotensin II

ET-1: Endothelin-1

ATP: Adenosine triphosphate

ABCG2: ATP-binding cassette transporter subfamily G member 2

NRG-1: Neuregulin-1

BH4: Tetrahydrobiopterin
Trx: Thioredoxin
HUVECs: Human umbilical vein endothelial cells
TEM: Transmission electron microscopy
NTA: Nanoparticle tracking analysis
hiPSC-CCs: Human induced pluripotent stem cell-derived cardiac cells
hiPSC-CMs: Human induced pluripotent stem cell-derived cardiomyocytes
hiPSC-SMCs: Human induced pluripotent stem cell-derived smooth muscle cells
hiPSC-ECs: Human induced pluripotent stem cell-derived endothelial cells
MI: Myocardial infarction
VEGFA: Vascular endothelial growth factor
Mst1: Mammalian sterile 20-like kinase 1
HG: High glucose
HCMEC: Human cardiac microvascular endothelial cell
miRs: MicroRNAs
3'-UTR: 3 'untranslated region
mRNAs: Messenger RNA
SMC: Smooth muscle cell
NSCLC: Non-small-cell lung cancer
CCR1: C-C Motif Chemokine Receptor 1
PLXNB2: Plexin-B2
Pads: Parathyroid adenomas
RV: Right ventricle
EPCs: Endothelial progenitor cells
ICM: Ischemic cardiomyopathy
TRP: Transient receptor potential
KCa: Ca²⁺-activated potassium channels
BK: Big conductance Ca²⁺-activated potassium channel
SK4: Intermediate-conductance Ca²⁺-activated potassium channel
SK1: Small-conductance Ca²⁺-activated potassium channel, type 1

SK2: Small-conductance Ca^{2+} -activated potassium channel, type 2
SK3: Small-conductance Ca^{2+} -activated potassium channel, type 3
EDHF: Endothelium derived hyperpolarization factor
RP: Resting membrane potential
mV: Millivolt
 I_{to} : Transient outward current
 I_{Kr} : Rapidly activating delayed rectifier potassium channel current
 I_{Ca-L} : L-type calcium channel current
 I_{Ks} : Slowly activating delayed rectifier potassium channel current
 I_{K1} : Inward rectifier potassium current
ARVC: Arrhythmogenic right ventricular cardiomyopathy
HCM: Hypertrophic cardiomyopathy
HEK: Human embryonic kidney
CHO: Chinese hamster ovary
LTA: Life-threatening arrhythmias
GFR: Growth Factor Reduced
FBS: Fetal Bovine Serum
4-AP: 4-Aminopyridine
BSA: Bovine Serum Albumin
AT1R: Angiotensin II subtype-1 receptor
Los: Losartan
AT2R: Angiotensin II subtype-2 receptor
PD: PD123 319
PKA: Protein kinase A
EMV2: Endothelial Cell Growth Medium MV2
 H_2O_2 : Hydrogen peroxide
NAC: N-Acetyl-L-cysteine
qPCR: Quantitative polymerase chain reaction
ELISA: Enzyme-linked immunosorbent assay
PI: Propidium iodide

DCFH-DA: 2', 7'-Dichlorofluorescein diacetate

MMP: Mitochondrial membrane potential

RGS3: G-protein signaling 3

MT: Mutant

V_{max}: The maximal depolarization velocity

APD10: The action potential duration at 10% repolarization

APD50: The action potential duration at 50% repolarization

APD90: The action potential duration at 90% repolarization

I_{Na}: Sodium current

I_{SK4}: Intermediate conductance calcium-activated potassium channel current

CRP: C-reactive protein

CCL2: C-C Motif Chemokine Ligand 2

TNF- α : Tumor necrosis factor alpha

$\Delta\psi_m$: Mitochondrial membrane potential level

I-V: Current-voltage relationship

ER: Endoplasmic reticulum

Wt-exo: Exosomes derived from HCMECs without challenge of Epi

Epi-exo: Exosomes isolated from HCMECs treated with Epi

Wt-exo+epi: Wt-Exo plus Epi

Epi-exo+epi: Epi-exo plus Epi

APA: Action potential amplitude

I_{Na-L}: Late Na⁺ current

I_{NCX}: Na⁺/Ca²⁺ exchanger current

Exo-mimic: Exosomes derived from HCMECs transfected with miR-126-3p mimic

Exo-inhibitor: Exosomes derived from HCMECs transfected with miR-126-3p inhibitor

Exo-NC: Exosomes derived from HCMECs transfected with miR-126-3p negative control

eNOS: Endothelial nitric oxide synthase

NOS3: Nitric oxide synthase 3

OFPAE: Ovine fetoplacental artery endothelial cells

NOX: Nicotinamide adenine dinucleotide phosphate oxidase

HAECs: Human aortic endothelial cells

VA: Ventricular arrhythmias

MSC: Mesenchymal stem cells

hECT: Human engineered cardiac tissue

CDCM: Childhood dilated cardiomyopathy

RGS3s: Short RGS3 isoform

GIRK: G protein-gated inwardly rectifying K⁺

2 INTRODUCTION

2.1 Takotsubo Syndrome

Takotsubo syndrome (TTS) is an acute cardiac disorder characterized by an acute, transient and reversible left ventricular (LV) systolic dysfunction with apical ballooning and abnormal ECG (ST-segment elevation or T-wave inversion) without obstructive coronary artery disease (CAD), and is frequently linked to emotional or physical stress [1,2]. It is also called Takotsubo cardiomyopathy (TTC) or broken heart syndrome or stress-induced cardiomyopathy. TTS can be identified in adults of all ages and even in children [3]. TTS was reported for the first time in Japan in 1990, in five patients suffering from chest pain with abnormal ECG, similar to acute myocardial infarction (AMI), but no coronary artery stenosis was detected by angiography [4]. The main differences between TTS and AMI are the absence of significant coronary stenosis contributing to the extent of contraction abnormalities [5,6], and the reverse of the wall motion and ejection fraction abnormality. TTS shows heart ventricular hypercontractility in the basal and mid segments, and wall dyskinesia in apical segment [7].

TTS and neurogenic stunned myocardium (NSM) share some common features, but are different in some clinical and laboratory features [8,9] (**Table 1**). For instance, hypokinesia in apical segment is more common in TTS patients, whereas hypokinesia in basal segment is typical in NSM-patients [10,11]. The process of NSM is predominantly connected with an increased plasma norepinephrine (NE) level, which is caused by neuronal NE but not adrenal epinephrine (Epi) [12].

Table 1. Clinical and experimental features between TTS and NSM

	TTS	NSM
Trigger factors	Emotional, physical, or combined factors	Neurological event, particularly subarachnoid hemorrhage (SAH)
Pathophysiology	Mainly Epi mediated cardiac damage	Mainly NE mediated cardiac damage
Clinical presentation	Chest pain, Heart failure	Heart failure, neurological damage, atrial fibrillation
ECG	ST segment elevation, ST-segment depression, T-wave inversion	Reversed/negative T waves, ST segment depression, QT interval prolongation, large U waves
LV wall motion	Apical hypokinesia, mid-ventricular dysfunction	Mid-ventricular regional wall motion abnormalities, basal hypokinesia
Cardiac markers	High levels of NTproBNP	LcTnI and TnT troponin increase, increased Brain natriuretic peptide (BNP)

Because of the initial unawareness of the disease and reversible feature, the prevalence of TTS was underestimated. Now, TTS has been increasingly recognized worldwide. TTS patients in South-East Asian are reported as 82% being female patients, 89% with an apical variant, with a high incidence of physical triggers and low cardiovascular mortality [13]. In the United States and Europe, TTS patients show a higher prevalence of neurological or psychiatric diseases [14]. Female predominance, mainly aged 56-84 years, was reported [15-17]. However, the clinical characteristics and the course of the disease between men and women are similar, although physical stress is more likely to lead to TTS with much worse outcomes in male patients compared with female patients [18,19]. Due to the increased notice of the disease, male TTS patients have also been increasingly reported with the highest incidence in younger

patients [14,20-22]. About 10% of TTS patients are younger than 50 years [22]. Female patients account for 90% of the cases, with an average age of approximately 65-75 years in most series, and females over 55 years of age have a five-fold increased risk of TTS [23].

TTS can be linked to severe or fatal complications. The possible triggers, such as the emotional stress, inflammatory state, physical stress of cancer surgery, systemic antineoplastic therapy and radiation treatment, may render patients to a higher risk for TTS. A rate of 11% incidence of TTS was described over a 6-year follow-up among 275 patients with cancer [24,25]. In another study, cancer was founded in 16.6% (290 of 1750) TTS patients, similar to that in patients with chronic obstructive pulmonary disease (16.2%) and CAD (15.3%) and much less than that in patients with neurologic and psychiatric disorders (46.8%) [26]. Some cardiovascular risk factors including CAD, hypertension, diabetes and morbid obesity are less prevalent in TTS patients with cancer; but those patients have a higher all-cause mortality [27]. TTS patients with cancer had atrial fibrillation (AF) more frequently than those without cancer. In our hospital, 14% of TTS patients had cancer at the time of the TTS event, and further, 11% of patients were found to have cancer during a 5-year follow-up [28]. TTS patients with arrhythmias had a lower survival rate than patients without them [29]. Left ventricular outflow tract obstruction (LVOTO) may also be a complication in the acute phase and after the recovery phase of TTS because LVOTO can enhance the increase in LV pressure and hence can be linked to hemodynamic instability, mitral regurgitation, systolic anterior motion (SAM) and cardiogenic shock [30,31].

So far, significant progress has been achieved with respect to the diagnosis, clinical characterization and first-line therapy of TTS. However, the prognosis does not seem to be as benign as expected, with a mortality of 5.6% per patient/year from any cause and a rate of in-hospital complications similar to ACS [14]. The rate of 30-day mortality in TTS patients is between ST-segment elevation myocardial infarction (STEMI) and non-STEMI (NSTEMI) patients [32]. Therefore, elucidating the pathophysiology of TTS and further studying its molecular mechanism will improve the clinical treatment of TTS.

Since catecholamine excess is important for the occurrence of TTS, 20–25% of TTS patients have received beta-blocker drugs during their initial event and 40% during a second episode, but so far, no specific drug has been found for treating TTS or preventing the recurrence or improving the outcome of TTS [33]. Due to the lack of ideal therapy for TTS, the application of experimental models or platforms for studying TTS pathogenesis and searching for therapeutic targets is needed.

2.2 The pathophysiological mechanism of TTS

The proposed mechanisms linked to the pathogenesis of TTS include increased concentration of circulating plasma catecholamines and its metabolites, coronary microvascular dysfunction, sympathetic hyperexcitability, inflammation, estrogen deficiency, basal hypercontractility with left ventricular outflow tract obstruction and signal trafficking/biased agonism, spasm of the epicardial coronary vessels, genetic predisposition and thyroidal dysfunction [7,34-38]. TTS probably results from a combination of actions of multiple factors, and as such, the precise mechanisms of TTS are still not fully clarified. Nevertheless, it is widely accepted that catecholamine excess should play a critical role in the occurrence or development of TTS because stress factors can be identified and elevation of plasma catecholamine levels can be detected in most TTS patients. Although the exact mechanisms of TTS remain unclear, some signaling that may be important in TTS pathophysiology have been described [39] (**Figure 1**).

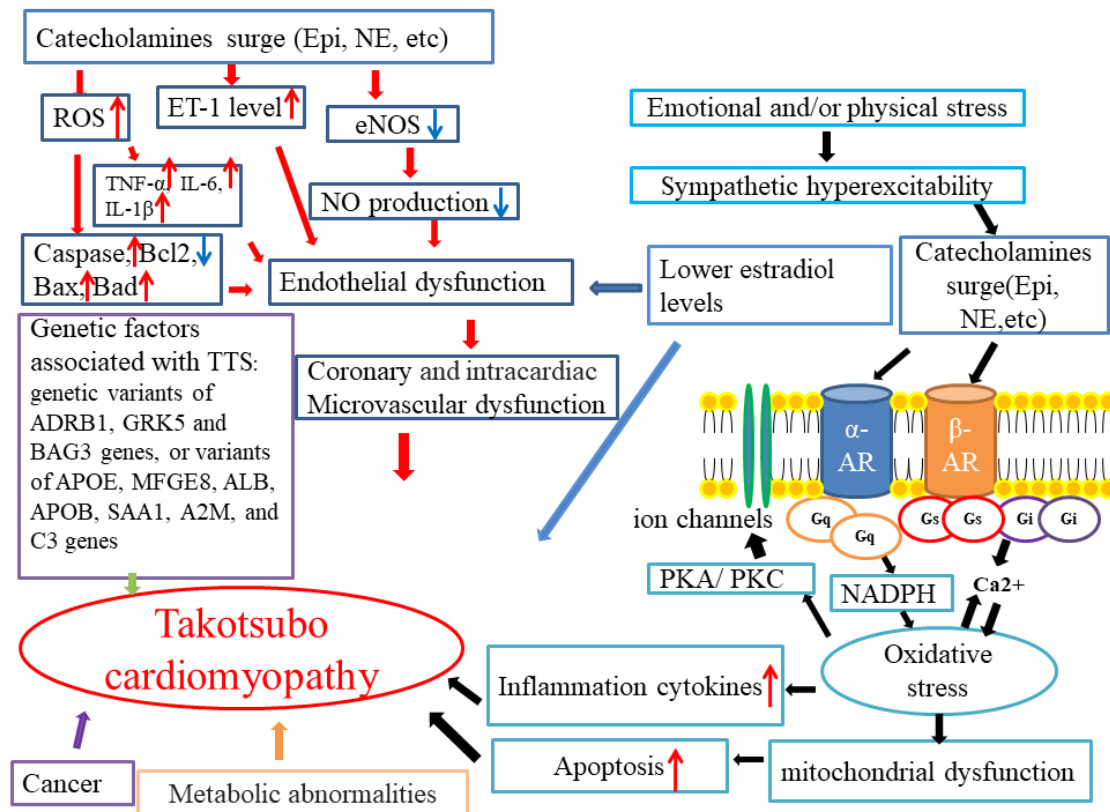


Figure 1. The possible mechanisms related to TTS. AR: adrenergic receptor; NE: norepinephrine; Epi: epinephrine. Emotional and/or physical stress trigger the activation of the sympathetic nervous system and further induce the release of catecholamines which can activate a variety of pathophysiological mechanisms to promote the development of TTS. Catecholamines can affect ion channel function through activating α and β -adrenoceptor signaling and increase oxidative stress. Oxidative stress promotes inflammatory factor release and cardiomyocyte apoptosis, which may contribute to TTS. Catecholamines surge leads to endothelial dysfunction through altering the levels of ET-1 and NO or elevated inflammatory factors and apoptosis-related proteins. Endothelial dysfunction further results in coronary and intracardiac microvascular dysfunction. Furthermore, metabolic abnormalities, cancer, and genetic factors may also be involved in the development of TTS. (Fan, X. et al. Takotsubo syndrome: Translational implications and pathomechanisms. *Int J Mol Sci* 2022, 23.)

Psychological or physical stress may lead to sympathetic hyperexcitability and a huge release of catecholamines, and in turn TTS. It was reported that intravenous

application of catecholamines or beta-agonists led to the clinical features similar to that of TTS [40,41]. Kido et al. reported that 68.2% of drug-induced TTS patients were associated with catecholamine, while 8.9% (14 of 157) of the patients were related to chemotherapy-induced coronary vasospasm [42]. Another study reported that the catecholamine level in TTS patients was significantly higher than that in patients with Killip class III MI [43]. In addition, it was detected that the response of the apical myocardium to sympathetic nerve stimulation was increased, which can render the apex more sensitive to acute elevation of the circulating catecholamine level [44]. When blood pressure was increased by catecholamines, basal akinesia was detected, whereas the apical segment preserved its function [45]. The regional dysfunction may be linked to differential distribution of adrenoceptors. It was demonstrated that the density of sympathetic innervation in the basal cardiomyocytes is higher than that in the apical myocytes. By contrast, the β -adrenoceptor (β -AR) density is higher in apical segment than that in basal segment [46]. Hence, catecholamine can exert stronger effects on the apical myocytes than basal cells.

Since β -adrenoceptors are important for heart function and TTS is related to catecholamine excess, most studies regarding the pathophysiology of TTS focused on β -receptor signaling. It is known that activation of β -receptors can activate Gs or Gi signaling, increase cellular reactive oxygen species (ROS) level (oxidative stress) and in turn can cause different cellular dysfunctions contributing to TTS phenotype. Beside β -receptors, other receptors like α -receptor and dopamine receptors, which can be detected in cardiomyocytes and are coupled to G-protein signaling, may also contribute to the pathogenesis of TTS [47,48]. Estradiol has been shown to have protective effects against toxic effects of catecholamine [36]. Lower estrogen levels may enhance catecholamine effects on cardiomyocytes and endothelial cells.

2.3 Endothelial dysfunction in TTS

Endothelial cells are located in the thin layer inside all blood vessels and play

important physiological roles in angiogenesis, inflammation, coagulation, smooth muscle cell proliferation, and vascular tone [49]. Endothelial cells, one of the most abundant non-myocyte cell types in the heart, have the ability to synthesize and release catecholamines [50]. Endothelial dysfunction is characterized by an imbalance between vasoconstriction and vasodilation factors [51], and may contribute to TTS pathogenesis. Endothelial dysfunction is also an early feature of atherosclerosis. A reduction of bioavailability of vascular and myocardial nitric oxide (NO) was detected in endothelial dysfunction in the presence of ROS [52,53]. Until now, different techniques have been applied for assessing endothelial dysfunction in the setting of TTS, such as flow-mediated dilation (FMD) of the brachial artery, coronary blood flow (CBF), and the peripheral arterial tonometry (PAT) [35,54,55]. Endothelin was suggested to be an important factor relating to endothelial dysfunction because selective endothelin-A receptor antagonism could prevent the dysfunction [56]. The plasma level of endothelin-1 in the acute phase of TTS is similar to the level in AMI patients. Notably, the plasma level of endothelin-1 is elevated transiently and recovered after the resolution of myocardial dysfunction. The biomarkers of endothelial dysfunction, which are von Willebrand factor (vWF) and plasminogen activator inhibitor-1 (PAI-1), were increased during the acute phase of TTS [57]. The surge of catecholamines in TTS may also lead to inflammatory reactions such as leukocytosis, the production of acute phase proteins and oxygen free radicals [58-61]. Wang et al. proposed that healthy coronary endothelial cells make happy cardiomyocytes [62]. At present, the evidence linking TTS to endothelial dysfunction is focused on clinical trials. However, how endothelial dysfunction affects the myocardium remains unclear. Protecting coronary vascular endothelial cells and maintaining healthy coronary circulation may be an effective therapeutic and anti-TTS strategy.

Besides, ROS can cause redox imbalance via different mechanisms, like the activation of proinflammatory signaling and secretion of proinflammatory cytokines, which may injure endothelial cell functions [63]. This implies that elevated ROS generation induced by catecholamine release in the setting of TTS may cause

endothelial dysfunction and in turn cause myocardial dysfunctions via a transient coronary spasm [64]. It was shown that the increased production of ROS decreased vascular NO bioavailability, and caused endothelial and myocardial dysfunction [52,53].

Regarding study on the mechanism of endothelial dysfunction, it was detected that the blood level of miRNA-125a-5p decreased, while the level of its target endothelin-1 increased in TTS, in agreement with the microvascular spasm hypothesis for TTS [65]. In female TTS patients, a reduction of citrulline production and an increase in thrombomodulin concentration were connected with endothelial dysfunction, but no change in the prostacyclin level was detected, suggesting that the endothelial dysfunction in TTS patients can exist even in the long term [66]. Thus, studies on reversing endothelial dysfunction and/or on improving the efficacy of therapeutics such as ACE-inhibitors, AT1-receptor blockers or statins are clinically relevant [64].

Angiotensin II (Ang II) stimulation for a long time can accelerate the endothelial senescence process in aging-related atherosclerosis [67]. Excess Ang II leads to vascular endothelial injury by increasing the synthesis and production of vasoconstrictor such as endothelin-1 (ET-1) and thromboxane A2 and decreasing the release of vasodilators such as NO [68,69]. Additionally, Ang II can induce hypertension, vascular endothelial dysfunction, activation of inflammatory molecules, oxidative damage [70,71]. Notably, Ang II could also stimulate ROS generation [72,73], suggesting that Ang II may contribute to catecholamine effects and pathogenesis of TTS.

2.4 Endothelial-cardiomyocyte interactions in cardiac remodeling and vascular regeneration

Cardiomyocytes and endothelial cells, the two most abundant cardiac cell types, also play a central role in myocardial development, diabetes and metabolic dysfunction, ischemia, cardiac remodeling and vascular regeneration [74,75]. The mechanisms

regulating crosstalk between cardiomyocytes and endothelial cells have not been fully elucidated. Endothelial cells and cardiomyocytes are in close proximity and communicate with each other in multiple ways, such as paracrine signaling, secreted molecules or vesicles, or direct cell-to-cell contact [75]. Deletion of the gene encoding VEGF in cardiomyocytes resulted in a decrease in basal systolic function, thinning of the ventricular wall, and decreased the number of coronary microvessels [76]. Cardiac endothelial cells have the normal functions of vascular endothelial cells, and also release various autocrine and paracrine factors, such as Ang II, NO, endothelin, prostaglandin I₂, which directly affect the contractile performance, growth, metabolism, and rhythmicity of the adult heart [77]. In addition, endothelial cells release various factors controlling cardiomyocyte contractility in the normal adult heart, such as ET-1, adenosine triphosphate (ATP)-binding cassette transporter subfamily G member 2 (ABCG2), neuregulin-1 (NRG-1), tetrahydrobiopterin (BH₄), thioredoxin (Trx) [78-82]. Accordingly, cardiomyocytes produce exosomes, proteins, or small molecules, which have been shown to regulate the function of endothelial cells. Exosomes secreted by glucose-starved cardiomyocytes significantly increase proliferation and tube formation in human umbilical vein endothelial cells (HUVECs) and stimulate glucose uptake and glycolysis in cardiac microvascular endothelial cells in vitro [83], suggesting that exosomes play an important role in cell-cell signaling both locally and remotely.

2.5 Roles of exosomes and microRNAs for communication between endothelial cells and cardiomyocytes

Almost all cell types can secrete exosomes, which range in size from 20 to 150 nm [84,85]. Currently, three main approaches have been used to verify exosomes in researches. First, transmission electron microscopy (TEM) was used to analyze the size and morphology of exosomes, which were displayed as double membrane "cup" vesicles [86-88]. Second, exosome markers were used to identify exosomes with western blotting [86-89]. Third, nanoparticle tracking analysis (NTA) was performed

to measure the size and concentration of exosomes [87,88,90]. Currently, exosomes have been proved to mediate communication between endothelial cells and smooth muscle cells, cardiomyocytes and endothelial cells, and fibroblasts and cardiomyocytes [88,91-93]. Exosomes can mediate cell-to-cell communication in maintaining homeostasis through three mechanisms: (1) receptor-ligand interactions, (2) internalization by cells, (3) direct fusion to the cell membrane [94-96].

At present, many studies have focused on the intercellular signaling and information exchange mediated by exosomes between endothelial cells and cardiomyocytes. Zhang et al. reported that exosomes secreted by hiPSC-derived cardiac cells (hiPSC-CCs) including cardiomyocytes (hiPSC-CMs), smooth muscle cells (hiPSC-SMCs) and endothelial cells (hiPSC-ECs) enhanced the ability of angiogenesis, prevented hypoxic injury, and improved cardiac function in a porcine myocardial infarction (MI) model [97]. Exosomes derived from H9C2 cardiomyocytes were increased by glucose deprivation [98]. miR-29a-enriched exosomes secreted by Ang II-treated cardiomyocytes inhibited the proliferation, migration, and angiogenesis of cardiac microvascular endothelial cells by inhibiting vascular endothelial growth factor (VEGFA) expression [99]. Mammalian sterile 20-like kinase 1 (Mst1)-enriched exosomes derived from endothelial cells inhibited autophagy and glucose uptake, but enhanced apoptosis in high glucose (HG) cultured cardiomyocytes [100]. The co-culture of miR-199b-5p-enriched exosomes derived from hiPSC-ECs and HUVECs significantly improved the migration, proliferation and tube formation of HUVECs via inhibition of Jagged1/Notch1 signaling [101]. Exosomes secreted by lipopolysaccharide-challenged endothelial cells could alleviate rat cardiomyocyte injury and apoptosis [102]. Whether exosomes secreted by human cardiac microvascular endothelial cells (HCMECs) can regulate the ion channel and electrophysiological properties of cardiomyocytes has not been elucidated.

microRNAs (miRs) are small noncoding RNAs, consisting of 22 to 25 nucleotides, that regulate gene expression after transcription by binding to the 3' untranslated region

(3'-UTR) of target messenger RNA (mRNAs). miRNAs inhibit and degrade mRNA or stimulate mRNA translation or directly regulate more than 60% of protein-coding genes [103,104]. miRNA activation can regulate smooth muscle cell (SMC)-endothelial cell crosstalk, endothelial cell-cardiomyocyte crosstalk, etc. [92,93,105,106]. Importantly, miRNAs can alter cardiac excitability, conduction, repolarization, and automaticity by targeting ion channel genes and even affect arrhythmia. Cardiac miR-133a, miR-1, miR-26, and miR-328 regulate ion channel genes involved in cardiac conduction, rhythmicity, and automaticity [107-113]. Recently, Fu et al. found that miRNAs modulate cardiac action potential by direct binding to ion channels [114], which may provide new insights into the pathogenesis of arrhythmias. Schreier et al. reported that miR-221 and miR-222 downregulate L-type Ca^{2+} channel current density and KCNJ5 channel expression by targeting the 3'-UTR of CACNA1C or KCNJ5 gene [115]. These suggest that miRNAs from non-cardiac cells such as endothelial cells can participate in the electrical remodeling of cardiomyocytes by regulating the expression of ion channel genes, which is an important mechanism of arrhythmia.

miR-126-3p, which is highly enriched in endothelial cells and located on human chromosome 9, plays a very critical role in vascular development by maintaining vascular integrity and promoting angiogenesis [116,117]. miR-126 has been studied in many human cancers. The upregulation of miR-126-3p can inhibit the growth, colony formation, invasion and migration of non-small-cell lung cancer (NSCLC) cells by targeting C-C Motif Chemokine Receptor 1 (CCR1), and can inhibit ovarian cancer proliferation and invasion via targeting plexin-B2 (PLXNB2) [118-120]. The downregulation of miR-126-3p promotes neovascularization of parathyroid adenomas (Pads), possibly through VEGFA overexpression [121]. These researches suggest that miR-126-3p may be used as a molecular target for tumor therapy. In addition, miR-126-3p plays an important role in maintaining cardiovascular function. Potus et al. confirmed that miR-126 overexpression can promote the regeneration ability of vascular endothelial cells in the right ventricle (RV) and improve RV function in patients with right heart failure [122]. miR-126-3p was significantly downregulated in

AMI patients, while miR-126-3p overexpression increased migration and tube-like structures of endothelial progenitor cells (EPCs) to improve the heart function of ischemic cardiomyopathy (ICM) patients [123,124].

Taking together, miRNAs, which are from either endothelial cells or cardiomyocytes, may participate in the regulation of endothelial or cardiac function. However, little is known about whether exosomal miR-126-3p in endothelial cells can modulate the ion channel function and electrophysiological properties of cardiomyocytes.

2.6 Ion channel functions in endothelial cells and cardiomyocytes

Numerous ion channels have been detected in endothelial cells and some of them were shown to be important for endothelium functions [125-127]. Ca^{2+} -activated potassium channels, ATP-sensitive potassium channel, inward rectifier potassium channels, P/Q-type and T-type calcium channels may be involved in determining endothelial cell membrane potential or modulating smooth muscle contraction and coronary blood flow [128-132]. Opening of potassium channels in endothelial cells can hyperpolarize the cell membrane potential and thus can increase the driving force for calcium influx conducted by transient receptor potential (TRP) channels in endothelial cells, and then causes vasodilation via intracellular calcium activating signaling. In addition, the hyperpolarization in endothelial cells can hyperpolarize smooth muscle cells via myo-endothelial gap-junctions, leading to vasodilation [126,133,134]. Furthermore, opening of calcium-conducting channels can increase intracellular calcium concentration, which can stimulate release of vasodilating factors, leading to vasodilation.

In endothelial cells, the most frequently studied ion channels are the Ca^{2+} -activated potassium (KCa) channels, which consist of three groups: big conductance (>200 pS) Ca^{2+} -activated potassium channel (KCa1.1, BK), intermediate-conductance (20-40 pS) Ca^{2+} -activated potassium channel (KCa3.1, SK4) and small-conductance (5-10 pS)

Ca²⁺-activated potassium channel, which include three subtypes, type 1 (KCa2.1, SK1), type 2 (KCa2.2, SK2) and type 3 (KCa2.3, SK3) [126]. In freshly isolated endothelial cells, BK channels are poorly expressed [135]. In contrast to BK channels, the SK channels are constitutively expressed in endothelial cells [136]. The endothelial SK channels have been suggested to play an important role in endothelium derived hyperpolarization factor (EDHF)-induced cell hyperpolarization. Although endothelial dysfunction is usually associated with decreased NO production, alteration of the EDHF-pathway may also participate in endothelial dysfunction or conversely can compensate the loss of NO bioavailability [137]. Alterations in EDHF-mediated responses were reported in diseases like hypertension, atherosclerosis, hypercholesterolemia, heart failure, diabetes, sepsis [136].

Given that ion channels in endothelial cells may modulate endothelial functions, abnormal modulation of ion channels may lead to dysfunctions in endothelial cells. However, whether ion channel dysfunctions in endothelial cells participate in endothelial dysfunction in TTS is unclear.

TTS is characterized by acute and transient left ventricular systolic dysfunction, which may be linked to cardiac ion channel dysfunctions because cardiac contraction is initiated by the cell excitation. When cardiomyocytes are excited, bioelectrical signals (action potentials) initiate contractions of the heart via excitation-contraction coupling [138]. Action potentials are determined by the opening/activation and closing/inhibition of transmembrane proteins forming ion channels/transporters [139,140]. The cardiac action potential is a transmembrane potential variation with an amplitude between 60 and 120 millivolts (mV) [141]. The resting membrane potential (RP), which can be roughly estimated from the Nernst equation, is around -80 mV mainly because of the uneven distribution of potassium ions across the cell membrane. The action potential of the heart has five distinct stages (**Figure 2**). Phase 0 is the rapid depolarization caused by a sudden increase in sodium influx, which is mainly due to

the activation of Na^+ channels, especially Nav1.5 channels [142]. A negative value is returned after an overshoot (above 0 mV), which is called repolarization that includes phases 1, 2, and 3. Phase 1 is characterized by a decrease in sodium inflow and a transient increase in potassium outflow and chloride inflow. During this phase, the transient outward current (I_{to}) channel opens shortly. During the second phase, the membrane potential remains almost constant or slowly decreases, caused by potassium outflow and simultaneous calcium (and some sodium) inflow, mainly through the rapidly activating delayed rectifier K^+ current (I_{Kr}) and L-type calcium channel current (I_{Ca-L}) [142]. In the third phase, the increase of potassium efflux and the decrease of calcium and sodium influx lead to the rapid repolarization. In phase 3, the outward K^+ channel currents include I_{Kr} and I_{Ks} (the slowly activating delayed rectifier K^+ current) [142]. Phase 4 represents the resting membrane potential. Inward rectifier potassium current (I_{K1}) is activated late in phase 3 and remains conducting throughout phase 4, and plays key roles in maintaining the RP. Any changes of the function of channels participating in the action potential generation may lead to abnormal action potentials and in turn abnormal contraction or arrhythmias.

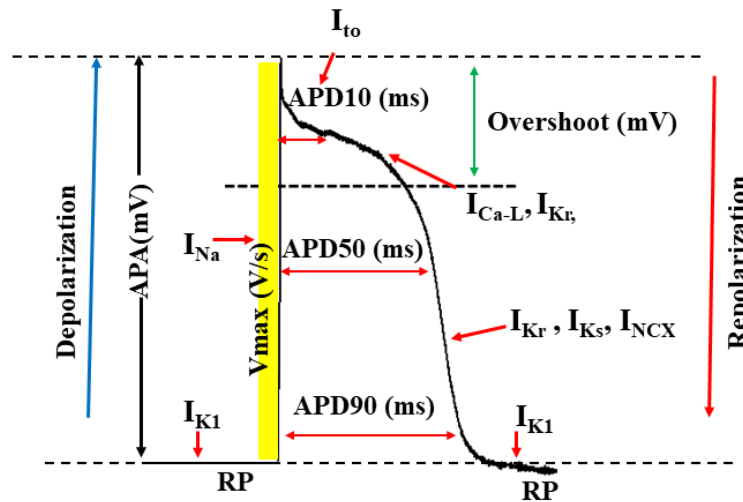


Figure 2. Analysis of action potential parameters in hiPSC-CMs.

2.7 The application of human induced pluripotent stem cell-derived cardiomyocytes in TTS

Understanding the critical role of endothelial dysfunction in the pathophysiology of TTS may facilitate early diagnosis and intervention. Experimental *in vivo* or *in vitro* studies are useful to explore the underlying pathophysiology of TTS and to search for effective therapy for the disease. Recently, experimental studies on TTS mainly used animal models, hiPSC-CMs models, other cell models and computational models, each of which possess advantages and disadvantages. The hiPSC-CMs have advantages in modeling genetic cardiac disorders like long-QT syndrome, short QT syndrome, arrhythmogenic right ventricular cardiomyopathy (ARVC), Brugada syndrome and familial hypertrophic cardiomyopathy (HCM) [39,143-152]. First, hiPSC-CMs have a human gene background, which can avoid a potential influence of the gene differences between humans and animals. Second, hiPSC-CMs may be a better platform for cardiac drug screening and ion channel research compared with *Xenopus* oocytes, human embryonic kidney (HEK) cells and Chinese hamster ovary (CHO) cells, which do not possess cardiac ion channel macromolecular complexes. Third, patient-specific mechanistic study and drug testing can be carried out. Additionally, genome editing combined with patient-specific iPSC-CMs can help to explore the genotype-phenotype correlation of unknown gene mutations or variants in patients.

Up to date, limited studies on TTS using hiPSC-CMs have been reported [47,153]. It is still unclear whether TTS is a genetic disease, but growing evidence suggests the involvement of genetic factors in TTS. For instance, variant in *RBM20*, encoding RNA-binding motif protein 20, or *CASQ2*, encoding calsequestrin 2, could be found to exist in TTS patients [154]. In addition, long QT syndrome has been reported in up to 70% of TTS patients and has connection with life-threatening arrhythmias (LTA) triggered by concomitant AF. El-Battrawy et al. used hiPSC-CMs to assess the toxic effects of catecholamine on cardiac ion channel function and the protective effects of estrogen, and found out that estrogen reduced the sensitivity of hiPSC-CMs to isoprenaline by reducing adrenoceptor expression [36]. That study supports a possible application of ROS-blockers, β -blockers and late sodium channel blockers for treating or preventing arrhythmias in TTS.

A second TTS model using hiPSC-CMs was established by the application of high doses of epinephrine (Epi), and G1/estrogen attenuated Epi-induced cardiac injury via decreasing the levels of brain natriuretic peptide in blood and the lactate dehydrogenase in the culture supernatant [153]. Huang et al. applied a high concentration of Epi to mimic the setting of TTS, and detected that Epi prolonged APD and induced arrhythmia events [47]. The Epi-effects was alleviated by an alpha-receptor blocker phentolamine [47]. An activator of alpha-1 receptor, but not alpha-2 receptor, mimicked the effects of Epi, implying that the alpha-1 adrenergic receptor signaling was involved in the arrhythmogenesis of TTS. Furthermore, NADPH-ROS-PKC signaling was proved to be important for the effects of the alpha-1 receptor activation [47,155], which provided novel information for searching for new therapy of TTS. Notably, Borchert et al. used, for the first time, hiPSC-CMs from two TTS patients in their study, and found that the response of β -adrenergic signaling to catecholamine challenge was enhanced in hiPSC-CMs from TTS patients, comparing with hiPSC-CMs from healthy donors [154]. The cardiac stress marker NR4A1 expression in TTS-hiPSC-CMs was also increased by catecholamine-challenge [154]. These data suggested the possible involvement of genetic factors in the pathogenesis of TTS and further support the use of hiPSC-CMs for studying TTS. However, pathogenic gene mutations for TTS have not been identified until now. Further efforts should be exerted to clarify whether and how genetic factors participate in the pathogenesis of TTS. From all the data reported so far, catecholamine-treated hiPSC-CMs or hiPSC-CMs from TTS patients mimicked TTS features, implying that hiPSC-CMs may provide a plausible platform for investigation of the pathogenic mechanism, drug effects, ion channel and gene function in TTS.

In summary, there is increasing evidence that endothelial dysfunction is associated with TTS, but the evidence is currently based on clinical trials. The exact pathophysiology of endothelial dysfunction in TTS remains unclear. Here, we hypothesize that secretions of endothelial cells challenged by catecholamine may be altered and contribute to endothelial cell or cardiomyocyte dysfunction, and hence

participate in TTS pathogenesis.

The aims of this study are to examine the contribution of Ang II signaling to epinephrine-induced endothelial dysfunction, the effects of exosomes from dysfunctional endothelial cells on cardiac ion channel functions, and to explore possible mechanisms underlying the endothelial Ang II and exosome effects. This study may provide experimental and theoretical bases for elucidating the pathophysiological mechanism of TTS and may reveal potentially new targets for the treatment of TTS.

3 MATERIALS AND METHODS

3.1 Ethics Statement

The skin biopsies from three healthy donors were obtained with written informed consent. The study was approved by the Ethics Committee of the Medical Faculty Mannheim, University of Heidelberg (approval number: 2018-565N-MA) and by the Ethics Committee of the University Medical Center Göttingen (approval number: 10/9/15). The study was performed in accordance with the approved guidelines and conducted in accordance with the Helsinki Declaration of 1975 (<https://www.wma.net/what-we-do/medical-ethics/declaration-of-helsinki/>), revised in 2013.

3.2 Materials and reagents

Table 2. Cell culture reagents in this study

Name	Cat No.	Company
Human Cardiac Microvascular Endothelial Cells (HCMEC)	C-12285	Promocell
TeSR™-E8™	05990	StemCell Technologies
RPMI 1640 Medium, GlutaMAX™ Supplement	61870044	Thermo Fisher Scientific

B-27™ Supplement (50×), serum free	17504001	Thermo Fisher Scientific
Matrigel Growth Factor Reduced (GFR)	354230	Corning
Basement Membrane Matrix, LDEV-free		
Penicillin-Streptomycin	15140-122	Thermo Fisher Scientific
Sodium Pyruvate (100 mM)	11360-039	Thermo Fisher Scientific
RPMI 1640 Medium, no glucose, no glutamine	01-101-1A	Biological Industries
L-Ascorbic acid 2-phosphate	A8960	Sigma-Aldrich
Sesquimagnesium salt hydrate		
StemMACS CHIR99021	130-103-926	StemMACS
StemMACS™ Y27632	130-103-922	Miltenyi
IWP-2	72122	StemCell Technologies
DPBS, no calcium, no magnesium	14190250	Thermo Fisher Scientific
Trypsin-EDTA 0.05%	25300054	Gibco
HEPES 1M Solution	15630080	Thermo Fisher Scientific
Sodium DL-lactate solution	BCBQ6934V	Sigma-Aldrich
Collagenase, Type 1	LS004194	Worthington
0.5 M EDTA Solution (Ph 8.0)	A4892.0500	AppliChem
2-Mercaptoethanol (50 mM)	31350010	Gibco
Endothelial Cell Growth Medium MV2	C-22022	PromoCell
Fetal Bovine Serum (FBS)	10500-056	Gibco
Dimethyl Sulfoxide	D2650	Sigma-Aldrich
DMEM (1×) + GlutaMAX™-1	2340225	Gibco
HEK293T cells	CRL-3216	ATCC
L-glutamine (2 mM)	25030123	Thermo Fisher Scientific
Opti-MEM™ I Reduced Serum Medium	31985-062	Thermo Fisher Scientific

Table 3. Drugs and chemicals used in this study

Name	Cat No.	Company
Angiotensin II	A9525	Sigma-Aldrich
Losartan	61188	Sigma-Aldrich
PD 123 319	P186	Sigma-Aldrich
NS309	N8161	Sigma-Aldrich
Hydrogen peroxide	1072100250	Sigma-Aldrich
N-Acetyl-L-cysteine	A7250	Sigma-Aldrich
Sp-8-Br-cAMPS	127634-20-2	BIOLOG Life Science Institute
Tetrodotoxin	6973.1	Carl Roth
Nifedipine	N7634	Sigma-Aldrich
Chromanol 293B	C2615	Sigma- Aldrich
Nickel chloride	339350	Sigma-Aldrich
4-Aminopyridine (4-AP)	275875	Sigma-Aldrich
E-4031	M5060	Sigma-Aldrich
Niflumic acid	N0630	Sigma-Aldrich
Lidocaine	L7757	Sigma-Aldrich
Dihydroouabain	D0670	Sigma-Aldrich
(±)-Epinephrine hydrochloride	E4642	Sigma-Aldrich
Tram-34	T6700	Sigma-Aldrich

Table 4. Kits and chemicals

Name	Cat No	Company
Angiogenesis Assay Kit	PK-CA577-K905	Promocell
Endothelin-1 enzyme-linked immunosorbent assay	ELH-EDN1-1	RayBiotech
ELISA Kit for Angiotensin II	USC-CEA005HU-96	Cloud clone

JC-10 Mitochondrial Membrane Potential Assay Kit	ab1121	Abcam
ATP Assay Kit	ab83355	Abcam
2',7'-dichlorofluorescein diacetate	D6883	Sigma-Aldrich
Nitric Oxide Assay Kit	EMSNO	Thermo Fisher scientific
HotRox Master Mix	119405	BIORON
High-Capacity cDNA Reverse Transcription Kit	4368814	Thermo Fisher scientific
Dual-Luciferase Reporter Assay System	E1910	Promega
psiCheck2-let-7-WT	78260	Addgene
TaqMan™ Fast Advanced Master Mix	4444557	Thermo Fisher scientific
High-Capacity cDNA Reverse Transcription Kit	4368814	Thermo Fisher scientific
Dual-Luciferase Reporter Assay System	E1910	Promega
TaqMan™ Fast Advanced Master Mix	4444557	Thermo Fisher scientific
psiCheck2-let-7-WT	78260	Addgene
Hsa-miR-126-3p	Assay ID.002228	Thermo Fisher scientific
Hsa-RNU6B	Assay ID.001093	Thermo Fisher scientific
Hsa-miR-16	Assay ID.000391	Thermo Fisher scientific
Hsa-miR-26a	Assay ID.000405	Thermo Fisher scientific
Hsa-miR-133a	Assay ID.002246	Thermo Fisher scientific
Hsa-miR-126-3p mimic	4464066	Thermo Fisher scientific
Hsa-miR-126-3p inhibitor	4464084	Thermo Fisher scientific

Lipofectamine™ RNAiMAX Transfection Reagent	13778075	Thermo Fisher scientific
Lipofectamine™ 2000 Transfection Reagent	11668030	Thermo Fisher scientific
FITC Annexin V Apoptosis Detection Kit I	556547	BD Biosciences
PKH26 Red Fluorescent Cell Linker Kit for General Cell Membrane Labeling	PKH26GL-1KT	Sigma-Aldrich
Protease Inhibitor Cocktail	P8340	Sigma-Aldrich
BCA Protein Assay Kit	23227	Thermo Fisher Scientific
Tris	5429.1	Carl Roth
Glycine	3570	Merck Millipore
Sodium dodecyl sulfate, SDS pellets	20765	Serva
Ammonium Persulfate	1610700	Bio-Rad
30 % Acrylamide	3029.1	Carl Roth
TEMED	1610800	Bio-Rad
RIPA buffer	R0278	Sigma-Aldrich
PVDF Transfer Membrane	GE1060009	Merck Millipore
Milchpulver	T145.3	Carl Roth
Bovine Serum Albumin (BSA)	10270106	Thermo Fisher Scientific
ECL Western Blotting Substrate	32209	Thermo Fisher Scientific
Paraformaldehyde 4%	P087.4	Carl Roth
Triton X-100	3051.3	Carl Roth
Fluo-3 AM	F1242	Thermo Fisher Scientific
Calcium chloride	C3881	Sigma-Aldrich

Magnesium chloride hexahydrate	MD250	Sigma-Aldrich
Potassium chloride	P3911	Sigma-Aldrich
Glucose	G7528	Sigma-Aldrich
Sodium Chloride	S9625	Sigma-Aldrich
Cesium chloride	289329	Sigma-Aldrich
EGTA	E4378	Sigma-Aldrich
Sodium hydroxide	S-5881	Sigma-Aldrich
HEPEs	H-3375	Sigma-Aldrich
Hydrochloric acid	H1758	Sigma-Aldrich
Barium chloride	449644	Sigma-Aldrich
Cesium hydroxide solution	232068	Sigma-Aldrich
TEA-Cl	T2265	Sigma-Aldrich
Tryptone	T9410	Sigma-Aldrich
Yeast Extract	Y1625	Sigma-Aldrich
Agarose	A5030	Sigma-Aldrich
Ampicillin, sodium salt	11593027	Thermo Fisher Scientific
GenElute HP Plasmid mimiprep kit	NA0160-1KT	Sigma-Aldrich
Herculase II Fusion DNA Polymerases	699675	Agilent
Not I-HF	R3189S	NEB
Xho I	R0146S	NEB
T4 DNA Ligase	M0202S	NEB

Table 5. Primary antibodies for experiments

Name	Cat No.	Company
Recombinant Anti-PKA alpha/beta/gamma (catalytic subunit) (phospho T197) antibody [EP2606Y]	ab75991	Abcam
Anti-KCNN4 (KCa3.1, SK4) Antibody	APC-064	Allomone
BAD Polyclonal antibody	10435-1-AP	Proteintech
Mouse monoclonal anti-bcl2	sc-7382	Santa Cruz
Anti-Bax Antibody	sc-20067	Cell Signaling technology
Rabbit polyclonal anti- cleaved caspase 3	ab2302	Abcam
Recombinant Anti-Cardiac Troponin T antibody [EPR20266]	ab209813	Abcam
RGS3 Polyclonal Antibody	66790-1-Ig	Proteintech
Glyceraldehyde 3-phosphate dehydrogenase (GAPDH) (14C10) antibody	2118S	Cell Signaling
Anti-GNAS	10150-2-AP	Proteintech
CD9 Polyclonal Antibody	PA5-11559	Thermo Fisher scientific
CD63 Monoclonal Antibody (Ts63)	10628D	Thermo Fisher scientific
CD81 Monoclonal Antibody	MA5-13548	Thermo Fisher scientific
Anti-GRP94 antibody	ab13509	Abcam
GM130 antibody	sc-55591	Santa Cruz

Table 6. Secondary antibodies used in this study

Name	Cat No.	Company
Goat anti-Rabbit IgG (H+L) Cross-Adsorbed Secondary Antibody, Alexa Fluor 488	A-11008	Thermo Fisher scientific
Anti-Rabbit IgG (whole molecule)-Peroxidase antibody produced in goat	A0545	Sigma-Aldrich
Anti-Mouse IgG (Fab specific)-Peroxidase antibody produced in goat	A3682	Sigma-Aldrich

Table 7. Primers for real-time polymerase chain reaction (qPCR)

Gene name	Cat No. Primers	Company
CACNA1C (L-type Ca ²⁺ channel)	PPH01378G	Qiagen
SCN5A (Na ⁺ channel, Nav1.5)	PPH01671F	Qiagen
SCN10A (Na ⁺ channel, Nav1.8)	PPH15064A	Qiagen
SLC8A1 (NCX1)	PPH12509B	Qiagen
KCND3 (Ito, Kv4.3)	PPH06923A	Qiagen
KCNH2 (I _{Kr} , Kv11.1)	PPH01660A	Qiagen
KCNQ1 (I _{Ks} , Kv7.1)	PPH01419A	Qiagen
KCNN4 (SK4)	PPH01418C	Qiagen
TNF- α	PPH00341F	Qiagen

Table 8. Primer sequence for qPCR

Gene name	Primer sequence (5'-3')	Company
RGS3	F: CCG CTC GAG GGG CCA CTG GAG TCG AGC TC	Sigma-
wildtype	R: AAG GAA AAA AGC GGC CGC AAG GGT CAA GAA CAA GAA AT	Aldrich

RGS3 mutant	F: CAACCTTAACCCTCAGACCACACAGT R: TAAGGTTGTTCCCAAAGCCCCCGAGG	Sigma- Aldrich
NOS3	F: GAC CAG AAA CTG TCT CAC CTG R: CGA ACA TCG AAC GTC TCA CA	Eurofins
CRP	F: AGA CAT GTC GAG GAA GGC TTT T R: TCG AGG ACA GTT CCG TGT AGA A	Eurofins
CCL2	F: CTC TCG CCT CCA GCA TGA AA R: TTT GCT TGT CCA GGT GGT CC	Eurofins
RGS3	F: GTTCTGGTTGGCTTGTGAGG R: CCAGGTAGAGGTCAGAACGG	Eurofins

Table 9. Disposable items

Name	Cat No.	Company
35mm Cell Culture Dish	81151	Ibidi
μ-Dish 35 mm, high	81156	Ibidi
15mL High Clarity PP Centrifuge Tube	352096	Falcon
50mL High Clarity PP Centrifuge Tube	352070	Falcon
75cm ² Rectangular Canted Neck Cell Culture Flask with Vented Cap	353136	Falcon
24 Well Cell Culture Plate	353047	Falcon
12 Well Cell Culture Plate	353043	Falcon
Falcon® 4-well Culture Slide	354114	Corning
Cell Scrapers	353085	Thermo Fisher Scientific
EMD Millipore Stericup Sterile Vacuum Filter	SCVPU11RE	Thermo Fisher Scientific
MicroAmp™ Fast Optical 96-	4346907	Thermo Fisher Scientific

Well Reaction Plate, 0.1 ml		
Falcon® 10 mL Serological	357551	Corning
Pipet, Polystyrene		
Falcon® 25 mL Serological	357525	Corning
Pipet, Polystyrene		
Eppendorf® epT.I.P.S.	EP0030000919	Eppendorf
standard, volume range 50-1000 µl, blue polypropylene		
Eppendorf® epT.I.P.S.	EP0030000870	eppendorf
standard, volume range 2-200 µl, yellow polypropylene		
Eppendorf® epT.I.P.S.	EP0030000811	Eppendorf
standard volume range 0.1-10 µl		
Eppendorf® ep Dualfilter	EP0030078551	Sigma-Aldrich
T.I.P.S.® PCR clean, sterile, tip volume × L 2-200 µl × 55 mm, yellow tip		
Eppendorf® ep Dualfilter	EP0030078519	Sigma-Aldrich
T.I.P.S.® volume × L 0.1-10 µL × 34 mm		
Eppendorf® ep Dualfilter	EP0030078578	Sigma-Aldrich
T.I.P.S.® PCR clean, sterile, tip volume × L 50-1000 µl × 76 mm		

Table 10. The main instruments used in this study

Name	Company
Fluorescence microscope	Leica DMRE DFC3000G

PCR Amplifier	PeQSTAR PeQlab
qPCR	Applied Biosystems stepone Plus
Multi-function-reader Spark 10M	Tecan infinite m200
Incubator	Thermo HeRacell 240
Centrifuge	M&S Laborgerate GMBH
Electrophoresis Chambers	BIO-RAD
Chemiluminescence reader	PeQlab
Cytometry plate	BRAND
Patch electrodes	World Precision Instruments MTW 150F
DMZ-Universal Puller	Zeitz-InstrumenteVertriebs GmbH
HEKA patch clamp system	HEKA
FACSCanto II	BD-Becton Dickinson
Gel-Documentation System	Intas Science Imaging Instruments GmbH
Ultracentrifuge	Beckman Coulter
Nanosight NS300	Malvern Panalytical

3.3 Methods

3.3.1 Study design

To investigate the possible roles of endothelial dysfunction in TTS, we designed the following experiments (**Figure 3**):

- (1) To determine if Ang II plays important roles in endothelial dysfunction under conditions of high concentrations of catecholamines, we measured the concentration of Ang II in the supernatant of HCMECs treated with Epi.
- (2) To examine the roles of Ang II in catecholamine-induced endothelial dysfunction, we detected changes of endothelial cell functions monitored by the levels of ET-1 and NO, tube formation, mitochondrial function, inflammatory factors and apoptosis in HCMECs.
- (3) Ang II subtype-1 receptor (AT1R) blocker Losartan (Los) or Ang II subtype-2 receptor (AT2R) blocker PD123 319 (PD) was used to identify receptors mediating

Ang II effects in HCMECs.

- (4) An activator (NS309) and a blocker (Tram-34) of intermediate-conductance Ca^{2+} -activated K^+ channels (SK4 channels) were used to explore the involvement of SK4 in Ang II-induced endothelial functions.
- (5) SK4 channel current and membrane potential were measured to clarify the ionic mechanism by which Ang II caused endothelial dysfunction.
- (6) Blocker or activator of ROS and Protein kinase A (PKA) was applied to examine the involvement of ROS and PKA signaling in the regulation of SK4 channel by Ang II.

Next, we examined the effects of endothelial cell secretions on ion channel functions in hiPSC-CMs in the setting of TTS. The following experiments were performed.

- (1) To examine whether exosomes derived from endothelial cells can influence the function of cardiomyocytes, we isolated exosomes from HCMECs, characterized them and applied them to hiPSC-CMs.
- (2) We investigated the effects of exosomes from HCMECs with and without treatment of Epi on ion channel function, action potential and arrhythmia events in hiPSC-CMs to clarify whether exosomes from endothelial cells with and without Epi-challenge exert differential effects in cardiomyocytes.
- (3) To elucidate the mechanism by which exosomes alter Epi-induced changes in hiPSC-CMs, we assessed Epi-effects on expression levels of miRNAs in HCMECs and exosomes from HCMECs.
- (4) After it was revealed that miR-126-3p in exosomes derived from HCMECs challenged by Epi plays a key role in modulating the electrophysiological properties of hiPSC-CMs, we applied miR-126-3p-mimic or miR-126-3p-inhibitor to treat HCMECs to overexpress or suppress miR-126-3p and then isolated exosomes, and applied the exosomes again to hiPSC-CMs to confirm the importance of miR126-3p for the exosome effects in hiPSC-CMs.
- (5) Next, we further explored possible targets of miR-126-3p in hiPSC-CMs.

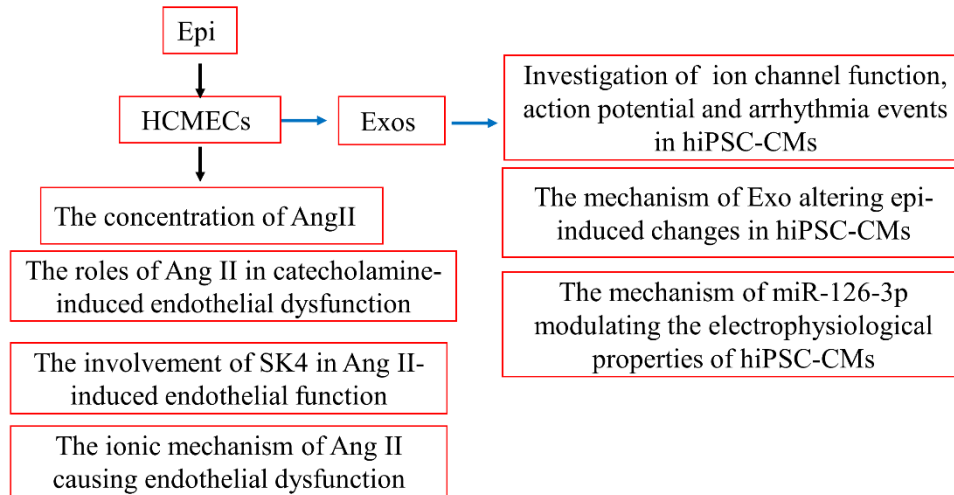


Figure 3. Study design. Epi. Epinephrine; HCMECs, Human Cardiac Microvascular Endothelial Cells; Exo, exosome; Ang II, angiotensin II; SK4, intermediate conductance calcium-activated potassium channel.

3.3.2 HCMECs culture

HCMECs were purchased from PromoCell (Heidelberg, Germany) and were cultured according to the manufacturer's instructions. They were characterized by vWF (Factor VIII) and CD31 (PECAM-1) positive staining as well as smooth muscle α -actin negative staining using immunofluorescence method within the first two passages. Their functions were measured by Dil-Ac-LDL uptake assay performed by the company. The cells were grown in Endothelial Cell Growth Medium MV2 (EMV2) supplemented with SupplementMix (C-22022, Promocell). Cells were cultured in Matrigel coated flasks and maintained in a humidified atmosphere of 5% carbon dioxide/95% air at 37°C. The medium was changed every other day until they reached 90% confluence before experiments. Ang II (1 μ M, final concentration) was added into HCMECs for 24 hours. AT1R antagonist Los (10 μ M, final concentration) and AT2R antagonist PD (10 μ M, final concentration) were used to treat HCMECs for 24 h, respectively. HCMECs were separately administered with vehicle (control), Ang II (1 μ M), hydrogen peroxide (H₂O₂, 100 μ M), Ang II with H₂O₂, and Ang II with N-Acetyl-L-cysteine (NAC) (1mM) for 24 h, and then the SK4 current was measured.

3.3.3 Differentiation and culture of hiPSCs

In this study, iPSCs (provided by Dr. Lukas Cyganek, Stem Cell Center, Göttingen) were differentiated into cardiomyocytes by the following methods (**Figure 4**). hiPSCs were generated from healthy donor fibroblasts from skin biopsies at the Department of Dermatology at the University Medical Center Mannheim. hiPSCs were maintained in TeSR™-E8™ medium (05990, StemCell Technologies) supplemented with TeSR™-E8™ 25×supplement. hiPSCs were put into a 24-well plate coated with Matrigel when they reached 80-90% confluence in a T-75 flask. After 2 days, hiPSCs were started to differentiate into cardiomyocytes (hiPSCs-CMs) in a 24-well plate. The cardiac differentiation medium included RPMI 1640 Medium with GlutaMAX™ Supplement (61870044, Thermo Fisher Scientific), 1% Pen/Strep (15140-122, Thermo Fisher Scientific), 1% Sodium Pyruvate (11360-039, Thermo Fisher Scientific), 2% B27 (17504001, Thermo Fisher Scientific), 0.2 mg/ml L-ascorbic acid 2-phosphate (A8960, Sigma-Aldrich). On day 0, hiPSCs were treated with 6 μM CHIR99021 (130-103-926, StemMACS). On day 2, 5 μM IWP-2 (72122, StemCell Technologies) was used to treat hiPSCs. On day 4, normal cardiac differentiation medium was used to feed the cells. On day 13, the cells were fed with cardio-selection medium containing RPMI 1640 without glucose and glutamine supplemented with 5 mM Sodium DL-Lactate Solution (BCBQ6934V, Sigma Aldrich), 50 mM 2-mercaptoethanol (31350010, Gibco). The differentiated hiPSC-CMs were cultured for 50-60 days for maturity. After that, hiPSC-CMs were used for biological studies or were digested into single cell for patch clamp measurement.

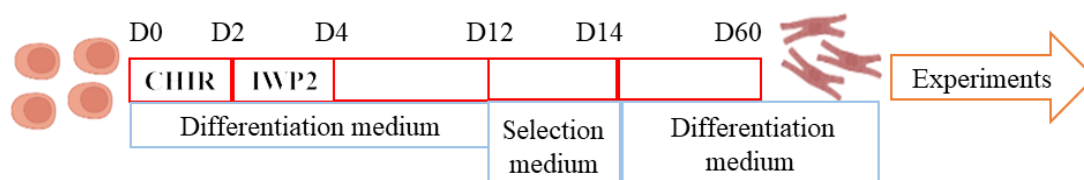


Figure 4. Schematic representation of differentiating hiPSCs into cardiomyocytes in this study.

3.3.4 Real-time quantitative PCR

Total RNA was extracted from HCMECs and hiPSC-CMs using the RNeasy Mini kit (74106, Qiagen), followed by the synthesis of cDNA using a high capacity cDNA reverse transcription kit (4368814, Thermo Fisher Scientific) according to manufacturers' recommendations. The reaction for RT-PCR was prepared (**Table 11**). The procedure of obtaining cDNA was performed with the following cycle conditions: 10 min at 25 °C, 120 min at 37 °C, 5 min at 85°C and store at 4°C. Quantitative polymerase chain reaction (qPCR) was performed on the StepOne Plus Real-Time PCR platform (Applied Biosystems) using HotRox Master Mix (119405, BIORON). The reaction for qPCR was prepared (**Table 12**). Cyclor conditions were as follows: 94°C for 2 min; 94°C for 10 s, 60°C for 20 s, 72°C for 1 min, 40 cycles, followed by a melting curve analysis. Relative mRNA expression level was calculated as the expression of target gene relative to GAPDH in samples, which was analyzed by the $2^{-\Delta(\Delta CT)}$ method, where $\Delta CT = CT_{\text{target gene}} - CT_{\text{GAPDH}}$ and $\Delta(\Delta CT) = \Delta CT_{\text{treated}} - \Delta CT_{\text{control}}$.

Table 11. Components for RT-PCR

Component	Volume (μl)
10× RT Buffer	2
25× dNTP Mix (100 mM)	0.8
10× RT Random Primers	2
MultiScribe™ Reverse Transcriptase	1
Nuclease-free H ₂ O	4.2
Total per reaction	10

Table 12. Components for qPCR

Component	Volume (μl)/25 μl PCR reaction
2× HotRox Master Mix	12.5
Forward primer	1

Reverse Primer	1
Template DNA	1
Nuclease-free H ₂ O	9.5
Total per reaction	25

3.3.5 Levels of ET-1 and NO

The supernatant from HCMECS treated with Ang II, Los and PD for 24 h, respectively, were collected to determine the levels of NO and ET-1. The concentration of ET-1 in the supernatant was detected according to the instructions of enzyme-linked immunosorbent assay (ELH-EDN1-1, RayBiotech). Total NO production in culture medium was determined by measuring the concentration of nitrate and nitrite according to the protocol of Nitric Oxide Assay Kit (EMSNO, Thermo Fisher Scientific).

3.3.6 Tube formation assay

Tube formation measurements were performed by using the Angiogenesis Assay Kit (PK-CA577-K905, PromoCell) according to the manufacturer's recommendations. 96-well plates were coated with extracellular matrix solution at 37°C for 1 h. After that, 2x10⁴ cells/well were seeded into 96-well plates for 14 h. At the same time, HCMECs were treated with Ang II, Los, and PD, respectively. The medium was carefully removed. The cells were gently washed with 100 µl of wash buffer, dyed by 100 µl/well of staining dye working solution, and incubated for 30 min at 37°C. The endothelial tube formation was examined using Leica fluorescence microscopy. Images were analyzed by Angiogenesis Analyzer for Image J.

3.3.7 Enzyme-linked immunosorbent assay (ELISA) for Ang II

The concentration of Ang II was measured by human Ang II Elisa Kit (USC-CEA005HU-96, Cloud-Clone) according to the manufacturer's instructions. HCMECs were treated with 100 µM Epi. Cell culture supernatant was centrifuged for 20 min at

1,000×g and then the Ang II levels in the collected the medium were examined. Ang II levels were quantified using Spark® multimode microplate reader with 450 nm filter.

3.3.8 Apoptosis assay

The apoptosis in HCMECs was determined by using a FITC annexin V apoptosis detection kit I (556547, BD Biosciences). The PBS-washed HCMECs were digested with 0.05% trypsin-EDTA for 1 min at 37°C. The cells were then harvested and centrifuged for 5 min (200 g, 4 °C). After removing the supernatant, PBS was used to wash the HCMECs 3 times and centrifuged again. Then 5 µl of Annexin V-FITC and 5 µl of propidium iodide (PI) were added into 100 µl cell suspension. After being thoroughly mixed, they were left at room temperature for 15 min in the dark, and then they were analyzed using BD FACS Canto TM II (Becton Dickinson, Heidelberg, Germany).

3.3.9 Measurement of ROS

The ROS production in HCMECs was evaluated by 2', 7'-Dichlorofluorescein diacetate (DCFH-DA, D6883, Sigma) method according to the ROS assay instructions. HCMECs were harvested. After being washed 3 times with PBS, they were incubated with 10 µM DCFH-DA at 37°C for 30 min in the dark. Then the cells were washed 3 times with PBS, the results were measured by BD FACS Canto TM II (Becton Dickinson, Heidelberg, Germany).

3.3.10 Measurement of the mitochondrial membrane potential (MMP)

The MMP was determined using the fluorescent dye, JC-10 (ab1121, Abcam), which is capable of reversibly changing its color from green to orange as membrane potentials increase. HCMECs were seeded into a 96-well plate at a density of 8×10^4 cells/well and then cells were treated with Ang II, Los or PD, and cultured in a 37 °C, 5% CO₂ incubator for 24 h. JC-10 dye-loading solution (50 µl/well) was added into the 96-well plate and incubated in a 37°C, 5% CO₂ incubator for 1 h. Fluorescence intensities were

measured at Ex/Em = 490/525 nm and 540/590 nm for ratio analysis using Spark® multimode microplate reader.

3.3.11 ATP detection

Total ATP production from HCMECs was measured through an ATP Assay Kit (ab83355, Abcam). In brief, HCMECs were harvested, washed with cold PBS, and then resuspended in 100 µl of ATP assay buffer, followed by centrifuging 5 min (4 °C at 13,000 g). After that, the supernatant was collected. Deproteinizing Sample Preparation Kit-TCA (ab204708, Abcam) was used to remove enzymes that can interfere with the ATP assay from HCMECs and then the cells were incubated with the ATP probe at room temperature for 30 min in the dark. The ATP content was measured at Ex/Em = 535/587 nm using Spark® multimode microplate reader.

3.3.12 Detection of intracellular calcium transients

hiPSC-CMs were loaded with the fluorescent Ca²⁺-indicator Fluo-3 AM (F1242, Thermo Fisher scientific) to measure the intracellular Ca²⁺ transients. First, the membrane permeable acetoxymethyl-ester derivative of Fluo-3 AM (50 µg) was dissolved in 44 µl of the Pluronic F-127 stock solution (20% w/v in DMSO) to get a 1 mM Fluo-3 AM stock solution, which can be stored at -20 °C for several weeks. Pre-incubated PSS (see below) was used to wash hiPSC-CMs in dishes 2 times. Then, Fluo-3 AM stock solution (10 µl) was added into 1 ml PSS to prepare a final concentration of 10 µM Fluo-3, which was used to incubate hiPSC-CMs for 10 min at room temperature in the dark. Thereafter, the PSS was carefully sucked out, and hiPSC-CMs were washed with PSS 4-5 times. Finally, the cells were kept in PSS at room temperature for about 30 min for de-esterification before measurements. After de-esterification the fluorescence of the cells was measured by using Cairn Optoscan calcium imaging system (Cairn Research, UK). Fluorescence is excited by 488 nm and emitted at 520 nm.

3.3.13 Isolation and quantification of exosomes

The exosomes secreted by HCMECs was isolated by ultracentrifugation as previously described [156]. In short, the supernatant from medium of HCMECs cultured for 48 h with exosome-free serum was collected and processed for gradient centrifugation at 200 g for 10 min, 2000 g for 20 min and 10,000 g for 30 min, respectively. Then, the resultant supernatant was further centrifuged at 100,000 g for 70 min to pellet exosomes. Thereafter, the pellets were washed with PBS and centrifuged at 100,000 g for 70 min to harvest exosomes. The size and concentration of exosomes were measured by ZetaView instrument (Particle Metrix, Meerbusch, Germany).

3.3.14 Confirmation of exosomes by flow cytometry

Exosomes were isolated from the collected EMV2 medium that was used to culture HCMECs and then stained for flow cytometry according to ExoStep Cell Culture (ExoS-25-C9, Immunostep) recommendations. First, CD63⁺ exosomes were isolated according to the following steps: The capture beads (50 μ l) resuspended by vortex for approximately 20 s and about 10-15 μ g of exosomes were added into a 12 \times 75 mm cytometer tube; They were gently mixed by pipetting up and down several times with a 1 ml pipette and vortexed for few seconds; After that, they were incubated overnight at room temperature in the dark; On the next day, the bead-bound exosome was washed by adding 1 ml of 1 \times assay buffer, and then the magnetic beads were collected by placing tubes on a magnetic rack by incubating for 5 min; The supernatant was removed from tubes by aspiration; The primary detection antibody (5 μ l) was added to the bead-bound exosome tube and incubated in the dark for 60 min at 2-8 $^{\circ}$ C; After that, the magnetic beads were collected and then the supernatant was removed from tubes; The sample was resuspended in 350 μ l 1 \times assay buffer and acquired on a flow cytometer or stored in the dark maximal up to 2 h at 2-8 $^{\circ}$ C. The isolated exosomes were measured by BD FACS CantoTM II (Becton Dickinson, Heidelberg, Germany). Data analysis was conducted using the BD FACS Diva software (Version 8.0.1).

3.3.15 Exosome labeling for myocyte uptake assessments

The uptake of exosome by cardiomyocytes was monitored with a PKH26 Red Fluorescent Cell Linker Kit for General Cell Membrane Labeling (PKH26GL-1KT, Sigma-Aldrich). Exosomes isolated from HCMECs supernatant and 4 μ l PKH26 or 4 μ l PBS were mixed up with 0.5 mL Diluent C and then incubated at room temperature for 5 min in the dark. FBS (2 ml) was used to stop over-staining. The labeled exosomes were centrifuged at $110,000 \times g$ for 1 h to remove residual dye, then the exosome pellet was resuspended in 200 μ l PBS. The labeled exosomes (20 μ g), PBS and unlabeled exosomes were added into hiPSC-CMs, and incubated for 8 h in the dark in a 37°C cell incubator. Thereafter, the medium was removed from slides and slides were washed 3 times with PBS. Then, hiPSC-CMs in all slides were fixed with 4% paraformaldehyde at room temperature for 10 min in the dark and washed 3 times with PBS. DAPI (Biozol) was used to incubate hiPSC-CMs for 10 min at room temperature in the dark. The uptake of exosome by cardiomyocytes was observed using the confocal microscope TCS SP-8 upright (Leica, Germany) with Plan-Apochromat 40 \times /0.6 objective.

3.3.16 Immunofluorescence staining

hiPSC-CMs in the 24-well plate were digested into 4-well Culture Slide as separated single cells. The following steps were performed to prepare the single cell from 24-well plate to dishes: Collagenase I (2 mg/ml) in PRMI1640 medium was added into each well of 24-well plate; Then the cells were incubated for 40 min at 37 °C; After that, the cells were pipetted up and down about 10 times; Then the cell suspension was centrifuged at 250 g for 5 min at room temperature; PRMI 1640 medium (300 μ l) and 10% FBS were used to stop the reaction and then cell suspension was centrifuged at 250 g for 2 min at room temperature; Cardio-differentiation medium was added to resuspend the cells, and then the cell suspension was added to dishes for patch clamp experiment.

hiPSC-CMs were treated with exosomes before PBS was used to wash them 3 times.

The cells in 4-well culture slide were fixed with 4% paraformaldehyde (P087.4, Carl Roth) at room temperature for 15 min and permeabilized with 0.1% triton X-100 (3051.3, Carl Roth) for 10 min. Then, after the cells were washed 3 times with PBS, they were blocked with 5% bovine serum albumin (BSA, Sigma-Aldrich) in PBS at room temperature for 1 h. Recombinant Anti-Cardiac Troponin T antibody [EPR20266] (ab209813, Abcam) in 5% BSA was added into the slides to incubate the cells at 4 °C overnight. On the next day, hiPSC-CMs in 4-well culture slide were washed with PBS 3 times before incubated with Goat anti-Rabbit IgG (H+L) Cross-Adsorbed Secondary Antibody, Alexa Fluor 488 (A-11008, Thermo Fisher Scientific) for 1 h at room temperature in the dark. Thereafter, the cells were washed 3 times with PBS. Finally, hiPSC-CMs were incubated with VECTASHIELD Antifade Mounting Medium with DAPI (VEC-H-1200, BIOZOL) for 10 min at room temperature in the dark. Images were photographed using the confocal microscope TCS SP-8 upright (Leica, Germany) with Plan-Apochromat 40×/0.6 objective.

3.3.17 Dual-Luciferase assay

PsiCHECK2-LET-7 WT vector (Plasmid #78260) was purchased from Addgene. The plasmid was amplified before it was extracted with GenElute HP plasmid mimiprep kit (NA0160-1KT, Sigma-Aldrich). The following steps were carried out.

- (1) Harvest and lyse bacteria: 5 ml of an overnight culture was centrifuged at $12,000 \times g$ for 1 min and then supernatant was discarded. Resuspension solution (200 μ l) was used to resuspend cells. Lysis buffer (200 μ l) was added and the tube was gently inverted 6-8 times until the solution was clear.
- (2) Prepare cleared lysate: neutralization/binding buffer (350 μ l) was added into Eppendorf tubes and the tube was gently inverted 4-6 times to mix and then centrifuged at $12,000 \times g$ for 10 min. At the same time, the GenElute HP Miniprep Binding Column was inserted into microcentrifuge tube. Column preparation solution (500 μ l) was added to miniprep binding column and then centrifuged at $12,000 \times g$ for 1 min. The flow-through liquid was discarded.

- (3) Bind plasmid DNA to column: the cleared lysate was transferred to the column and centrifuged at $12,000 \times g$ for 1 min. The flow-through liquid was discarded.
- (4) Wash to remove contaminants: 500 μ l of wash solution 1 was added to the column and then centrifuged at $12,000 \times g$ for 1 min. The flow-through liquid was discarded. Next, 750 μ l of wash solution 2 was added to the binding column and centrifuged at $12,000 \times g$ for 1 min. The flow-through liquid was discarded. The column was centrifuged at $12,000 \times g$ for an additional 1 min to remove excess ethanol.
- (5) Elute purified plasmid DNA: the binding column was transferred to a fresh collection tube. 30 μ l of ddH₂O was added to the column and then centrifuged at $12,000 \times g$ for 1 min. The concentration of plasmid DNA was measured by using Spark® multimode microplate reader.

After PsiCHECK2-LET-7 WT vector was digested with Not I-HF and Xho I at 37°C overnight (**Table 13**), psiCHECK2-WT and G-protein signaling 3 (RGS3)-WT, psiCHECK2-WT and RGS3-MT (mutant) were ligated with T4 DNA ligase (**Table 14**).

Table 13. Plasmid digestion reaction

Component	50 μ l reaction
DNA	1 μ g (Calculate volume)
10x rCutSmart Buffer	5 μ l (1x)
Not I-HF	1 μ l (20 unites)
Xho I	1 μ l (20 unites)
Nuclease-free water	To 50 μ l

Table 14. Ligation

Component	20 μ l reaction (RGS3-WT)	20 μ l reaction (RGS3-MT)
T4 DNA ligase buffer(10x)	2 μ l	2 μ l
Psi CHECK2 vector DNA(6.2kb)	3.6 μ l (50 ng)	3.6 μ l (50 ng)

RGS3 CDS DNA (0.79kb)	1.4 μ l (31.85 ng, 5:1)	1.5 μ l (31.85 ng, 5:1)
T4 DNA ligase	1 μ l	1 μ l
water	12 μ l	11.9 μ l
In total	20 μ l	20 μ l

The ligation products (10 μ l) were subjected to transformation reaction, and then the plasmid was extracted. After PCR reaction, 1% gel was run for identification. HEK293T cells (CRL-3216, ATCC) were cultured in DMEM supplemented with 1% penicillin-streptomycin (15140122, Thermo Fisher Scientific), 10% FCS, and 2 mM L-glutamine (25030123, Thermo Fisher Scientific). Then, the following steps were performed:

A. miRNA-126-3p-mimic (5 μ l, 20 μ M) stock solution and 1 μ l RGS3-psiCHECK 2 recombinant plasmid (the amount of transfected plasmid was 1 μ g) were added into 125 μ l Opti-MEM, mixed gently, incubated at room temperature for 5 min.

B. Lipofectamine 2000 (5 μ l) was added to 125 μ l serum-free medium Opti-MEM, mixed gently and incubated at room temperature for 5 min.

C. samples from A and B were gently mixed, and incubated at room temperature for 20 min

D. The mixture from C was added to a six-well plate containing 1750 μ l medium of cells, mixed gently, and cultured for 48 h.

Dual-Luciferase experiment was performed according to Dual-Luciferase® Reporter Assay instructions. TargetScan and miRDB (https://www.targetscan.org/vert_80/ and <https://mirdb.org/>) were used to predict if RGS3 was indeed a target gene of miR-126-3p. Human embryo kidney (HEK293T) cells were cultured in DMEM containing 10% FBS at 37°C with 5% CO₂. The cDNA fragment in RGS3 3'UTR containing miR-126-3p binding sites was inserted into psiCHECK2 WT vector. The cDNA fragments of RGS3 3'UTR with binding site mutation were inserted into psiCHECK2 WT vector.

The recombinant vector of psiCHECK2 WT-RGS3 or psiCHECK2 MT-RGS3 was co-transfected with miR-126-3p-mimic or miR-126-3p-NC (negative control) into HEK293T cells by Lipofectamine 2000 Transfection Reagent (11668030, Thermo Fisher Scientific), respectively. HEK293T cells were then cultured for 48 h. Subsequently, the growth medium was removed from the cultured hiPSC-CMs, and the cells were gently washed with a sufficient volume of PBS. hiPSC-CMs were covered with 100 μ l 1 \times PLB and shaken at room temperature for 15 min. Lysate (20 μ l) was transferred into a 96-well plate. Thereafter, 100 μ l of LAR II was added to each well and firefly luciferase luminescence was measured. Then, 100 μ l of Stop & Glo[®] Reagent was added and the renilla luciferase activity measurement was recorded. The renilla luciferase and firefly luciferase activities were detected by Spark[®] multimode microplate reader.

3.3.18 Single-cell contraction measurement

Single hiPSC-CM contraction was measured by a single cell contraction measuring system (MyoCam-S IonOptix). The shortening of spontaneously beating hiPSC-CMs was recorded at 37°C. The rhythmic and arrhythmic events were analyzed in the absence and presence of a drug. The data were analyzed by MyoCam-S IonOptix.

3.3.19 Electrophysiological recording in single cell

Patch electrodes we used in patch clamp experiment were thin wall borosilicate glass capillaries (TW150F-4, world Precision Instruments) and were pulled with DMZ-Universal Puller (Zeitz-InstrumenteVertriebs GmbH, Martinsried, Germany) and filled with pre-filtered pipette solution for different current recording. The pipette resistance ranged from 2-4 M Ω for measurements.

For action potential recording, pulses of 800-1000 pA for about 5 ms were applied to trigger the AP under current-clamp in the whole-cell configuration. All the recordings were performed at room temperature (22-25°C). APs were recorded at 1 Hz with the

bath solution containing (mM): 130 NaCl, 5.9 KCl, 2.4 CaCl₂, 1.2 MgCl₂, 11 Glucose, and 10 HEPES (pH 7.4 (NaOH)). The pipette solution contained (mM): 20 KCl, 110 K-aspartate, 1 MgCl₂, 0.5 EGTA, 2 ATP, 0.5 GTP, and 10 HEPES (pH 7.2 (KOH)). The cell RP, the maximal depolarization velocity (V_{max}), the action potential duration at 10% repolarization (APD₁₀), the action potential duration at 50% repolarization (APD₅₀), the action potential duration at 90% repolarization (APD₉₀) were analyzed by FitMaster software.

Different ion channel currents in hiPSC-CMs were recorded in voltage-clamp mode. Sodium current (I_{Na}) was measured with the bath solution containing (mM): 20 NaCl, 110 CsCl, 1.8 CaCl₂, 1 MgCl₂, 10 HEPES, 10 Glucose, and 0.001 nifedipine (pH 7.4(CsOH)). The pipette solution contained (mM): 10 NaCl, 135 CsCl, 2 CaCl₂, 3 MgATP, 2 TEA-Cl, 5 EGTA, and 10 HEPES (pH 7.2 (CsOH)). The peak I_{Na} density or gating kinetics including the channel activation, inactivation, and recovery from inactivation or late I_{Na} density were analyzed using FitMaster software.

For L-type calcium channel current (I_{Ca-L}) recording, we used the bath solution containing (mM): 140 TEA-Cl, 5 CaCl₂, 1 MgCl₂, 10 HEPES, 0.003 E-4031, 0.02 TTX, and 3 4-AP (pH 7.4 (CsOH)). The electrode solution used in this experiment contained (mM): 10 NaCl, 135 CsCl, 2 CaCl₂, 3 MgATP, 2 TEA-Cl, 5 EGTA, and 10 HEPES (pH 7.2 (CsOH)). The I_{Ca-L} density or gating kinetics including the activation, inactivation, and recovery from inactivation were analyzed using FitMaster software.

For recording Na⁺/Ca²⁺ exchanger current (I_{NCX}), the extracellular solution contained (mM): 135 NaCl, 10 CsCl, 2 CaCl₂, 1 MgCl₂, 10 HEPES, 10 glucose, 0.01 nifedipine, 0.1 niflumic acid, 0.05 lidocaine, and 0.02 dihydroouabain (pH 7.4 (CsOH)). The intracellular solution contained (mM): 150 CsOH, 75 aspartic acid, 10 NaOH, 5 EGTA, 2 CaCl₂, 1 MgCl₂, (pH7.2 (CsOH)). The I_{NCX} density were analyzed by FitMaster software.

For measuring the rapidly activating delayed rectifier channel current (I_{Kr}), Cs^+ is used as the charge carrier instead of the K^+ ion. The following bath solution was used (mM): 140 CsCl, 2 MgCl₂, 10 HEPES, and 10 glucose (pH 7.4 (CsOH)). Pipette solution contained 140 CsCl, 2 MgCl₂, 10 HEPES, and 10 EGTA (pH 7.2 (CsOH)). The I_{Kr} density were analyzed by FitMaster software.

For recording I_{to} and I_{Ks} , the following bath solution was used (mM): 130 NaCl, 5.9 KCl, 2.4 CaCl₂, 1.2 MgCl₂, 11 Glucose, and 10 HEPES (pH 7.4 (NaOH)). The pipette solution contained (mM): 20 KCl, 110 K-aspartate, 1 MgCl₂, 0.5 EGTA, 2 ATP, 0.5 GTP, and 10 HEPES (pH 7.2 (KOH)). Importantly, 10 μ M nifedipine, 10 μ M TTX, and 3 μ M E-4031 were added into the bath solution to avoid interference of I_{Ca-L} , I_{Na} , and I_{Kr} when I_{to} was recorded. For I_{Ks} recording, 10 μ M TTX, 10 μ M nifedipine, 3 mM 4-AP were added in the bath solution.

Intermediate conductance calcium-activated potassium channel currents (I_{SK4}) were measured by standard patch-clamp recording techniques in the whole-cell configuration at room temperature. To isolate I_{SK4} from others, a specific channel blocker Tram-34 (1 μ M) was used. The extracellular solution contained 130 mmol/L NaCl, 11 mmol/L glucose, and 10 mmol/L HEPES, 5.9 mmol/L KCl, 2.4 mmol/L CaCl₂, 1.2 mmol/L MgCl₂, (pH 7.4 (NaOH)). The pipette solution contained 126 mM KCl, 11 mM glucose, 10 mM HEPES, 6 mM NaCl, 5 mM EGTA, 1.2 mM MgCl₂, and 1 mM MgATP (pH 7.4 (KOH)). Appropriate amount of CaCl₂ was added to the pipette solution to get the final free Ca^{2+} concentration of 0.5 μ M according to the calculation by the software MAXCHELATOR (<http://web.stanford.edu/~cpatton/downloads.htm>).

3.3.20 Western blot

Equal amounts of total proteins added into each lane were separated by 10% separation gel and 15% separation gel, respectively, and then transferred to a PVDF membrane (Millipore, USA). The membrane was incubated in 5% non-fat milk in

TBST for 1 h at room temperature and incubated with the corresponding primary antibodies overnight at 4 °C. The primary antibodies are as follows: Anti-KCNN4 (KCa3.1, SK4) Antibody (APC-064, Alomone, Israel), Anti-Bcl-2 antibody (sc-7382, Santa Cruz Biotechnology), Anti-Cleaved Caspase-3 antibody (ab2302, abcam), Anti-Bax Antibody (sc-20067, Santa Cruz Biotechnology), BAD Polyclonal antibody (10435-1-AP, proteintech), Anti-PKA alpha/beta/gamma (catalytic subunit) (phospho T197) antibody (ab75991, abcam), Anti-CD9 Polyclonal Antibody (PA5-11559, ThermoFisher scientific), Anti-CD63 Monoclonal Antibody (Ts63) (10628D, ThermoFisher scientific), Anti-CD81 Monoclonal Antibody (MA5-13548, ThermoFisher scientific), Anti-GM130 antibody (sc-55591, Santa Cruz), Anti-GRP94 antibody (ab13509, Abcam), RGS3 Polyclonal Antibody (66790-1-Ig, Proteintech), mouse-anti-GAPDH (5G4MAb6C5, HyTest).

On the next day, the membranes were washed for 10 min 3 times in TBST and then incubated with the corresponding secondary antibodies for 60 min. The secondary antibodies were anti-Mouse IgG (Fab specific)-Peroxidase antibody produced in goat (A3682, Sigma-Aldrich) and anti-Rabbit IgG (whole molecule)-Peroxidase antibody produced in goat (A0545, Sigma-Aldrich). After washing for 10 min 3 times in TBST, the results were visualized with chemiluminescence, and the density of the bands was analyzed by Image J software.

3.2.21 Statistics

All data are shown as mean \pm SD and were analyzed by SigmaPlot 14.0 (Systat GmbH, Germany) and GraphPad Prism 7 (GraphPad Software Inc., California, USA). Unpaired Student's t-test analysis was performed to compare two independent groups with normal distribution. One-way ANOVA followed with Holm-Sidak post-test was used for comparison of more than two groups. To compare categorical variables, the Fisher test was used. P value less than 0.05 were considered statistically significant.

4. RESULTS

Part I. Catecholamine could induce endothelial dysfunction via Ang II, SK4 channel and ROS signaling

4.1 Catecholamine-induced changes of ET-1 and NO release in HCMECs contained roles of Ang II and SK channels

To examine the possible involvement of Ang II in the catecholamine-induced endothelial dysfunction, we first measured the levels of ET-1 and NO in supernatant of HCMECs treated with epinephrine (Epi) or Epi plus AT1R blocker losartan (Los) or AT2R blocker PD123319 (PD) or both together. The concentration of ET-1 in the collected medium from HCMECs treated by Epi was significantly increased compared with control group, while the concentration of NO was decreased by the Epi treatment (**Figure 5A-B**). Los or PD significantly attenuated the effects of Epi on ET-1 level (**Figure 5A**) and NO level (**Figure 5B**), suggesting involvement of Ang II in Epi effects. Next, Ang II effects were examined. Like Epi, Ang II increased ET-1 level and reduced NO level in HCMECs, and Los or PD blocked Ang II effects (**Figure 5C-D**). Importantly, we found that Epi treatment of HCMECs could significantly increase the level of Ang II (**Figure 5E**). Furthermore, a calcium activated potassium (SK) channel activator NS309 attenuated Ang II-induced elevation of ET-1 level and Ang II-induced reduction of NO level in the supernatant of HCMECs (**Figure 5F-G**). Tram-34, an SK4 channel blocker, mimicked Ang II effects (**Figure 5F-G**), suggesting involvement of SK4 channel in Ang II effects.

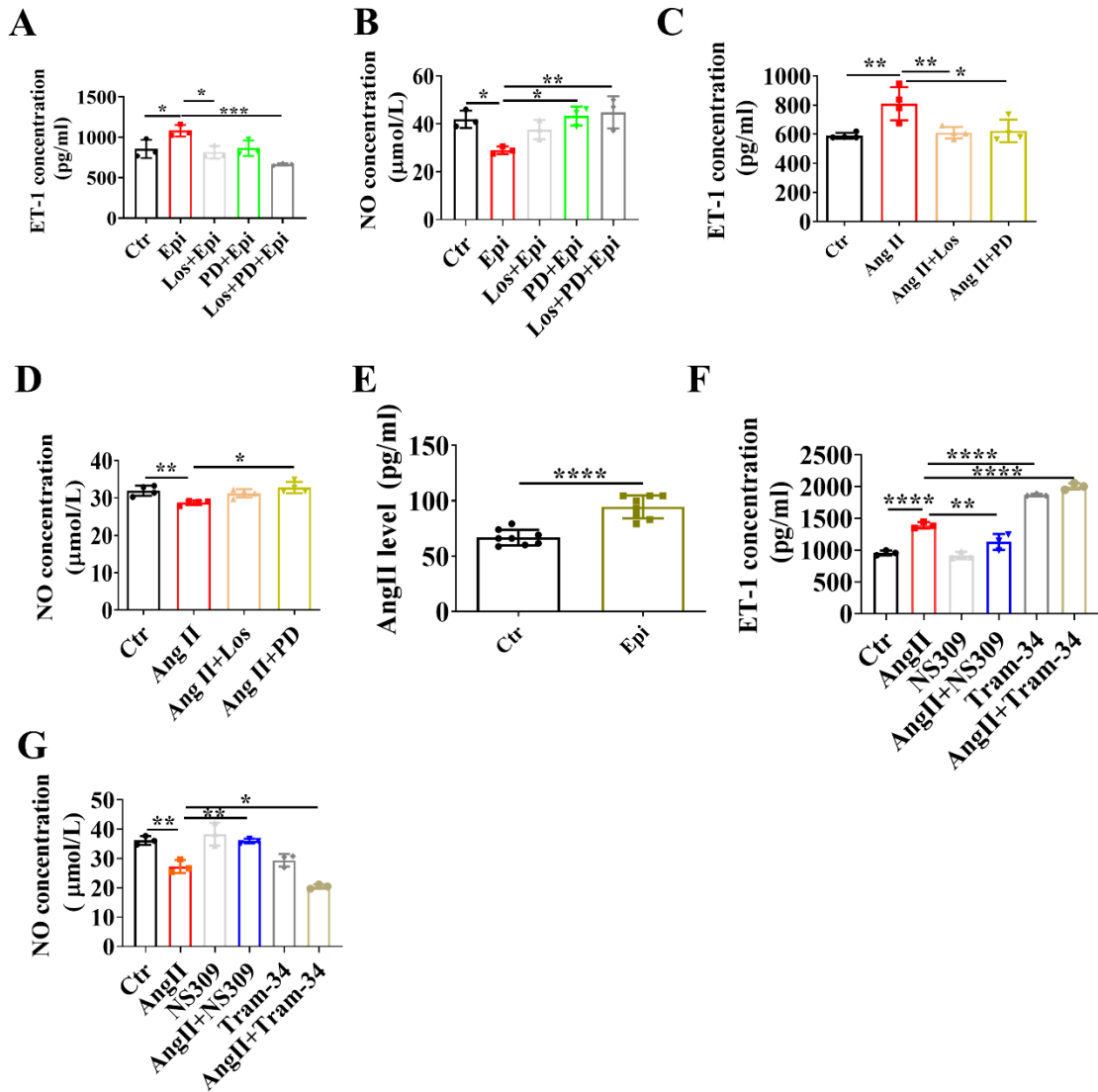


Figure 5. Ang II and SK4 channel contributed to epinephrine-induced endothelial dysfunction.

Endothelin-1 (ET-1) and nitric oxide (NO) in the supernatant of HCMECs were measured by ELISA kits. HCMECs were treated with vehicle (Ctr) or 100 μ M epinephrine (Epi) or 1 μ M angiotensin II (Ang II) in the absence or presence of losartan (Los, 10 μ M) or PD123319 (PD, 10 μ M). (A) Los and PD reduced the effect of Epi on ET-1 production in HCMECs (n= 3). (B) Los and PD reversed the effect of Epi on NO production in HCMECs (n= 3). (C) Ang II increased ET-1 level in the collected supernatant of HCMECs compared with control group, Los and PD inhibited the effect of Ang II (n=4). (D) Ang II reduced the concentration of NO in the supernatant of HCMECs, and PD reversed Ang II effect (n=4). (E) Epi increased the level of Ang II in the collected supernatant of HCMECs (n=8). Then, HCMECs were treated with vehicle (Ctr) or 1 μ M angiotensin II (Ang II) for 24 h in the absence or presence of NS309 (1 μ M) or Tram-34 (1 μ M) or NS309 or Tram-34 alone. (F) NS309, an SK channel activator, reduced the ET-1 concentration in the supernatant of HCMECs

stimulated by Ang II, while an SK4 inhibitor Tram-34 increased ET-1 level (n=3). (G) NS309 rescued NO production reduced by Ang II, while Tram-34 decreased NO generation in the presence of Ang II. (n=3). All results are presented as means \pm SD. The n-number represent replicates of different experiments. * $P < 0.05$, ** $P < 0.01$, *** $P < 0.001$, **** $P < 0.0001$ determined by one-way ANOVA with Holm-Sidak post-hoc test.

4.2 SK4 channels contributed to Ang II-effects on endothelial cell functions

To further investigate roles of SK4 channel for endothelial functions besides ET-1/NO generation, we treated HCMECs with Ang II with or without NS309 or Tram-34 to measure the tube formation, which is an important function character of endothelial cells. **Figure 6A** showed that the tube formation ability of HCMECs was reduced by Ang II. NS309 significantly increased tube formation compared with Ang II group, while Tram-34 further reduced tube formation (**Figure 6B**), implying that SK4 channels are important for endothelial tube-forming function.

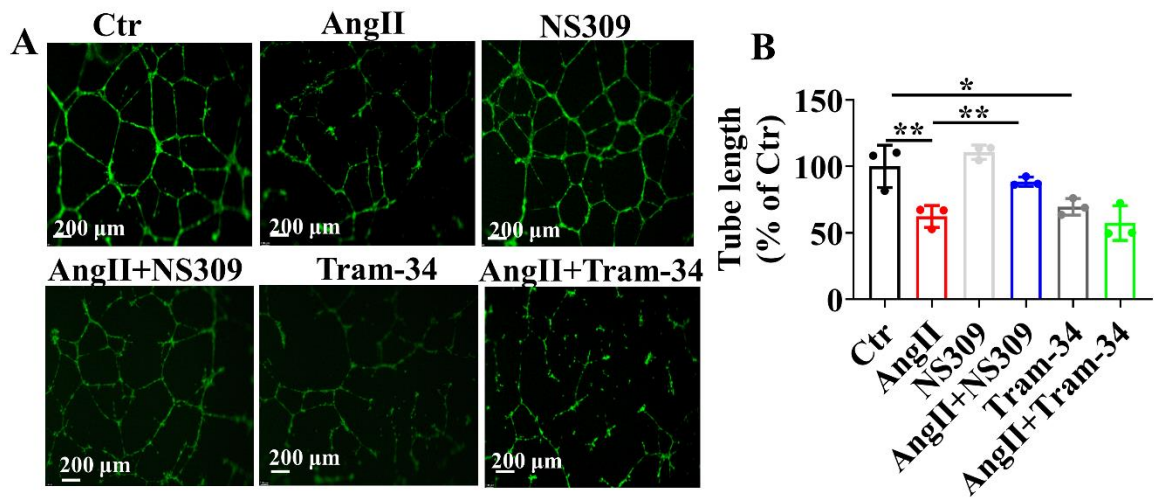


Figure 6. SK4 channel activator rescued and SK4 channel blocker mimicked Ang II effect on tube formation. HCMECs were treated with vehicle (Ctr) or 1 μ M angiotensin II (Ang II) for 24 h in the absence or presence of NS309 (1 μ M) or Tram-34 (1 μ M) or NS309 or Tram-34 alone. (A) Representative images demonstrating tube formation in HCMECs. (B) The total tube length

reflecting tube formation in indicated groups. Triplicate tube formation experiments were performed. Data are presented as mean \pm SD and are expressed as % of control. * $P < 0.05$, ** $P < 0.01$ determined by one-way ANOVA with Holm-Sidak post-hoc test.

To further characterize the roles of Ang II for endothelial dysfunction, we examined its roles in inflammation, mitochondrial impairment and apoptosis of HCMECs. We first treated HCMECs with Ang II with or without Los and PD to measure the expression of inflammatory factors. **Figure 7A** showed that Ang II reduced NOS3 mRNA expression, which could be reversed Ang II receptor blockers. The expression levels of c-reactive protein (CRP), C-C Motif Chemokine Ligand 2 (CCL2), and tumor necrosis factor alpha (TNF- α) gene expression were upregulated in response to Ang II in HCMECs, which were abolished or attenuated by Los and PD (**Figure 7B-D**). Then, we assessed the cellular energy metabolism and apoptosis in HCMECs. The results showed that Ang II promoted mitochondrial damage by reducing the mitochondrial membrane potential ($\Delta\psi_m$) (**Figure 7E**) and reducing ATP level (**Figure 7F**). Both effects could be reversed by Los but not PD (**Figure 7E-F**). In addition, Ang II increased apoptotic cells, which was attenuated by both Los and PD (**Figure 7G-H**). These results indicated that Ang II can promote endothelial cell apoptosis, mitochondrial impairment and inflammation leading to endothelial dysfunction.

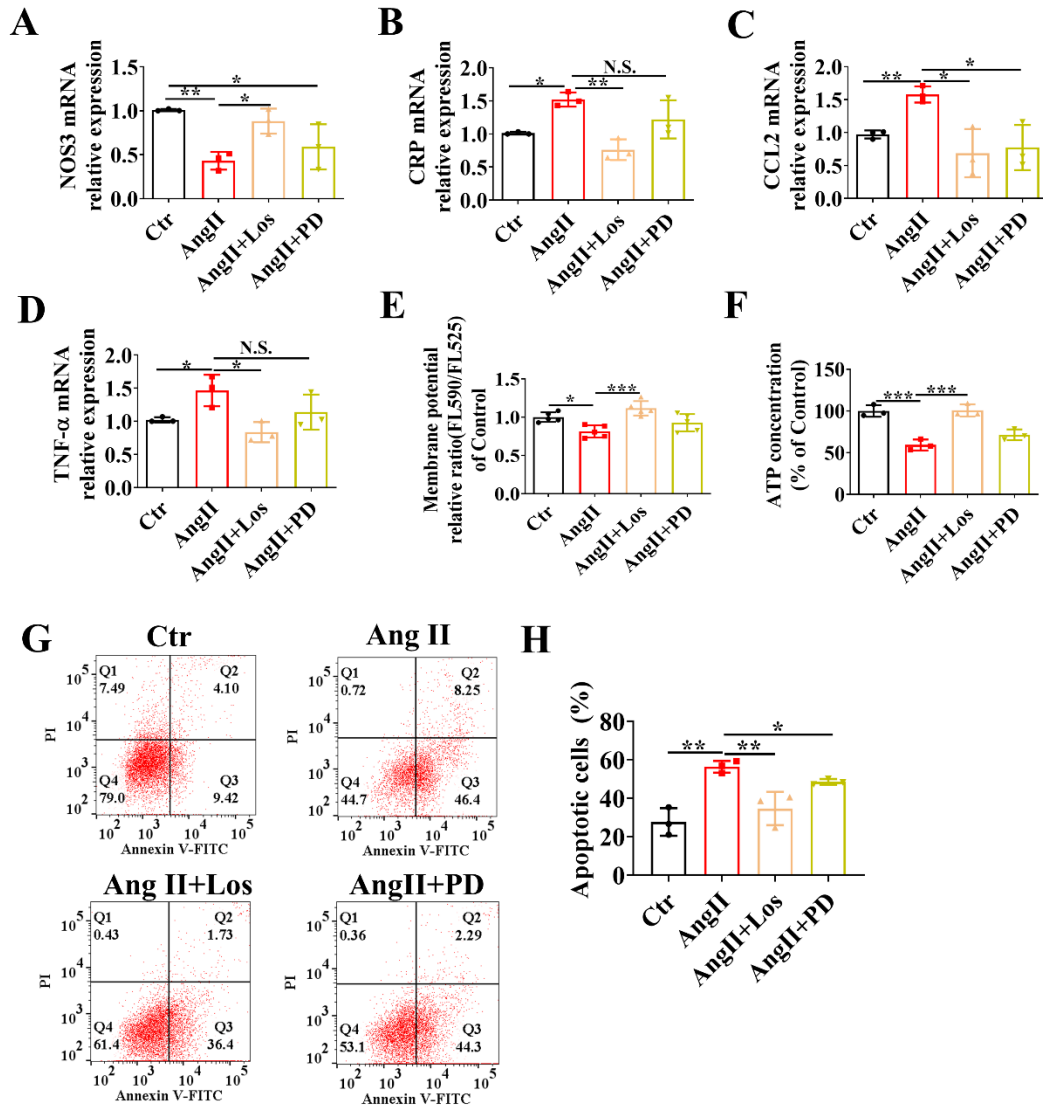


Figure 7. The effects of Ang II on inflammation-related factors, mitochondrial membrane potential ($\Delta\psi_m$), ATP production and apoptosis. HCMECs were treated by vehicle (Ctr) or 1 μM angiotensin II (Ang II) for 24 h in the absence or presence of losartan (Los, 10 μM) or PD123319 (PD, 10 μM). **(A)** Ang II reduced NOS3 gene expression, and Los reversed Ang II effect (n=3). **(B)** Ang II increased CRP gene expression, and Los blocked the effect of Ang II (n=3). **(C)** Ang II increased CCL2 mRNA expression, Los and PD blocked Ang II effect (n=3). **(D)** Ang II increased TNF- α gene expression, and Los prevented Ang II effect (n=3). **(E)** Fluorescence intensity ratio [590/525] relative to control showing changes of mitochondrial membrane potential ($\Delta\psi_m$) in HCMECs (n=5). **(F)** Ang II reduced cellular ATP content in HCMECs and Los rescued it (n=3). **(G-H)** Representative flow cytometry measurements (G) and statistical data (H) showing that Ang II increased cell apoptosis. Cell apoptosis of HCMECs was assessed using FITC Annexin V Apoptosis

assay (n=3). All data shown are mean \pm SD. * $P < 0.05$, ** $P < 0.01$, *** $P < 0.001$ determined by one-way ANOVA with Holm-Sidak post-hoc test.

Interestingly, we found that apoptosis is associated with SK4 channel function. Ang II significantly decreased the protein expression of Bcl2, (**Figure 8A, B**) and increased the expression levels of cleaved caspase 3, Bax and Bad (**Figure 8A, C-E**), which are commonly used markers for cell apoptosis. Ang II also increased the number of apoptotic cells (**Figure 8G-H, 9F-G**). Strikingly, all these effects could be reversed by NS309 and mimicked by Tram-34 (**Figure 8**), suggesting that SK4 channel function may play an important role in Ang II induced apoptosis. In addition, KCl (10 mM), which could depolarize the cell membrane (**Figure 9A**), also increased cell apoptosis (**Figure 9B-C**), suggesting alteration of cell membrane potential, which could be caused by changing the potassium channel current, may play a critical role for endothelial apoptosis.

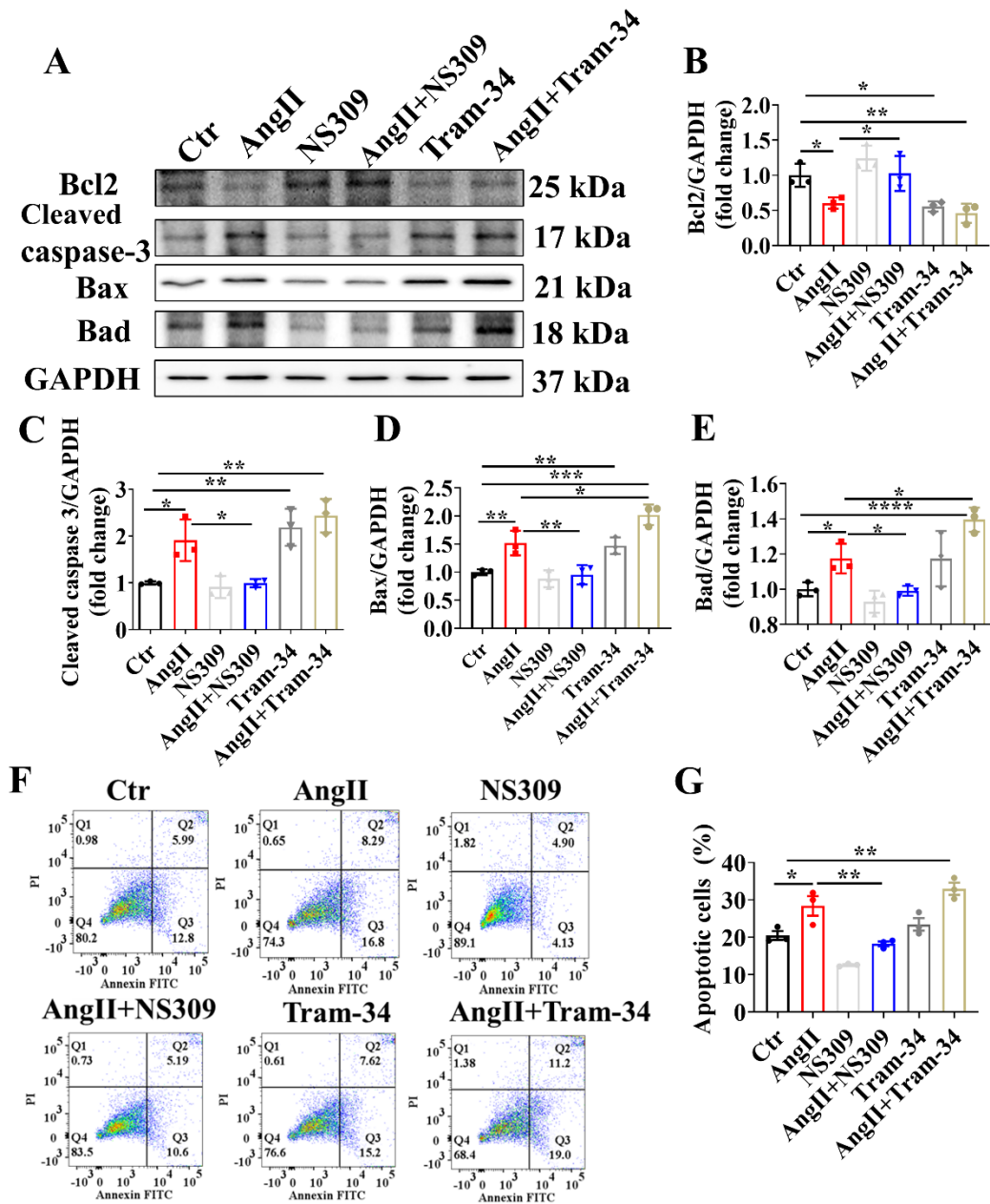


Figure 8. NS309 restored and Tram-34 mimicked Ang II-effects on apoptosis in HCMECs.

HCMECs were treated with vehicle (Ctrl) or 1 μ M angiotensin II (Ang II) for 24 h in the absence or presence of NS309 (1 μ M) or Tram-34 (1 μ M) or NS309 or Tram-34 alone. (A) Representative western blot of each group showing Bcl2, cleaved caspase-3, Bax, and Bad expression in HCMECs. (B) Bcl2 relative protein expression in HCMECs. (C) Relative protein expression level of cleaved caspase-3 in HCMECs. (D) Bax relative protein expression in HCMECs. (E) Bad relative protein expression in HCMECs. All the protein levels shown are normalized to GAPDH. (F-G) Representative (F) and statistical (G) analyses of apoptotic cells by flow cytometry. All data shown

are mean \pm SD for triplicate experiments. * $P < 0.05$, ** $P < 0.01$ determined by one-way ANOVA with Holm-Sidak post-hoc test.

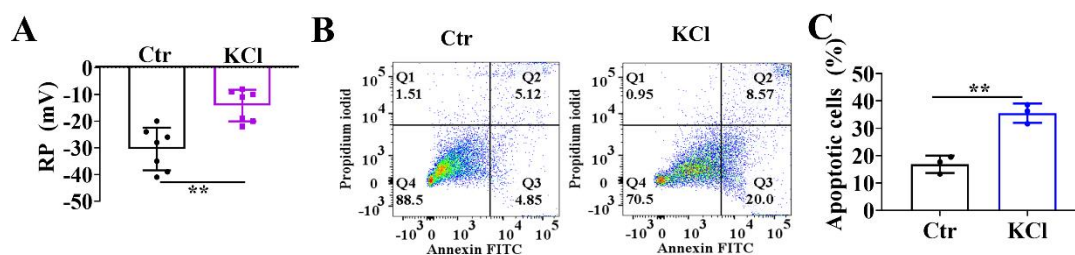


Figure 9. KCl depolarized cell membrane potential and increased cell apoptosis. HCMECs were treated with vehicle (Ctr) or 10 mM KCl for 1 h and then, patch clamp and flow cytometry analyses were performed to evaluate cell membrane potential and apoptosis. **(A)** KCl induced depolarization of cell membrane potential (RP) (n=7 cells). **(B)-(C)** Representative **(B)** and statistical data of flow cytometry analyses showing that KCl increased HCMECs apoptosis (n=3). Data are presented as means \pm SD, * $P < 0.05$, ** $P < 0.01$ determined by unpaired t-test.

4.3 Ang II could regulate membrane potential and SK4 channel function in HCMECs

In order to determine how Ang II could alter endothelial function via SK4 channels, we performed whole cell patch clamp measurements to record cell RP and SK4 channel current. **Figure 10A** showed that Ang II caused a depolarization and Los or PD, significantly restored the depolarization of membrane potential induced by Ang II in HCMECs. Tram-34-sensitive SK4 current (I_{SK4}) was obtained in HCMECs treated by Ang II and Ang II with Los or PD (**Figure 10B**). I_{SK4} density between -80 mV to +50 mV was calculated (**Figure 10C**). The data exhibited that Ang II significantly decreased the I_{SK4} and both Los and PD blocked the effect of Ang II on I_{SK4} (**Figure 10D**). These data indicated that Ang II could regulate the function of SK4 channels through both AT1R and AT2R signaling, and in turn change the RP of HCMECs.

We next conducted qPCR and western blot to further check possible effects of Ang II on the protein and gene level of SK4 channel. The protein expression level of SK4 under the condition of Ang II stimulation for 24 h showed no significant differences

compared with control group (**Figure 10E**), although qPCR results showed a down-regulation of KCNN4 gene expression by Ang II, which could be reversed by Ang II blockers (**Figure 10F**).

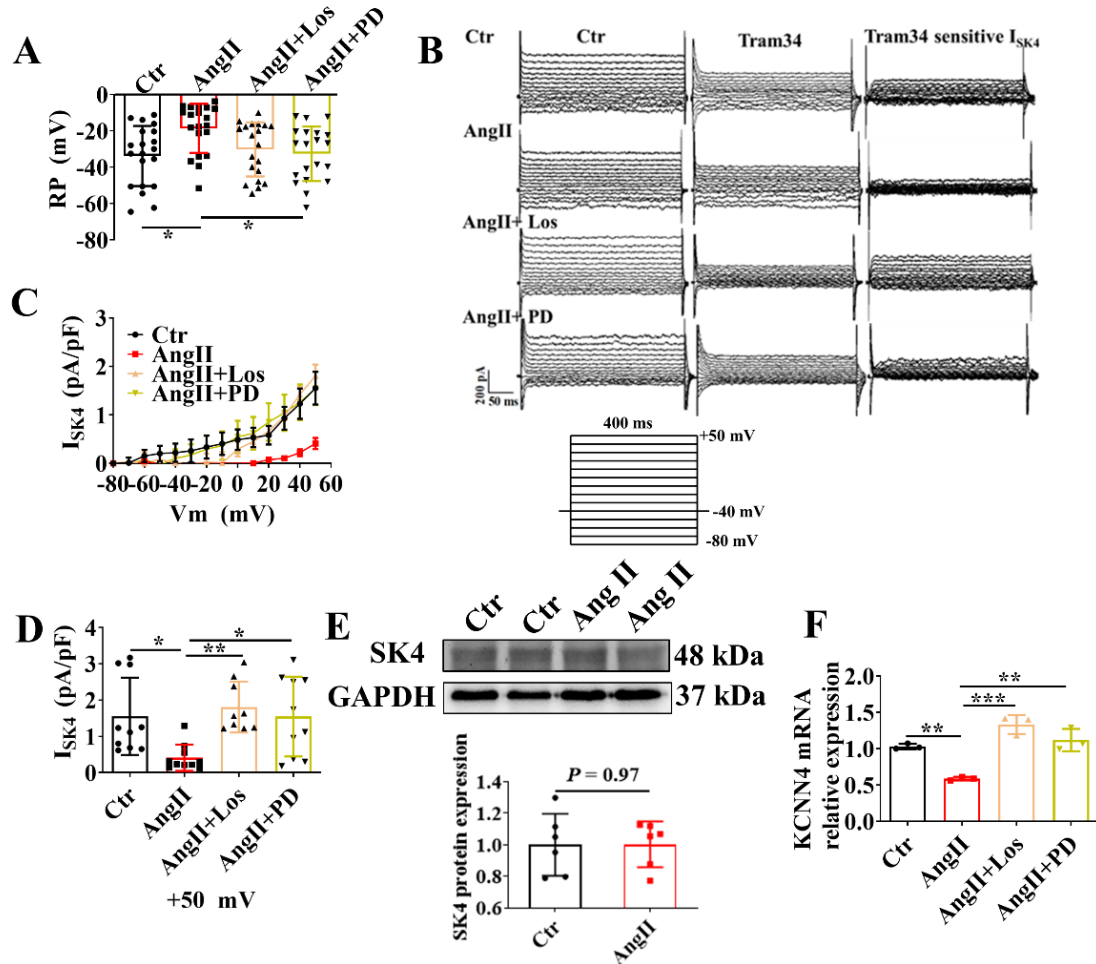


Figure 10. Ang II reduced RP and inhibited SK4 channel currents in HCMECs via PD-sensitive AT2R and Los-sensitive AT1R signaling. HCMECs were treated by vehicle (Ctr) or 1 μ M angiotensin II (Ang II) for 24 h in the absence or presence of losartan (Los, 10 μ M) or PD123319 (PD, 10 μ M). Patch clamp whole-cell recordings were performed to measure cell membrane potential and current. Tram-34 was used to isolate SK4 channel current (I_{SK4}) from other currents. **(A)** Ang II-induced depolarization of membrane potential (RP). **(B)** Representative SK4 channel current traces in HCMECs. **(C)** Current-voltage relationship (I-V) curves of I_{SK4} . **(D)** SK4 current density at +50 mV in indicated groups. **(E)** Representative bands (top panel) and statistical values (bottom panel) of western blot analyses showing SK4 protein expression levels in HCMECs of indicated groups. N=6 replicates. **(F)** The mRNA expression of SK4 channels. N=3 replicates in each group. Data are shown as means \pm SD. * P < 0.05, ** P < 0.01, *** P < 0.001 determined by

one-way ANOVA with Holm-Sidak post-hoc test (A, D, F) or unpaired t-test (E).

4.4 Ang II reduced SK4 channel current via promoting ROS production

Next, to explore the possible mechanisms by which Ang II reduced I_{SK4} , we investigated the effects of Ang II on ROS generation because ROS may mediate endothelial dysfunction. We observed that Ang II induced ROS generation in HCMECs and the effect could be blocked by Ang II blockers (**Figure 11A-B**). Then, we examined the effects of ROS on SK4 channel current. Tram-34-sensitive SK4 current was obtained in the presence of Ang II, H_2O_2 or Ang II plus NAC (**Figure 11C**). The results showed that Ang II inhibited I_{SK4} , and H_2O_2 mimicked Ang II effect on I_{SK4} (**Figure 11D-E**). NAC (ROS blocker) attenuated Ang II effect on I_{SK4} (**Figure 11D-E**). These data demonstrated that ROS was involved in the regulation of SK4 channels by Ang II.

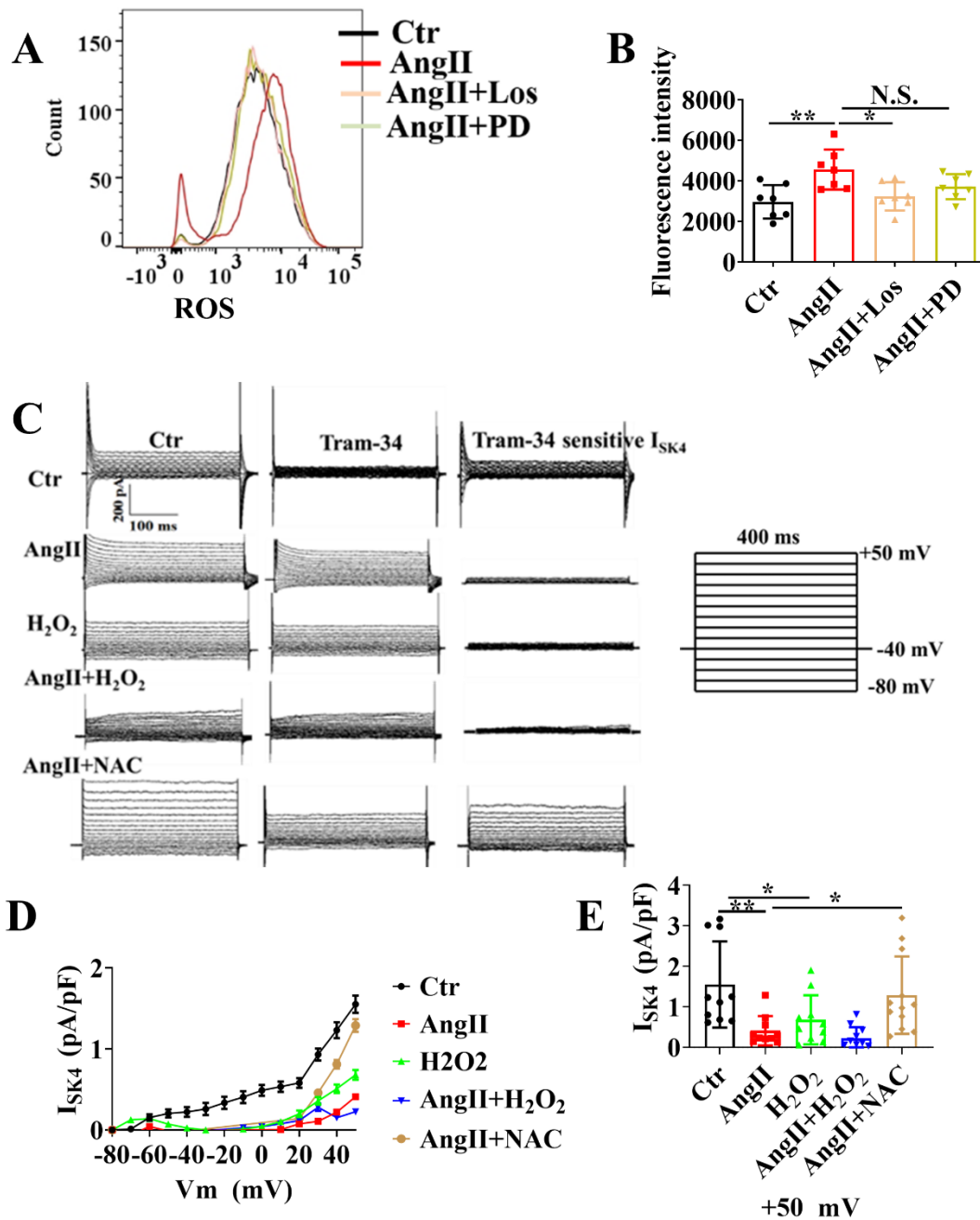


Figure 11. Ang II reduced SK4 channel current by increasing ROS production. HCMECs were treated by vehicle (Ctr) or 1 μ M angiotensin II (Ang II) for 24 h in the absence or presence of losartan (Los, 1 μ M) or PD123319 (PD, 1 μ M) or 100 μ M H_2O_2 or Ang II + H_2O_2 or Ang II+NAC. Flow cytometric analysis was performed to analyze ROS generation. Patch clamp whole-cell recordings were performed to measure SK4 current. Tram-34 was used to isolate SK4 channel current (I_{SK4}) from other currents. **(A)** Representative flow cytometric analysis of ROS in HCMECs treated with Ang II, Ang II plus Los, Ang II plus PD. **(B)** Mean values of ROS levels in HCMECs of indicated groups (n=7 in each group). **(C)** Representative SK4 channel current traces in HCMECs

treated by Ang II, H₂O₂, Ang II plus H₂O₂ and Ang II plus NAC. **(D)** I-V curves of I_{SK4} in indicated groups. **(E)** SK4 current density at +50 mV in indicated groups. Data are shown as means ± SD. Scatter plots show the value of every experiment (B) or measured cells (E). **P* < 0.05, ***P* < 0.01 determined by one-way ANOVA with Holm-Sidak post-hoc test. N.S., no significance.

4.5 Protein kinase A contributed to the effect of Ang II on SK4 channel

To further explore the mechanism by which Ang II affects SK4 channels, we examined PKA signaling. The results showed that Ang II treatment significantly reduced PKA protein expression in HCMECs (**Figure 12A**). Sp-8-Br-Camps, a PKA activator, significantly increased SK4 channel current (**Figure 12B-D**). These data implied that Ang II could inhibit SK4 channel by reducing PKA protein expression.

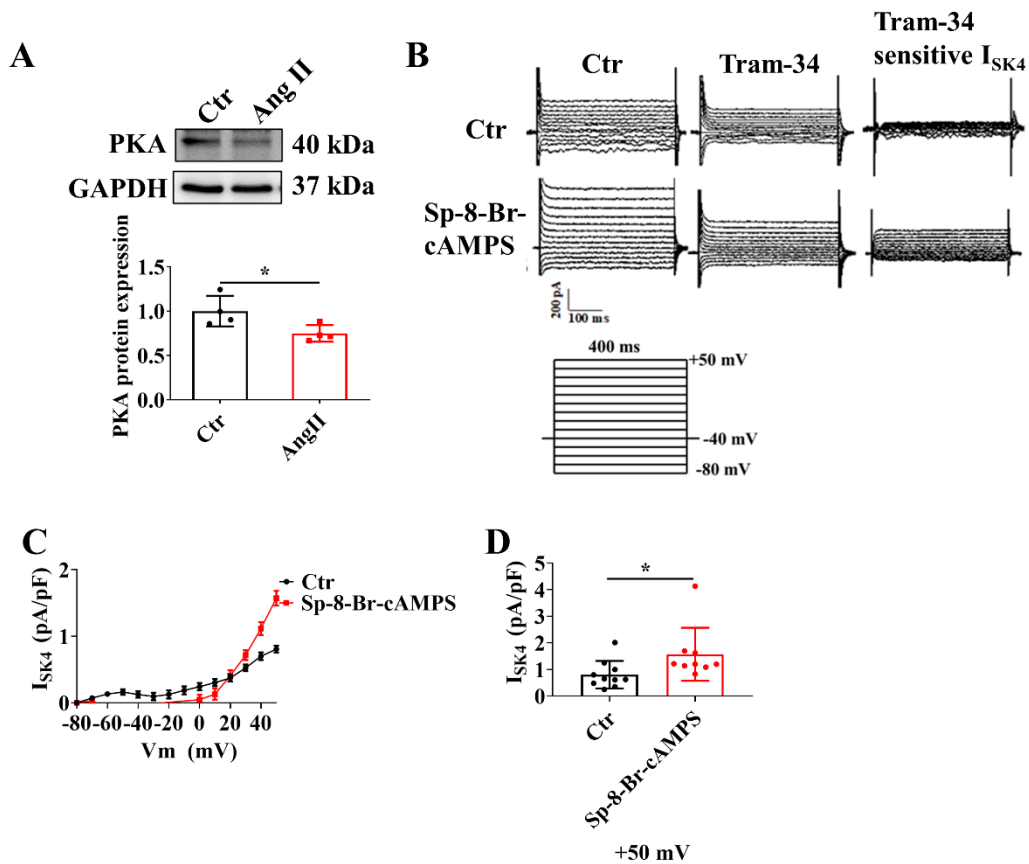


Figure 12. Ang II reduced SK4 channel current by inhibiting PKA expression. HCMECs were treated with vehicle (Ctrl) or 1 μM Ang II or 5 μM Sp-8-Br-cAMP, a PKA activator. Western blot and patch clamp were used to measure protein expression and SK4 channel current. **(A)** Representative bands (top panel) and statistical values (bottom panel) of western blot analyses

showing that Ang II decreased PKA protein expression. n=4 (each group). **(B)** Representative SK4 channel current traces after application of PKA activator Sp-8-Br-cAMP. **(C)** I-V curves of I_{SK4} with and without application of Sp-8-Br-cAMP. **(D)** SK4 current density at + 50 mV between control and Sp-8-Br-cAMP group. n=10 cells (control group), n=9 cells (Sp-8-Br-cAMPs group), * $P < 0.05$ determined by unpaired t-test.

Part II. Catecholamine could induce cardiac ion channel dysfunction through endothelial cell secreted exosomes

4.6 Isolation and characterization of exosomes derived from HCMECs

To explore possible factors secreted by endothelial cells, which may be involved in the pathogenesis of cardiac dysfunction in the setting of catecholamine excess, we purified exosomes from the culture supernatant of HCMECs by serial differential centrifugation plus ultracentrifugation (**Figure 13A**). To characterize endothelial exosomes, the expression of exosome makers was first assessed. Western blot results demonstrated that the widely recognized exosome markers CD9, CD63, and CD81 were highly expressed in our extracted exosomes from HCMECs (**Figure 13B**). However, endoplasmic reticulum (ER) stress-related proteins-GRP94 and Golgi marker GM130 were absent in exosomes but were present in HCMECs, ruling out cellular protein or intracellular debris contamination in exosome preparations (**Figure 13C**). In addition, the NTA demonstrated that the diameter of exosomes derived from HCMECs was around 100 nm (**Figure 13D**). Flow cytometry results confirmed that 97.5% of vesicles were CD9⁺ (**Figure 13E**). These data indicated that the exosome-isolation from HCMECs was successful.

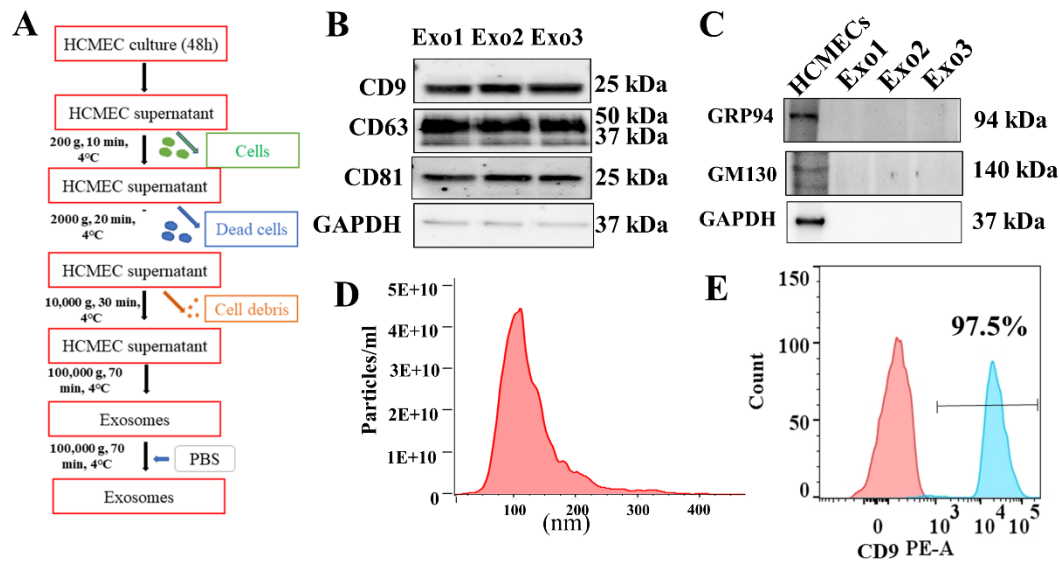


Figure 13. Isolation and characterization of exosomes from HCMEC culture supernatant. (A) Flow chart for obtaining exosomes from HCMECs supernatant by ultracentrifuge. (B) Western blot showing exosomal markers CD9 (~25 kDa), CD63 (between 37 and 50 kDa), and CD81 (~25 kDa) in exosomes (10 μ g lysates) isolated from supernatant of HCMECs of three samples (Exo 1, Exo 2, Exo 3). (C) GRP94 (~94 kDa) and GAPDH (~37 kDa) serve as a negative control and a loading control, respectively. (D) Size distribution of HCMECs-derived exosomes by ZetaView NTA analysis. (E) Percentage of CD9-positive exosomes displayed by flow cytometry.

4.7 Exosomes secreted by endothelial cells can be taken up by hiPSC-CMs

To examine the possibility that exosomes derived from HCMECs can affect cardiomyocytes, we first check the uptake of endothelial exosomes by hiPSC-CMs. hiPSC-CMs were marked with cardiomyocyte marker cTNT and treated with PBS or exosomes or exosomes plus PKH26, which was used to label exosomes. The results showed that exosomes isolated from HCMECs could be taken up by hiPSC-CMs (**Figure 14**), suggesting that exosomes may affect the function of hiPSC-CMs.

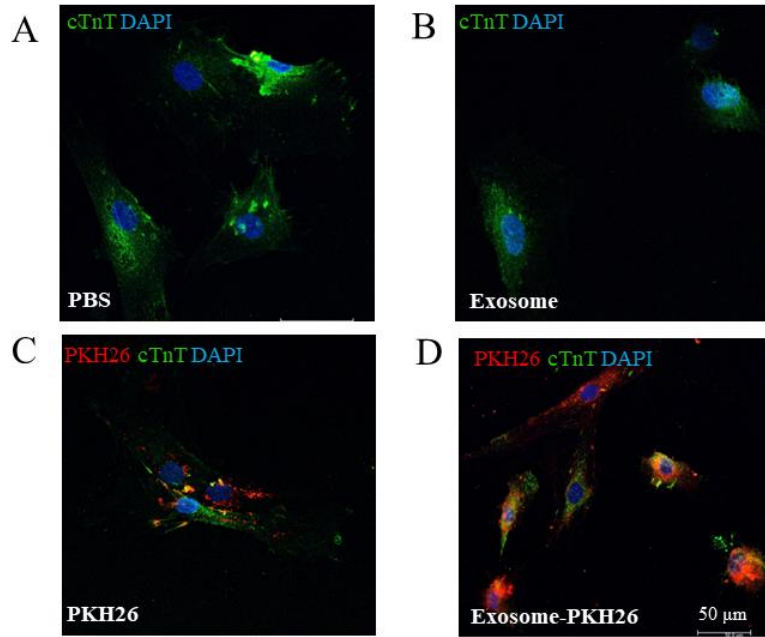


Figure 14. Exosomes secreted by endothelial cells can be taken up by hiPSC-CMs. hiPSC-CMs were labeled with cTnT (green) and exosomes were stained with PKH26 (red). DAPI was used to stain cell nuclei (blue). (A) hiPSC-CMs treated with PBS and stained with cTnT (green). (B) hiPSC-CMs treated with endothelial exosomes (Exo) and stained with cTnT (green). (C) hiPSC-CMs treated with PKH26 and stained with cTnT (green) and PKH26 (red). (D) hiPSC-CMs treated with exosomes that were labeled by PKH26 and stained with cTnT (green) and PKH26 (red) showing that exosomes labeled with PKH26 were taken up by hiPSC-CMs.

4.8 Endothelial cell-derived exosomes changed arrhythmic events induced by epinephrine in hiPSC-CMs

To investigate the effects of exosomes on arrhythmia events in hiPSC-CMs, the occurrence of arrhythmic events (such as irregular or triggered beats or EAD-like events) was assessed in spontaneously beating cells. Intriguingly, high concentration of Epi (500 μ M, 1 h) significantly decreased the beating frequency of hiPSC-CMs and triggered episodes of arrhythmic events such as extra contractions and irregular contractions. Interestingly, exosomes derived from HCMECs without challenge of Epi (Wt-exo) attenuated Epi-effects and exosomes isolated from HCMECs treated with Epi (Epi-exo) mimicked the Epi effect (**Figure 15A-C**). hiPSC-CMs treated with both Epi-exo and Epi further decreased the rate of beating and enhanced irregular contractions

(Figure 15A-C). These data indicated that endothelial exosomes may contribute to Epi-induced arrhythmias.

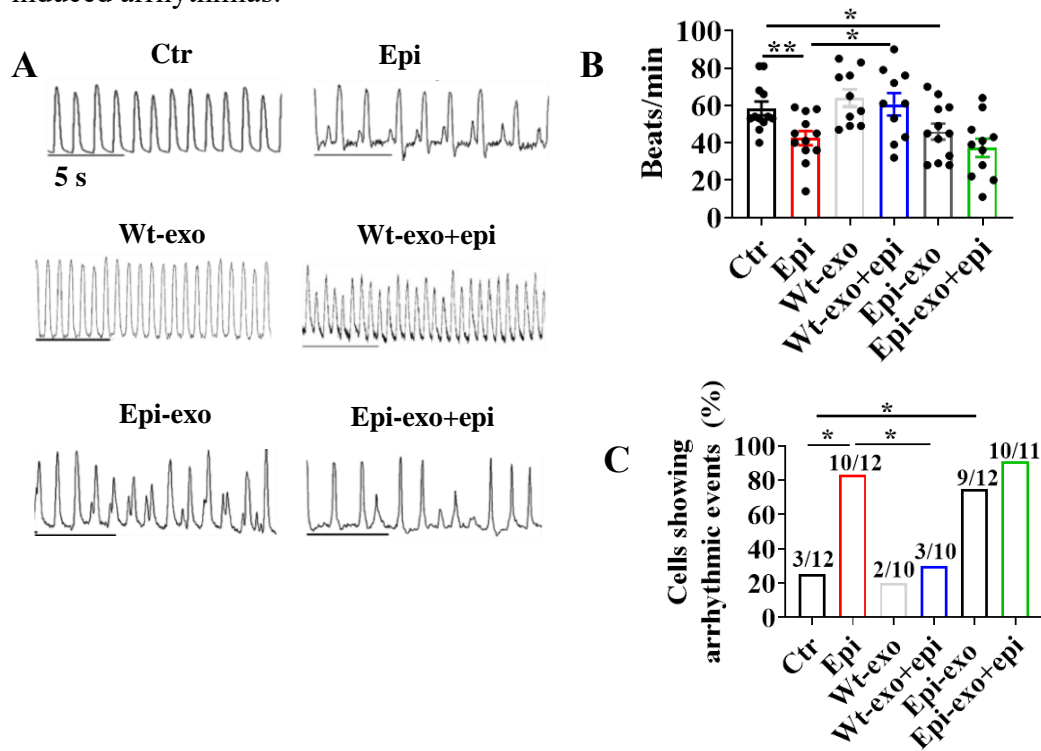


Figure 15. Exosome effects on arrhythmia events in hiPSC-CMs. hiPSC-CMs were treated with either vehicle (Ctr) or 500 μ M epinephrine (Epi), or exosomes from HCMECs without Epi treatment (Wt-exo), or Wt-exo plus epi (Wt-exo+epi), or exosomes secreted by HCMECs treated with Epi (Epi-exo), or Epi-exo plus Epi (Epi-exo+epi), respectively. (A) Representative traces of single-cell contractions in indicated groups. (B) Average values of beating rates of hiPSC-CMs in indicated groups. (C) Percentage of hiPSC-CMs with arrhythmia events in indicated groups. Data are shown as means \pm SD. Scatter plots show the value of every measured cell. Numbers given in C represent number of cells showing arrhythmic event/total number of measured cells. * $P < 0.05$, ** $P < 0.01$, *** $P < 0.001$ determined by one-way ANOVA with Holm-Sidak post-hoc test (B) or Fisher test (C).

4.9 Exosomes contributed to action potential changes induced by epinephrine

To examine the possible mechanisms underlying the occurrence of arrhythmias induced by high concentration of Epi (500 μ M, 1 h) and the contribution of endothelial

exosomes, we investigated the effects of exosomes on action potential in hiPSC-CMs challenged by Epi. The results showed that RP and action potential amplitude (APA) were not affected by Epi, Wt-exo with or without Epi, Epi-exo with or without Epi (**Figure 16A-C**). Epi significantly reduced maximum depolarization velocity (V_{max}) and prolonged action potential duration at 10% repolarization (APD10), action potential duration at 50% repolarization (APD50), and action potential duration at 90% repolarization (APD90), respectively, which were reversed by Wt-exo (**Figure 16A, 16D-G**). Strikingly, we found that Epi-exo alone mimicked the effects of Epi. In the presence of Epi, Epi-exo further decreased V_{max} and further prolonged APD10, APD50, and APD90, respectively (**Figure 16A, 16D-G**). These data indicated that exosomes secreted by HCMECs plays an important role in electrophysiological activities of hiPSC-CMs and can contribute to Epi-induced arrhythmic events via changing APs.

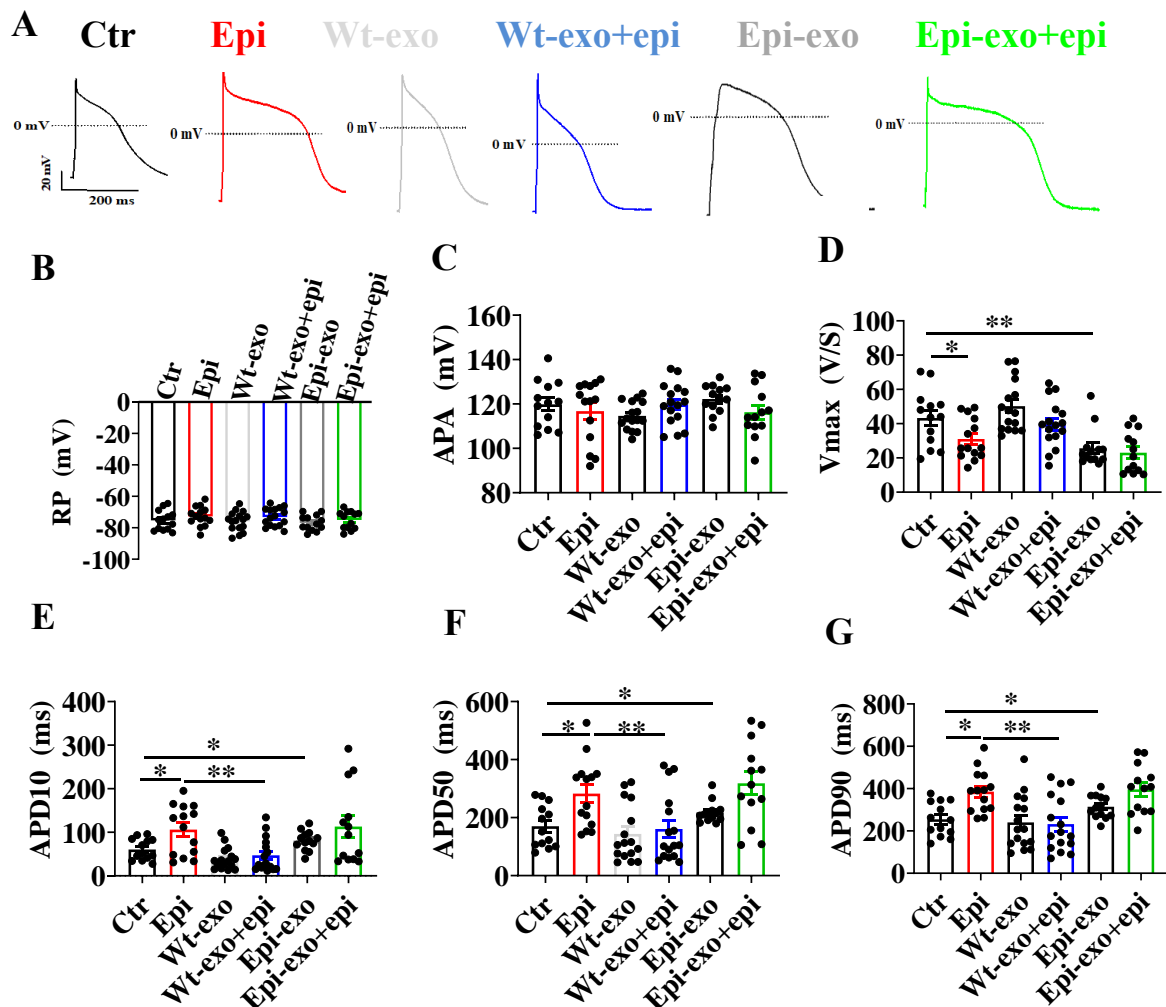


Figure 16. Exosomes derived from HCMECs contributed to action potential changes induced by Epi. hiPSC-CMs were treated with either vehicle (Ctr) or 500 μ M epinephrine (Epi), or exosome from HCMECs without Epi treatment (Wt-exo), or Wt-exo plus Epi (Wt-exo+epi), or exosomes secreted by HCMECs treated with Epi (Epi-exo), or Epi-exo plus Epi (Epi-exo+epi), respectively. Action potential (AP) was measured by patch clamp whole cell recording with pulses of 1 nA for 5 ms at 1 Hz. **(A)** Representative traces of APs in hiPSC-CMs of indicated groups. **(B)** Mean values of cell resting potential (RP) in indicated groups. **(C)** Mean values of action potential amplitude (APA) in indicated groups. **(D)** Mean values of maximal upstroke velocity of action potential (V_{max}) in indicated groups. **(E)** Mean values of APD at 10% repolarization (APD10) in indicated groups. **(F)** Mean values of APD at 50% repolarization (APD50) in indicated groups. **(G)** Mean values of APD at 90% repolarization (APD90) in indicated groups. Data are presented as means \pm SD. Scatter plots show the value of every measured cell. * $P < 0.05$, ** $P < 0.01$, *** $P < 0.001$ determined by one-way ANOVA with Holm-Sidak post-hoc test.

4.10 The ionic mechanisms of action potential changes induced by Epi and exosomes

To investigate the mechanism of action potential changes induced by exosomes in the TTS setting, the expression profile of the main ion channel associated with action potential changes was assessed by carrying out qPCR experiments. The results revealed that Epi significantly increased *CACNA1C* (coding L-type calcium channel), *SCN10A* (coding Nav1.8 sodium channel), and *SLC8A1* (coding $\text{Na}^+/\text{Ca}^{2+}$ -exchanger, NCX) gene expression (**Figure 17A-C**). Exosomes secreted by HCMECs (Wt-exo) reversed Epi-effects (**Figure 17A-C**). Exosomes derived from HCMECs challenged by Epi (Epi-exo) exhibited similar effects as Epi on the gene expression of *CACNA1C*, *SCN10A*, and *SLC8A1* (**Figure 17A-C**). In contrast, Epi clearly reduced gene expression of *SCN5A* (coding sodium channel, Nav1.5), *KCNH2* (coding I_{Kr} , also called HERG channel, Kv11.1) and *KCND3* (coding Ito channel, Kv4.3), which were reversed by Wt-exo (**Figure 17D-F**). Epi-exo showed the same effect as Epi on the gene expression of these three channels. However, Epi or Wt-exo or Epi-exo showed no influence on

KCNQ1 (coding IKs channels, Kv7.1) gene expression of hiPSC-CMs (**Figure 17G**).

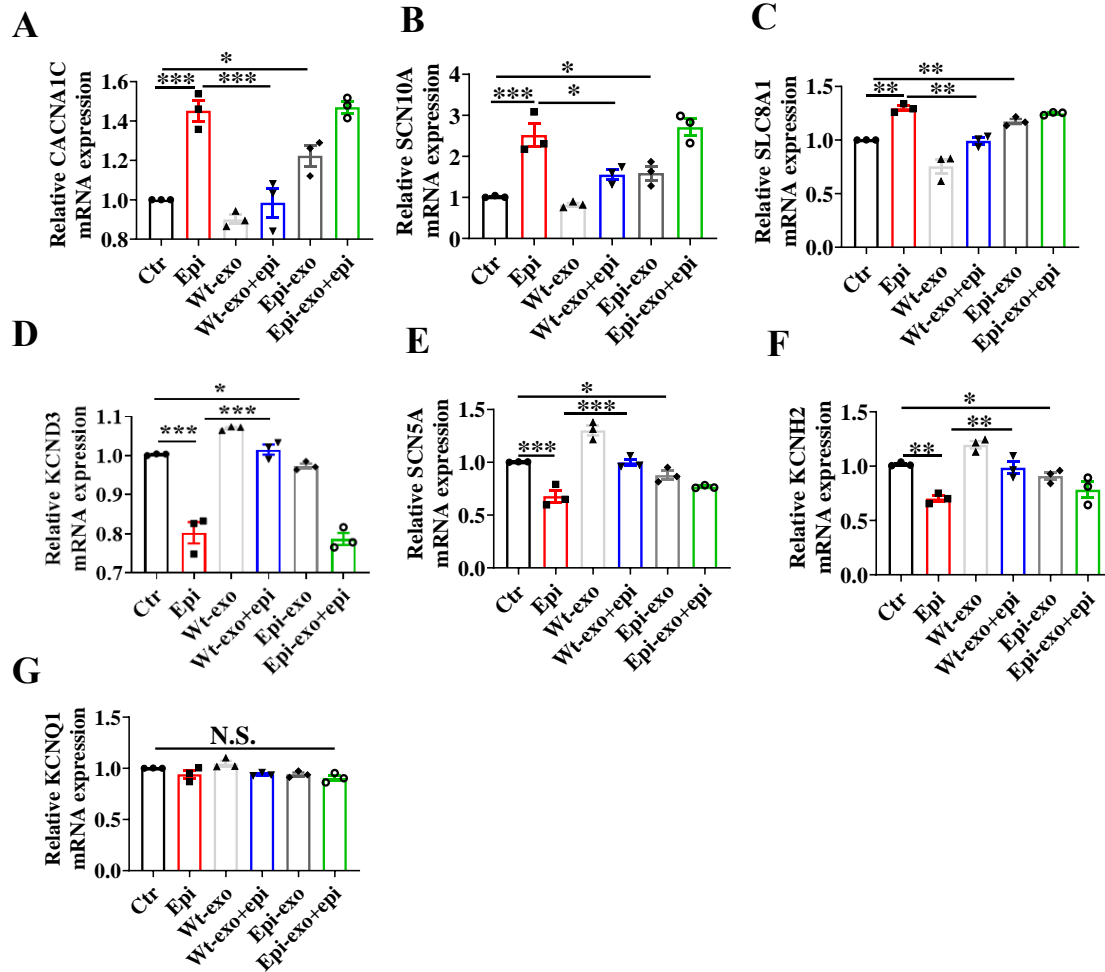


Figure 17. Ion channel gene expression of hiPSC-CMs was affected by exosomes derived from HCMECs. hiPSC-CMs were treated with either vehicle (Ctr) or 500 μ M epinephrine (Epi), or exosomes from HCMECs without Epi treatment (Wt-exo), or Wt-exo plus Epi (Wt-exo+epi), or exosomes secreted by HCMECs treated with Epi (Epi-exo), or Epi-exo plus Epi (Epi-exo+epi), respectively. qPCR analyses were performed to detect gene expression levels of different ion channels. **(A)** Gene expression of CACNA1C in indicated groups. **(B)** Gene expression of SCN10A in indicated groups. **(C)** Gene expression of SLC8A1 in indicated groups. **(D)** Gene expression of KCND3 in indicated groups. **(E)** Gene expression of SCN5A in indicated groups. **(F)** Gene expression of KCNH2 in indicated groups. **(G)** Gene expression of KCNQ1 in indicated groups. Data are presented as means \pm SD. Scatter plots show the value of every experiment. * $P < 0.05$, ** $P < 0.01$, *** $P < 0.001$ determined by one-way ANOVA with Holm-Sidak post-hoc test. N.S., no significance.

Next, we performed voltage clamp experiment to record ion channel currents including I_{Ca-L} , I_{Na} , late Na^+ current (I_{Na-L}), the Na^+/Ca^{2+} exchanger current (I_{NCX}) and several K^+ channel currents such as I_{Kr} , I_{Ks} , and I_{to} in each group of hiPSC-CMs. Wt-exo significantly reduced but Epi-exo mimicked Epi effect on I_{Ca-L} (Figure 18A-C). Epi or Wt-exo or Epi-exo did not influence the activation and inactivation of I_{Ca-L} , evaluated by the potential of 50% activation ($V_{0.5}$) and the potential of 50% inactivation ($V_{0.5}$) (Figure 18D-G). Interestingly, Epi increased the time constant of recovery from inactivation, which was reduced by Wt-exo and mimicked by Epi-exo (Figure 18H-I).

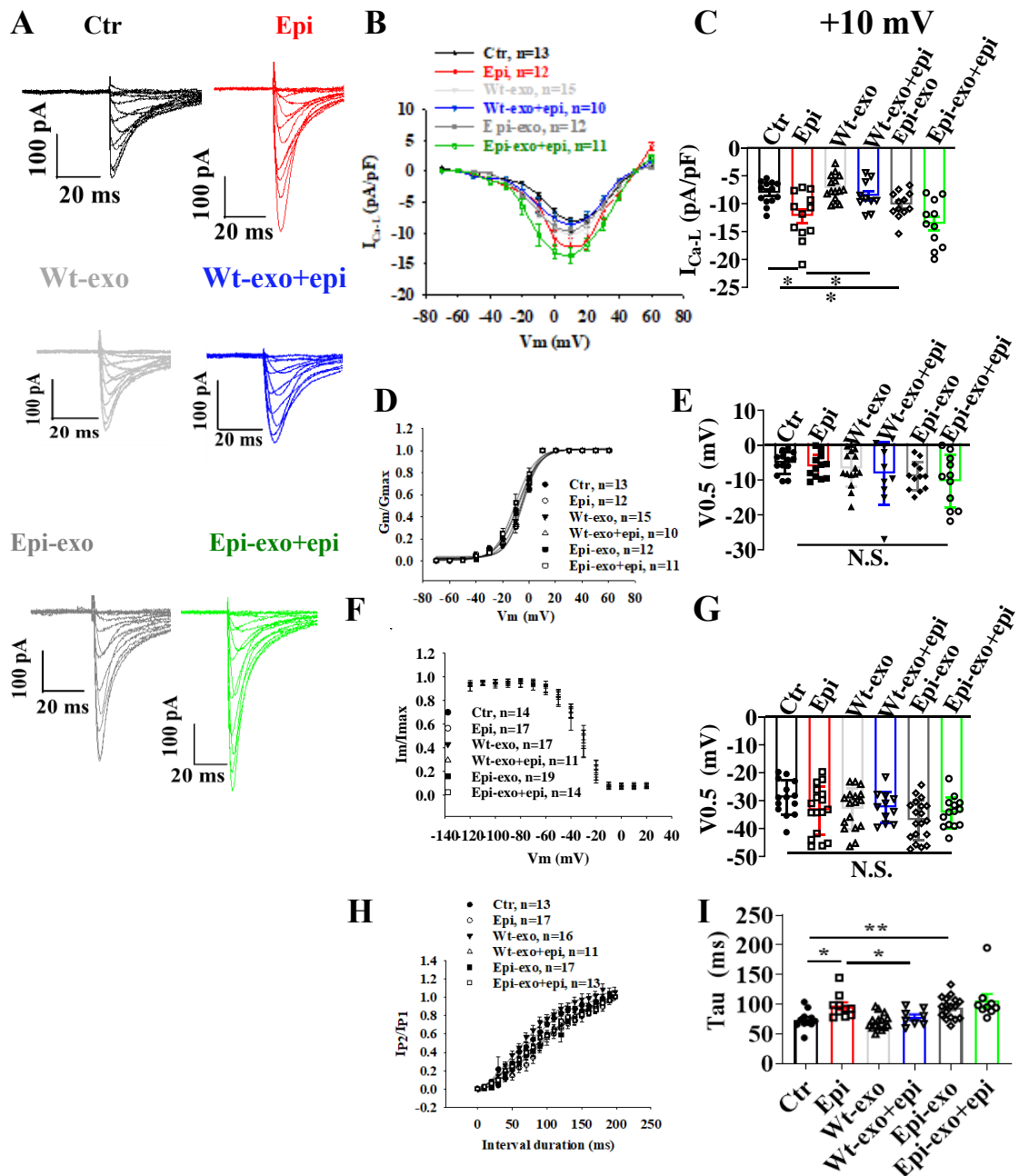


Figure 18. Effects of exosomes derived from HCMECs on the L-type calcium current (I_{Ca-L}) in hiPSC-CMs in the presence of Epi. hiPSC-CMs were treated with either vehicle (Ctr) or 500 μ M epinephrine (Epi), or exosomes from HCMECs without Epi treatment (Wt-exo), or Wt-exo plus Epi (Wt-exo+epi), or Exo secreted by HCMECs treated with Epi (Epi-exo), or Epi-exo plus Epi (Epi-exo+epi), respectively. Patch clamp whole cell recording techniques were used to measure L-type calcium channel current (I_{Ca-L}). **(A)** Representative traces of I_{Ca-L} in indicated groups. **(B)** Current-voltage (I-V) relation curves of I_{Ca-L} in indicated groups. **(C)** Current density of I_{Ca-L} at 10 mV in indicated groups. **(D)** Steady-state activation curves for I_{Ca-L} in indicated groups. **(E)** Mean values of potentials at 50% activation ($V_{0.5}$) in indicated groups. **(F)** Voltage-dependent inactivation of I_{Ca-L} in cells of indicated groups. **(G)** Half-maximal inactivation potential ($V_{0.5}$) in indicated groups. **(H)** Time course curves of recovery from inactivation in indicated groups. **(I)** Time constants (τ) of recovery from inactivation. Data are shown as means \pm SD. Scatter plots show the value of every measured cell. The n-numbers represent the number of measured cells. * $P < 0.05$, ** $P < 0.01$ determined by one-way ANOVA with Holm-Sidak post-hoc test. N.S., no significance.

The peak I_{Na} was reduced by Epi (**Figure 19A-C**). Wt-exo attenuated but Epi-exo mimicked the effects of Epi on peak I_{Na} in hiPSC-CMs (**Figure 19A-C**). Epi-exo+epi caused a significant shift of the steady-state activation curves toward more positive potentials (**Figure 19D**). No significant changes were observed in other biophysical properties of the peak sodium channel such as voltage-dependent inactivation and time dependent recovery from inactivation in hiPSC-CMs of each group (**Figure 19F-I**). Strikingly, I_{Na-L} that was increased by Epi was significantly reduced by Wt-exo and further enhanced by Epi-exo (**Figure 19J**).

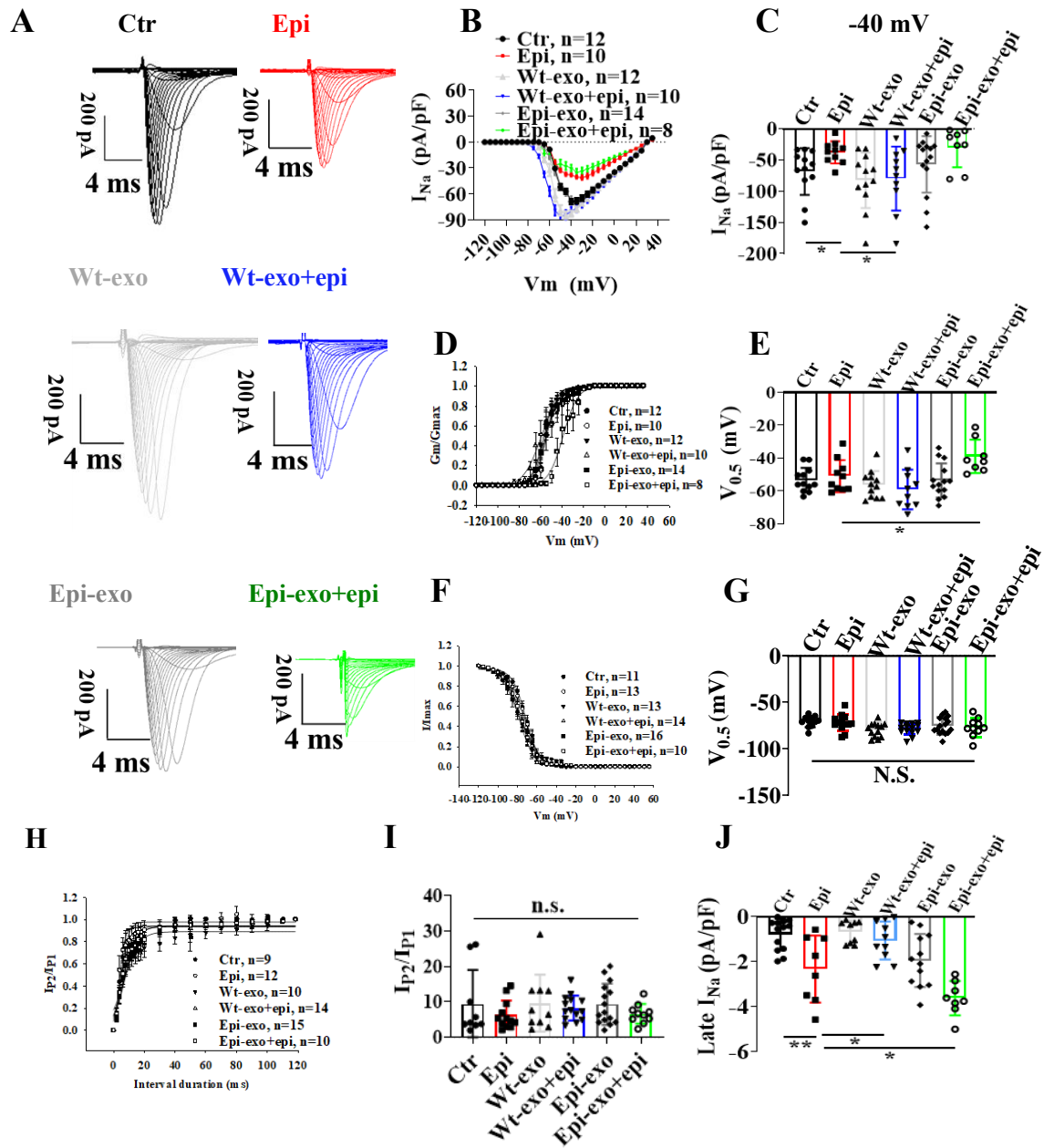


Figure 19. Exosome effects on biophysical properties of sodium channels. hiPSC-CMs were treated with either vehicle (Ctr) or 500 μ M epinephrine (Epi), or exosomes from HCMECs without Epi treatment (Wt-exo), or Wt-exo plus Epi (Wt-exo+epi), or Exo secreted by HCMECs treated with Epi (Epi-exo), or Epi-exo plus Epi (Epi-exo+epi), respectively. Patch clamp whole cell recording techniques were used to measure sodium channel current (I_{Na}). Peak and late I_{Na} as well as the channel gating kinetics including activation, inactivation and recovery from inactivation were analyzed. **(A)** Representative traces of I_{Na} in indicated groups. **(B)** I-V curves of peak I_{Na} in indicated groups. **(C)** Current density of peak I_{Na} at -40 mV in indicated groups. **(D)** Steady-state activation curves of peak I_{Na} in indicated groups. **(E)** Mean values of the half-maximal activation

potential ($V_{0.5}$) in indicated groups. **(F)** Voltage-dependent inactivation curves of peak I_{Na} in indicated groups. **(G)** Mean values of half-maximal inactivation potential ($V_{0.5}$) in indicated groups. **(H)** Time course curves of recovery from inactivation in indicated groups. **(I)** Time constants (τ) of recovery from inactivation in indicated groups. **(J)** Current density of late I_{Na} at -40 mV in indicated groups. The late I_{Na} was the current measured at 200 ms of the pulse. Data are shown as means \pm SD. Scatter plots show the value of every measured cell. The n-numbers represent the number of measured cells. * $P < 0.05$, *** $P < 0.001$ determined by one-way ANOVA with Holm-Sidak post-hoc test. N.S., no significance.

In addition, we checked whether I_{NCX} participated in action potential changes caused by Epi, Wt-exo, or Epi-exo. An increase in I_{NCX} in the presence of Epi in hiPSC-CMs was observed compared with control group at +50 mV and -85 mV (**Figure 20A-C**). Wt-exo restored and Epi-exo simulated the Epi effect on I_{NCX} at +50 mV and -85 mV (**Figure 20A-C**).

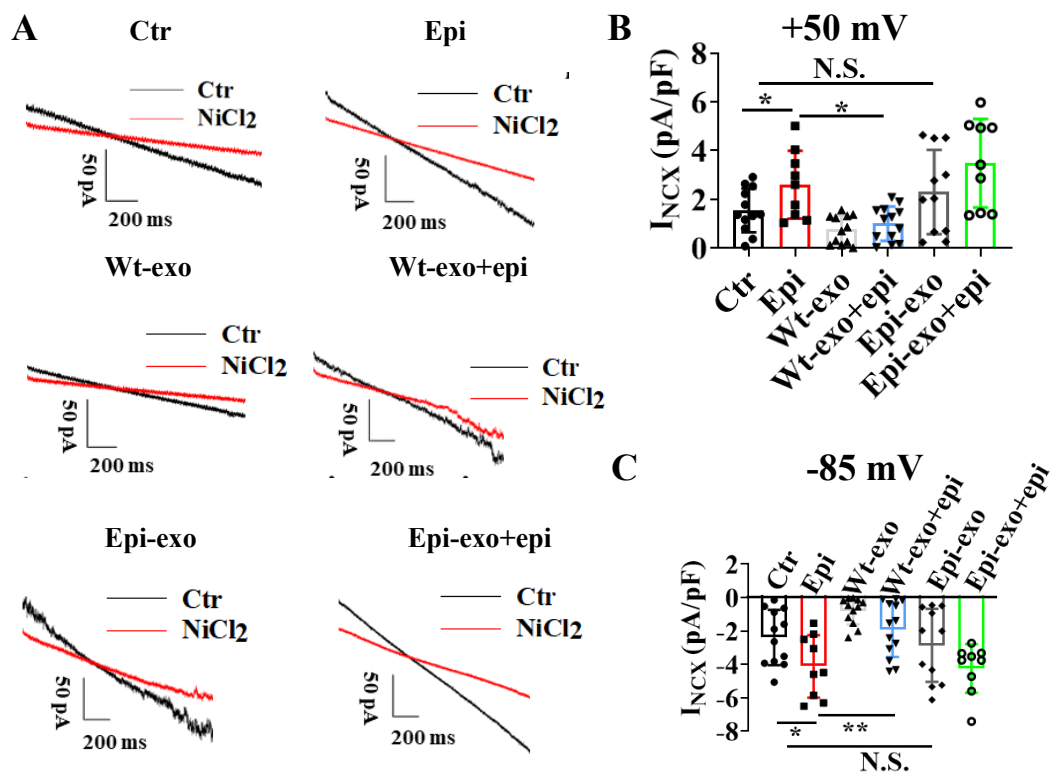


Figure 20. Effects of epinephrine and exosomes on I_{NCX} in hiPSC-CMs. hiPSC-CMs were treated with either vehicle (Ctr) or 500 μ M epinephrine (Epi), or exosomes from HCMECs without

Epi treatment (Wt-exo), or Wt-exo plus Epi (Wt-exo+epi), or Exo secreted by HCMECs treated with Epi (Epi-exo), or Epi-exo plus Epi (Epi-exo+epi), respectively. Patch clamp whole cell recording techniques were used to measure Na/Ca exchanger current (I_{NCX}). **(A)** Representative traces of I_{NCX} before and after application of 10 mM $NiCl_2$, an I_{NCX} blocker, in hiPSC-CMs of indicated groups. **(B)** Current density of I_{NCX} at +50 mV in indicated groups. **(C)** Current density of I_{NCX} at -85 mV in indicated groups. The results are shown as means \pm SD. Scatter plots show the value of every measured cell. * $P < 0.05$, ** $P < 0.01$ determined by one-way ANOVA with Holm-Sidak post-hoc test. N.S., no significance.

Next, we evaluated the effects of Epi, Wt-exo, Epi-exo on K^+ channels. Epi significantly reduced I_{Kr} and I_{to} , which was reversed by Wt-exo secreted by HCMECs (**Figure 21A-C and 22A-C**). Epi-exo mimicked the Epi effects on I_{Kr} and I_{to} , showing reduced I_{Kr} and I_{to} (**Figure 21A-C and 22A-C**). No significant difference was observed between Epi-exo+epi and Epi. I_{Ks} was not significantly influenced by Epi or Wt-exo or Epi-exo (**Figure 23A-C**).

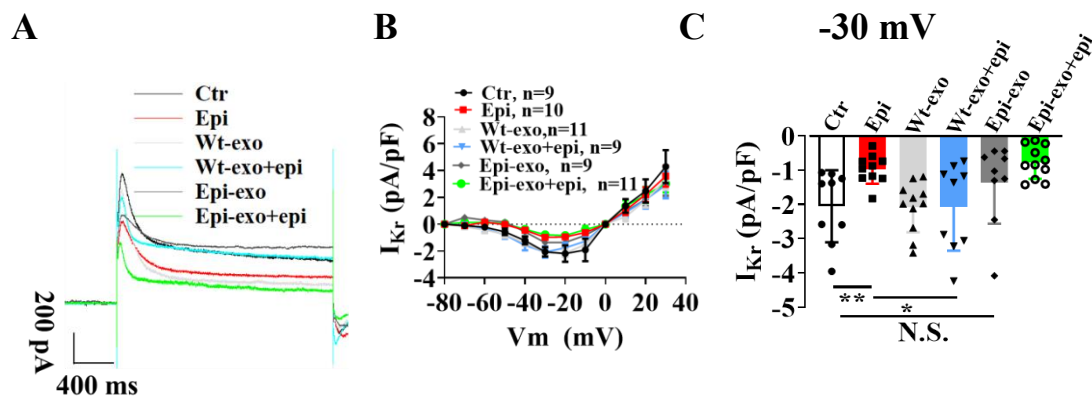


Figure 21. Effects of epinephrine and exosomes on I_{Kr} of hiPSC-CMs. hiPSC-CMs were treated with either vehicle (Ctr) or 500 μ M epinephrine (Epi), or exosomes from HCMECs without Epi treatment (Wt-exo), or Wt-exo plus Epi (Wt-exo+epi), or exosomes secreted by HCMECs treated with Epi (Epi-exo), or Epi-exo plus Epi (Epi-exo+epi), respectively. Patch clamp whole cell recording techniques were used to measure rapidly activating delayed rectifier potassium channel current (I_{Kr}). **(A)** Representative current traces of I_{Kr} at +30 mV in hiPSC-CMs of indicated groups. **(B)** I-V relationship curves of I_{Kr} from -80 mV to +40 mV in indicated groups. **(C)** Current density

of I_{Kr} at -30 mV in indicated groups. The results are shown as means \pm SD. Numbers given in B represent the number of measured cells. Scatter plots (C) show the value of every measured cell. * $P < 0.05$, ** $P < 0.01$ determined by one-way ANOVA with Holm-Sidak post-hoc tests. N.S., no significance.

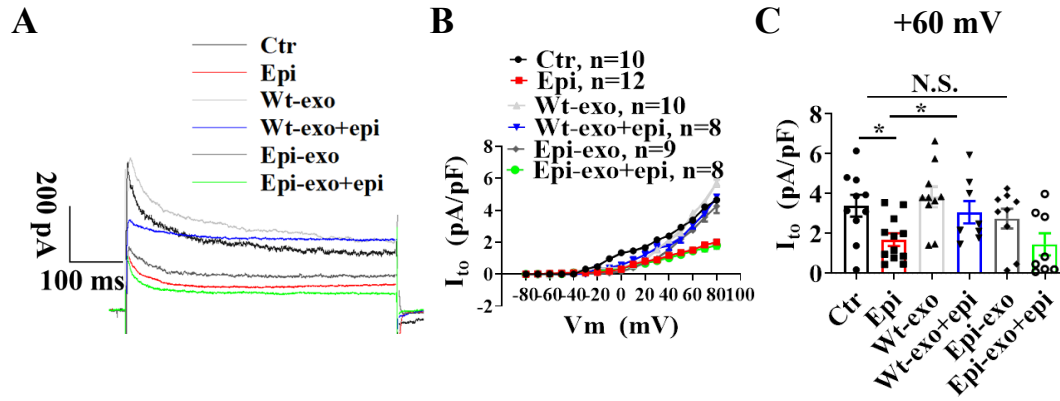


Figure 22. Measurements of I_{to} in hiPSC-CMs treated with epinephrine or exosomes. hiPSC-CMs were treated with either vehicle (Ctr) or 500 μ M epinephrine (Epi), or exosomes from HCMECs without Epi treatment (Wt-exo), or Wt-exo plus Epi (Wt-exo+epi), or exosomes secreted by HCMECs treated with Epi (Epi-exo), or Epi-exo plus Epi (Epi-exo+epi), respectively. Patch clamp whole cell recording techniques were used to measure transient outward potassium current (I_{to}). (A) The raw traces of I_{to} at +60 mV in hiPSC-CMs in indicated groups. (B) I-V curves of 4-AP (I_{to} blocker)-sensitive currents in hiPSC-CMs of indicated groups. (C) Current density of I_{to} at +60 mV in indicated groups. Data are shown as means \pm SD. Numbers given in B represent the number of measured cells. Scatter plots (C) show the value of every measured cell. * $P < 0.05$ determined by one-way ANOVA with Holm-Sidak post-hoc tests. N.S., no significance.

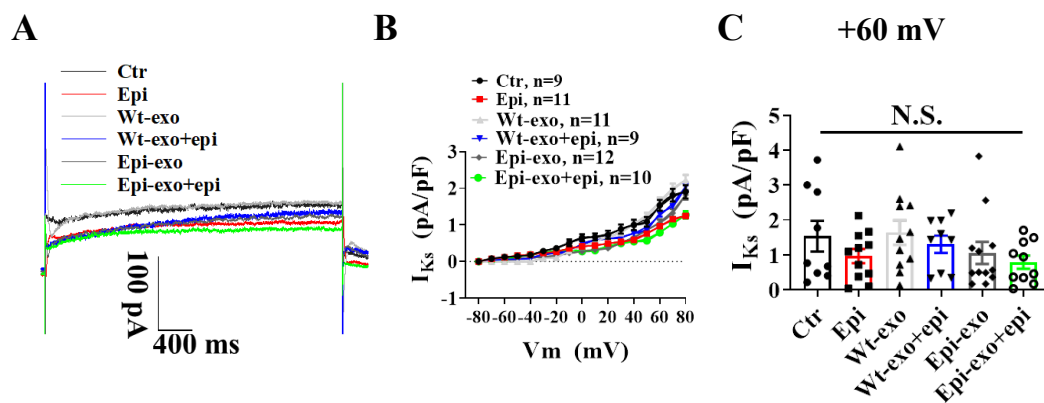


Figure 23. Measurements of I_{Ks} in hiPSC-CMs treated with epinephrine or exosomes. hiPSC-

CMs were treated with either vehicle (Ctr) or 500 μ M epinephrine (Epi), or exosomes from HCMECs without Epi treatment (Wt-exo), or Wt-exo plus Epi (Wt-exo+epi), or exosomes secreted by HCMECs treated with Epi (Epi-exo), or Epi-exo plus Epi (Epi-exo+epi), respectively. Patch clamp whole cell recording techniques were used to measure slowly activating delayed rectifier potassium channel current (I_{Ks}). **(A)** The raw traces of I_{Ks} at +60 mV in hiPSC-CMs in indicated groups. **(B)** I-V curves of I_{Ks} from -80 mV to +80 mV in hiPSC-CMs of indicated groups. **(C)** Current density of I_{Ks} at +60 mV in indicated groups. Data are shown as means \pm SD. Numbers given in B represent the number of measured cells. Scatter plots (C) show the value of every measured cell. N.S., no significance.

4.11 miR-126-3p was involved in the effects of endothelial exosomes

Since our results revealed that exosomes derived from HCMECs with or without Epi challenge could differentially influence Epi-induced ion channel dysfunction and arrhythmias in cardiomyocytes, we assumed that the Epi-challenge of HCMECs changed components of exosomes. We next studied in more detail which component of exosomes secreted by endothelial cells modulated the function of cardiomyocytes. Some studies proved that miR-16, miR-26a, miR-133a are related to TTS [157,158]. Further, miR-126-3p, one of the most important endothelial cell-restricted miRNAs, was shown to modulate vascular integrity and developmental angiogenesis [116,117]. Therefore, we measured the expression of miR-16, miR-26a, miR-133a and miR-126-3p in exosomes derived from HCMECs treated with vehicle or Epi. Consequently, we observed that miR-16, miR-26a and miR-133a were upregulated in exosomes derived from HCMECs treated with Epi (**Figure 24A-D**), consistent with previously reported data showing increased levels of those three miRNAs in the blood of TTS patients. Interestingly, the expression of miR-126-3p in exosomes derived from HCMECs treated with 500 μ M Epi was also increased compared with control group (**Figure 24D**), indicating that miR-126-3p may play an important role in the pathophysiology of TTS. Moreover, we found that exosomes secreted from HCMECs treated with Epi increased the expression of miR-126-3p in hiPSC-CMs compared with control group (**Figure**

24E). Considering that roles of miR-126-3p in TTS have not been reported, we focused on it in the subsequent assessments.

To study the effects of miR-126-3p in exosomes on hiPSC-CMs, we tried to increase and decrease miR-126-3p in exosomes using its mimic and inhibitor. We transfected miR-126-3p-mimic, miR-126-3p-inhibitor or miR-126-3p-NC (negative control) into HCMECs to measure the expression of miR-126-3p in cells and exosomes. miR-126-3p-mimic increased the expression of miR-126-3p in exosomes derived from HCMECs (**Figure 24F**) and also in HCMECs (**Figure 24G**) compared with control (vehicle) group. Accordingly, miR-126-3p-inhibitor reduced the expression of miR-126-3p in exosomes (**Figure 24F**) and HCMECs (**Figure 24G**) compared with control group. There was no significant difference in the expression of miR-126-3p in exosomes and HCMECs between the miR-126-3p-NC group and control group (**Figure 24F-G**). After hiPSC-CMs were treated with exosomes derived from HCMECs transfected with miR-126-3p mimic (Exo-mimic), miR-126-3p inhibitor (Exo-inhibitor), miR-126-3p negative control (Exo-NC), we observed that Exo-mimic increased miR-126-3p expression in hiPSC-CMs compared with control group, whereas Exo-inhibitor decreased miR-126-3p expression in hiPSC-CMs compared with control group (**Figure 24H**). These data suggested that Epi-induced increase in miR-126-3p could be involved in the observed effects of endothelial exosomes on ion channels in hiPSC-CMs.

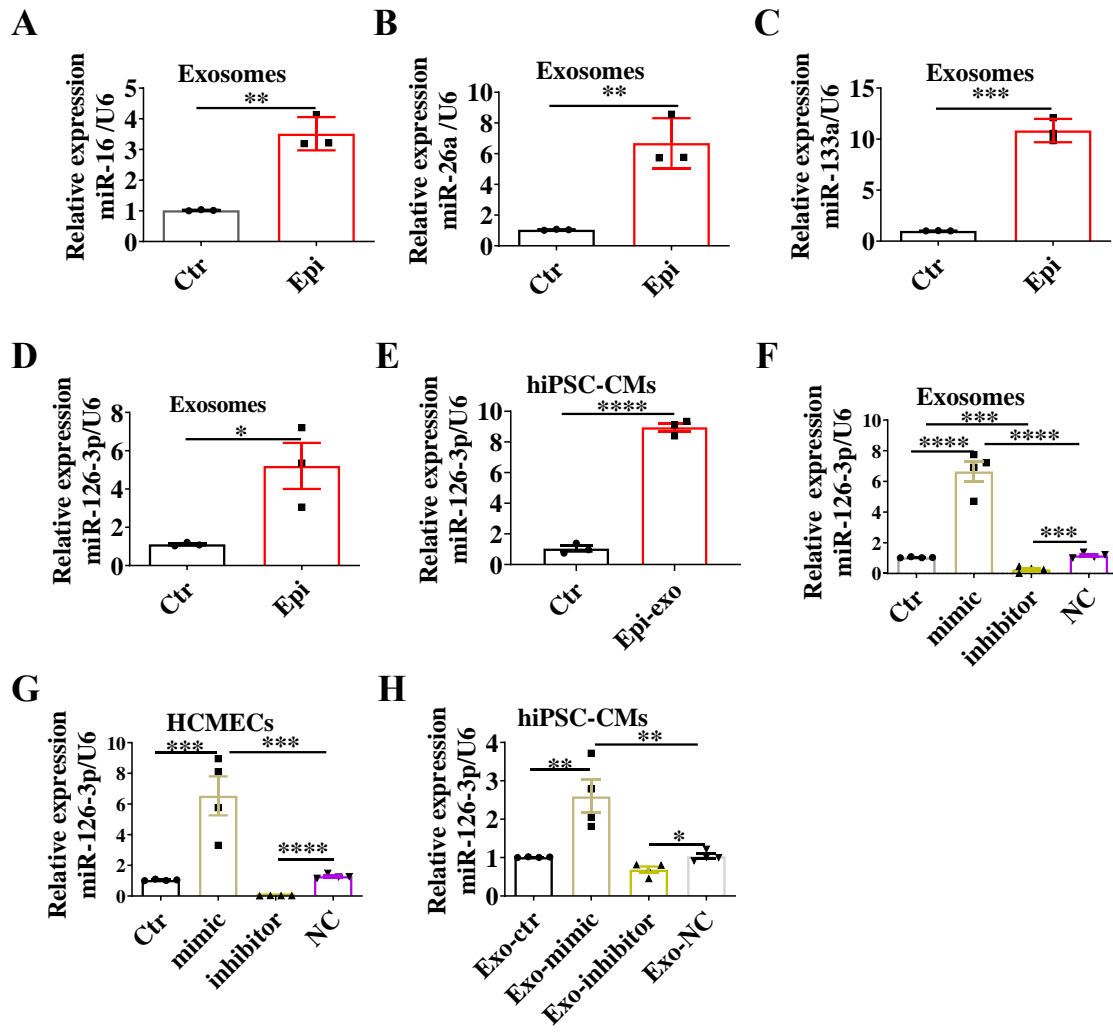


Figure 24. Changes of miRNAs in HCMECs or hiPSC-CMs treated with epinephrine, miR-126-3p activator and inhibitor. HCMECs were treated with vehicle (Ctr) or 500 μ M epinephrine (Epi) and different miRNAs were measured in exosomes. Then, HCMECs were transfected with vehicle (Ctr) or miR-126-3p mimic (mimic) or miR-126-3p inhibitor (inhibitor) or miR-126-3p negative control (NC), respectively. Exosomes (Exo) were isolated from HCMECs of each group (Exo-ctr, Exo-mimic, Exo-inhibitor and Exo-NC) and applied to hiPSC-CMs. **(A)** Epi increased the expression of miR-16 in Exo from HCMECs. **(B)** Epi increased the expression of miR-26a in Exo from HCMECs. **(C)** Epi increased the expression of miR-133a in Exo from HCMECs. **(D)** Epi increased the expression of miR-126-3p in Exo from HCMECs. **(E)** The expression of miR-126-3p in hiPSC-CMs treated with Exo derived from HCMECs pretreated by Epi (Epi-exo). **(F)** The expression of miR-126-3p in Exo derived from HCMECs transfected with miR-126-3p mimic, miR-126-3p inhibitor, miR-126-3p NC. **(G)** The expression of miR-126-3p in HCMECs transfected with miR-126-3p mimic, miR-126-3p inhibitor or miR-126-3p NC. **(H)** The expression of miR-126-3p

in hiPSC-CMs treated with Exo-ctr, Exo-mimic, Exo-inhibitor, Exo-NC. Data are presented as means \pm SD. Scatter plots show the value of every experiment. * $P < 0.05$, ** $P < 0.01$, *** $P < 0.001$, **** $P < 0.0001$ determined by unpaired t-test (A-E) or one-way ANOVA with Holm-Sidak post-hoc test (F-H).

To investigate if miR-126-3p in exosomes derived from HCMECs play a key role in modulating the electrophysiological properties of hiPSC-CMs in the setting of TTS, we also carried out current clamp experiment to record the AP of hiPSC-CMs treated with Exo-mimic (exosomes overexpressing miR-126-3p) or Exo-inhibitor (exosomes with low level of miR-126-3p) in the presence and absence of Epi. The results showed no significant effects of Epi and Exo-mimic on RP and APA (Figure 25A-C). Interestingly, the Exo-mimic but not Exo-inhibitor mimicked Epi-effects on Vmax, APD50 and APD90 (Figure 25A, 25D, 25F-G). These data indicated that miRNA-126-3p could contribute to effects of Epi on electrophysiological properties of hiPSC-CMs.

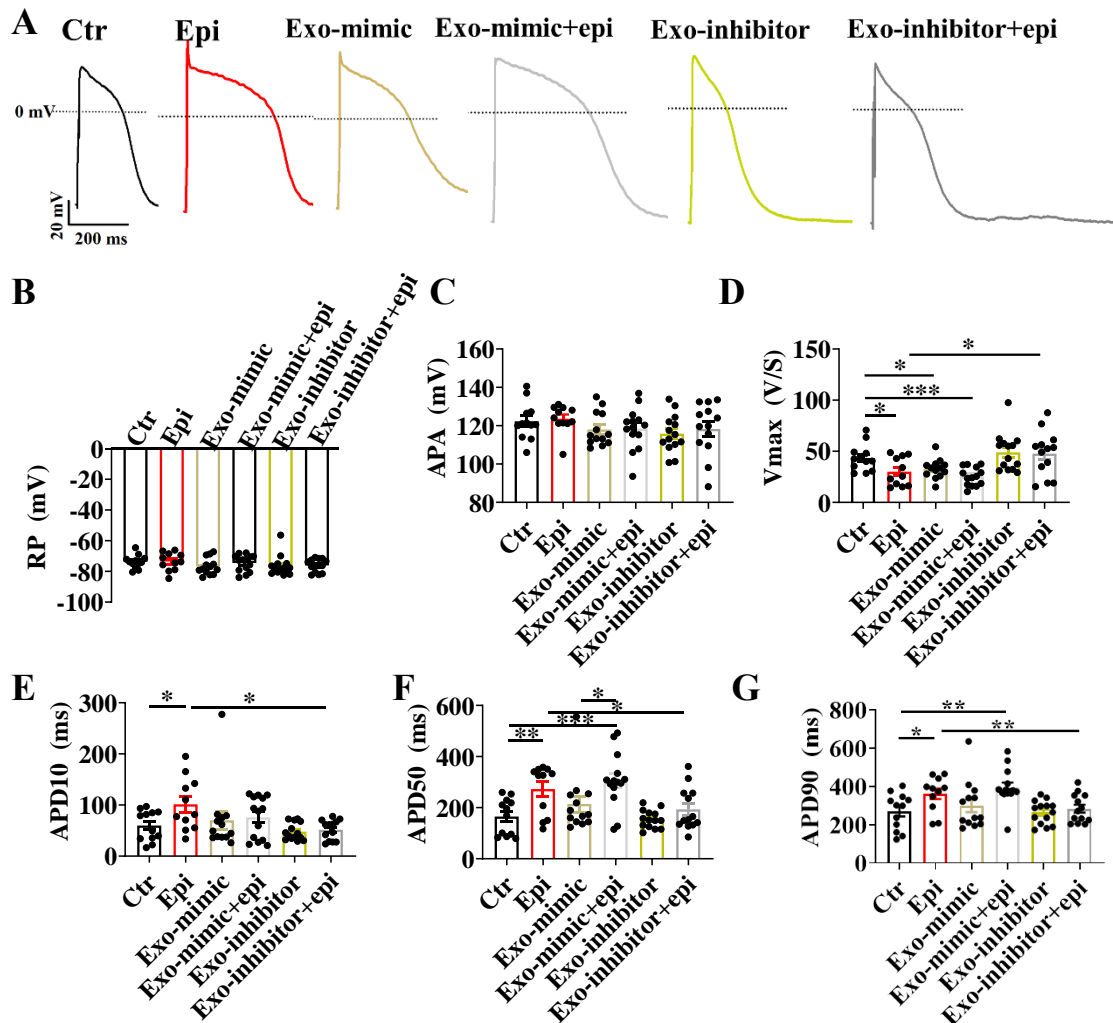


Figure 25. Exosomes secreted by endothelial cells overexpressing miR-126-3p mimicked the effects of epinephrine on action potential of hiPSC-CMs. hiPSC-CMs were treated with vehicle (Ctr) or 500 μ M epinephrine (Epi) or exosomes from HCMECs transfected by miR-126-3p mimic (Exo-mimic), or Exo-mimic plus Epi (Exo-mimic+epi), or exosomes from HCMECs transfected with miR-126-3p inhibitor (Exo-inhibitor), or Exo-miR-126-3p inhibitor plus Epi (Exo-inhibitor+epi), respectively. Patch clamp whole cell recording techniques were used to measure action potentials (AP). **(A)** Representative traces of AP recorded in hiPSC-CMs in indicated groups. **(B)** Mean values of resting potential (RP) in indicated groups. **(C)** Mean values of amplitude of action potential (APA) in indicated groups. **(D)** Mean values of maximal depolarization velocity (V_{max}) in indicated groups. **(E)** Mean values of action potential duration at 10% repolarization (APD10) in indicated groups. **(F)** Mean values of action potential duration at 50% repolarization (APD50) in indicated groups. **(G)** Mean values of action potential duration at 90% repolarization (APD90) in indicated groups. Data are presented as means \pm SD. Scatter plots show the value of every measured cell. * $P < 0.05$, ** $P < 0.01$, *** $P < 0.001$ determined by one-way ANOVA with Holm-Sidak post-hoc test.

4.12 Exosomes secreted by endothelial cells overexpressing miR-126-3p increased arrhythmia-like events of hiPSC-CMs

Since exosomes secreted by HCMECs overexpressing miR-126-3p (Exo-mimic) prolonged the APD, we performed calcium transient experiments to detect the arrhythmia-like events of hiPSC-CMs treated with Epi (500 μ M, 1 h), Exo-mimic or Exo-inhibitor in the presence and absence of Epi. In spontaneously beating hiPSC-CMs, Exo-mimic not only mimicked but also further significantly enhanced Epi-effects on beating intervals and the occurrence of arrhythmia-like events in hiPSC-CMs (**Figure 26A-C**). Exo-inhibitor significantly reduced Epi-effects (**Figure 26A-C**). These data suggested that exosomes derived from endothelial cells could induce arrhythmia events via miR-126-3p.

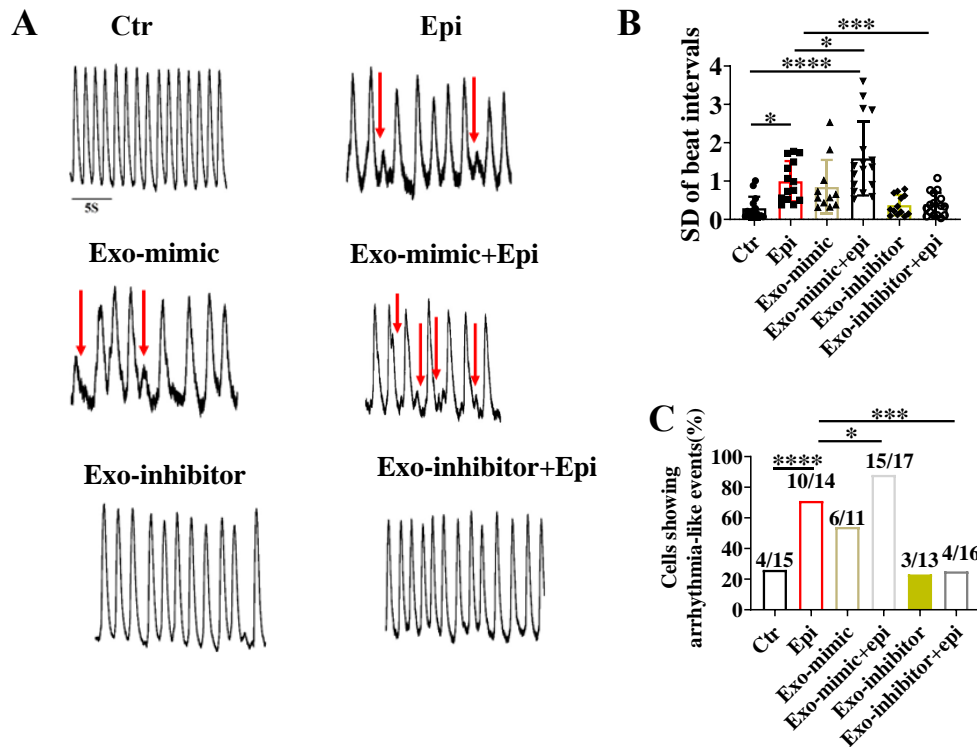


Figure 26. Exosomes derived from HCMECs could induce arrhythmia events of hiPSC-CMs via miR-126-3p. hiPSC-CMs were treated with vehicle (Ctr) or 500 μ M epinephrine (Epi) or exosomes from HCMECs transfected with miR-126-3p mimic (Exo-mimic), or Exo-miR-126-3p mimic plus Epi (Exo-mimic+epi), or exosomes from HCMECs transfected with miR-126-3p inhibitor (Exo-inhibitor), or Exo-miR-126-3p inhibitor plus Epi (Exo-inhibitor+epi), respectively. **(A)** Calcium transient traces obtained in spontaneously beating hiPS-CMs of indicated groups. Arrows indicate EAD- or DAD-like events. **(B)** Standard deviation (SD) of beat intervals in indicated groups. **(C)** The percentage of hiPSC-CMs showing arrhythmia events in indicated groups. Scatter plots show the value of every measured cell. Numbers given in C represent number of cells showing arrhythmic events/total number of measured cells. * $P < 0.05$, ** $P < 0.01$, *** $P < 0.001$, **** $P < 0.0001$ determined by one-way ANOVA with Holm-Sidak post-hoc test (B) or Fisher-test (C).

Next, we evaluated the effects of exosomes derived from HCMECs overexpressing miR-126-3p on single cell contractions of hiPSC-CMs. In spontaneously beating hiPSC-CMs, Exo-mimic further reduced beat frequency, increased the numbers of hiPSC-CMs showing arrhythmia events, increased SD of beat intervals of hiPSC-CMs (**Figure 27A-D**). By contrary, Exo-inhibitor significantly improved beats of hiPSC-

CMs, reduced Epi-induced arrhythmia events in hiPSC-CMs, and reduced SD of beat intervals (**Figure 27A-D**). The results in single cell contraction measurements are similar to the abovementioned results in calcium transient measurements, confirming that exosomes secreted by endothelial cells can alter the beat rhythm of cardiomyocytes via miR-126-3p.

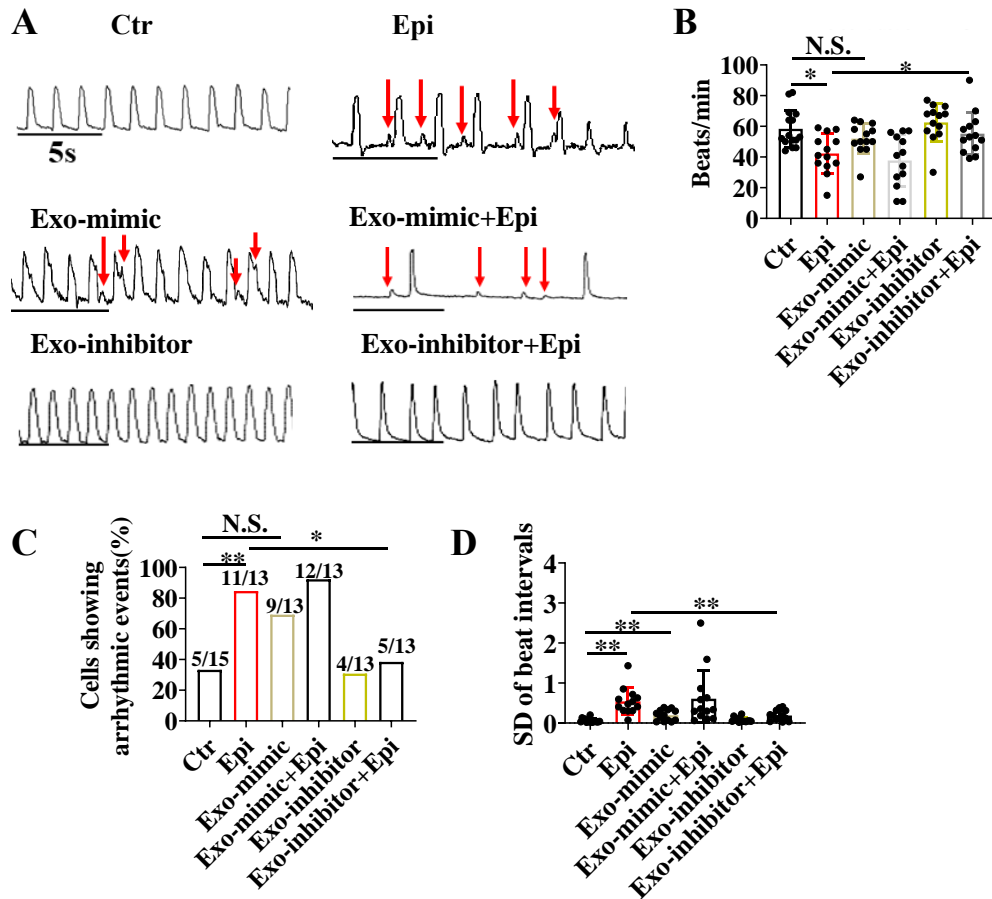


Figure 27. Effects of exosomes overexpressing miR-126-3p on single cell contractions of hiPSC-CMs. hiPSC-CMs were treated with vehicle (Ctr) or 500 μ M epinephrine (Epi) or exosomes from HCMECs transfected by miR-126-3p mimic (Exo-mimic), or Exo-miR-126-3p mimic plus Epi (Exo-mimic+epi), or exosomes from HCMECs transfected by miR-126-3p inhibitor (Exo-inhibitor), or Exo-miR-126-3p inhibitor plus Epi (Exo-inhibitor+epi), respectively. Single cell contraction measurements were performed. **(A)** Contraction traces of single hiPSC-CMs in indicated groups. Arrows indicate EAD- or DAD-like events. **(B)** The effects of Exo derived from HCMECs transfected with miR-126-3p mimic or inhibitor on beat frequency. **(C)** The percentage

of hiPSC-CMs showing arrhythmia events. **(D)** SD of beat intervals in indicated groups. Results are presented as means \pm SD. Scatter plots show the value of every measured cell. Numbers given in C represent number of cells showing arrhythmic events/total number of measured cells. * $P < 0.05$, ** $P < 0.01$, *** $P < 0.001$ determined by one-way ANOVA with Holm-Sidak post-hoc test (B, D) or Fisher-test (C). N.S., no significance.

4.13 The endothelial exosome overexpressing miR-126-3p affected ion channel expression in hiPSC-CMs

To investigate the mechanisms by which exosomes derived from HCMECs transfected with miR-126-3p affected the AP and arrhythmia events, we measured the mRNA expression of ion channels which are related to the alteration of action potential of hiPSC-CMs. Exo-mimic increased CACNA1C, SCN10A, and SLC8A1 mRNA levels compared with exosomes derived from HCMECs without transfection (Exo-ctr) or transfected with Exo-NC, while exosomes secreted by HCMECs transfected with miR-126-3p inhibitor (Exo-inhibitor) reduced the mRNA expression of CACNA1C, SCN10A, and SLC8A1 compared with Exo-ctr and Exo-NC (**Figure 28A-C**). The mRNA expression levels of SCN5A, KCND3, KCNH2, and KCNQ1 were decreased by Exo-mimic compared with Exo-ctr and Exo-NC (**Figure 28D-F**). But there was no significant difference in gene expression of KCNQ1 among Exo-ctr, Exo-mimic, Exo-inhibitor, Exo-NC groups. The detected changes of ion channel expression levels in hiPSC-CMs caused by exosomes overexpressing miR-126-3p are consistent with changes of ion channel expression (**Figure 17**) and currents (**Figure 18-23**) caused by exosomes from HCMECs challenged by Epi (Epi-exo). Thus, miR-126-3p probably mediated the observed effects of endothelial exosomes on the ion channel function in hiPSC-CMs.

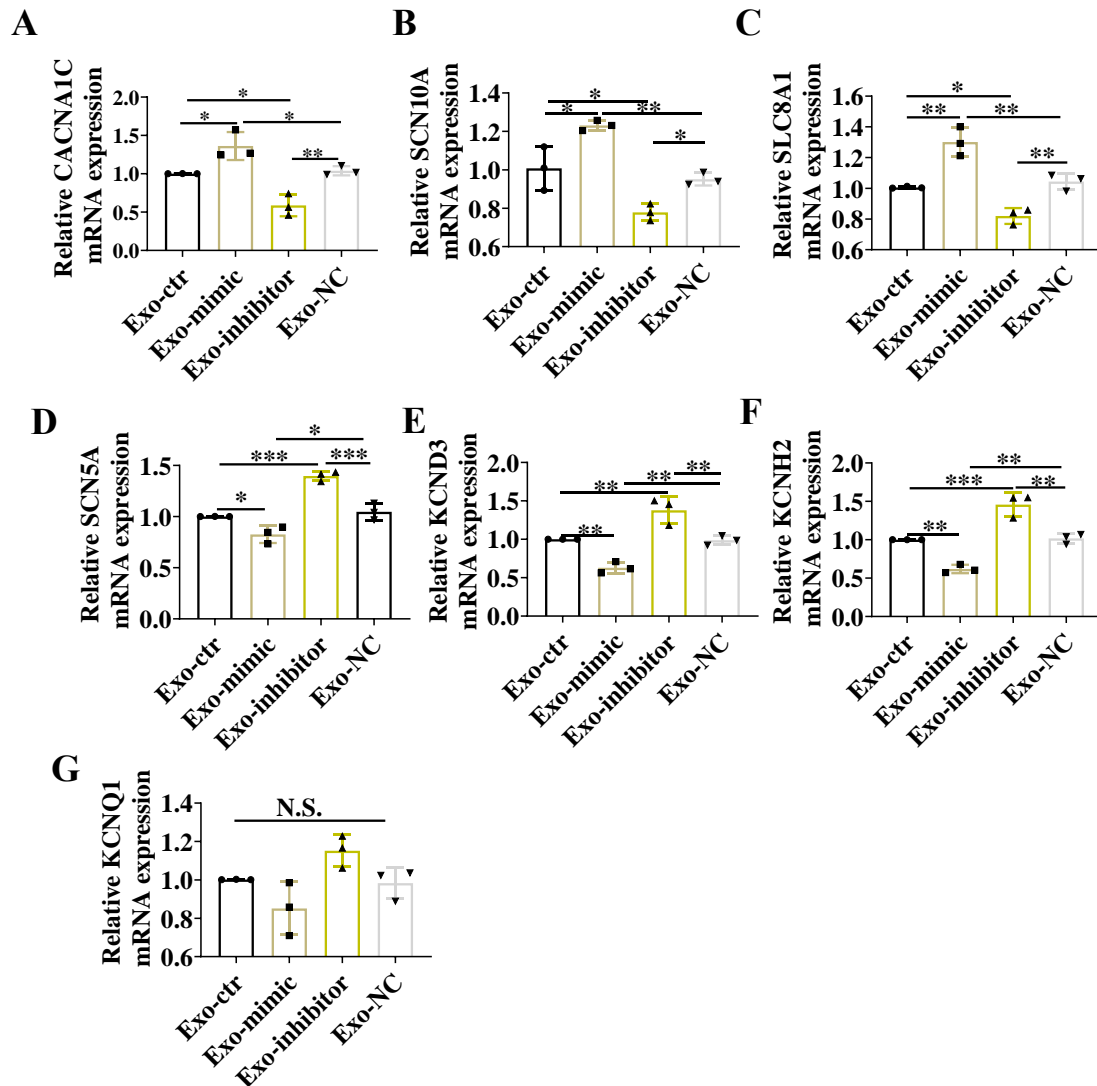


Figure 28. Effects of exosomes derived from HCMECs transfected with miR-126-3p on ion channel expression in hiPSC-CMs. hiPSC-CMs were treated with exosomes from HCMECs transfected with vehicle (Exo-ctr) or miR-126-3p mimic (Exo-mimic) or miR-126-3p inhibitor (Exo-inhibitor) or miR-126-3p inhibitor negative control (Exo-NC), respectively. qPCR was performed to measure gene expression. **(A)** The mRNA expression of CACNA1C in hiPSC-CMs of indicated groups. **(B)** The mRNA expression of SCN10A in hiPSC-CMs of indicated groups. **(C)** The mRNA expression of SLC8A1 in hiPSC-CMs of indicated groups. **(D)** The mRNA expression of SCN5A in hiPSC-CMs of indicated groups. **(E)** The mRNA expression of KCND3 in hiPSC-CMs of indicated groups. **(F)** The mRNA expression of KCNH2 in hiPSC-CMs of indicated groups. **(G)** The mRNA expression of KCNQ1 in hiPSC-CMs of indicated groups. Results are presented as means \pm SD (n=3 for each group). * P < 0.05, ** P < 0.01, *** P < 0.001 determined by one-way ANOVA with Holm-Sidak post-hoc test. N.S., no significance.

4.14 RGS3 is targeted by miR-126-3p in hiPSC-CMs

To further explore possible mechanisms underlying miR-126-3p effects, we tried to find out possible targets of miR-126-3p. Using TargetScan and miRDB (https://www.targetscan.org/vert_80/ and <https://mirdb.org/>), RGS3 was identified as a potential target for miR-126-3p (**Figure 29A**). miR-126-3p was detected to have a specific binding region for RGS3 within its 3'-UTR. To demonstrate that miR-126-3p can regulate RGS3 by binding to the predicted target site in the 3' UTR, a dual luciferase reporter gene assay was performed in HEK293T cells. Overexpression of miR-126-3p inhibited the luciferase activity of 3' UTR of RGS3-wild-type (WT) (**Figure 29A and B**). However, miR-126-3p showed no significant effect on the luciferase activity of 3'-UTR RGS3 mutant (RGS3 MT) (**Figure 29A and B**), indicating that RGS3 is a target of miR-126-3p. Western blot and qPCR analysis showed that miR-126-3p mimic reduced the gene expression and protein level of RGS3 in RGS3 WT group (**Figure 29C-E**).

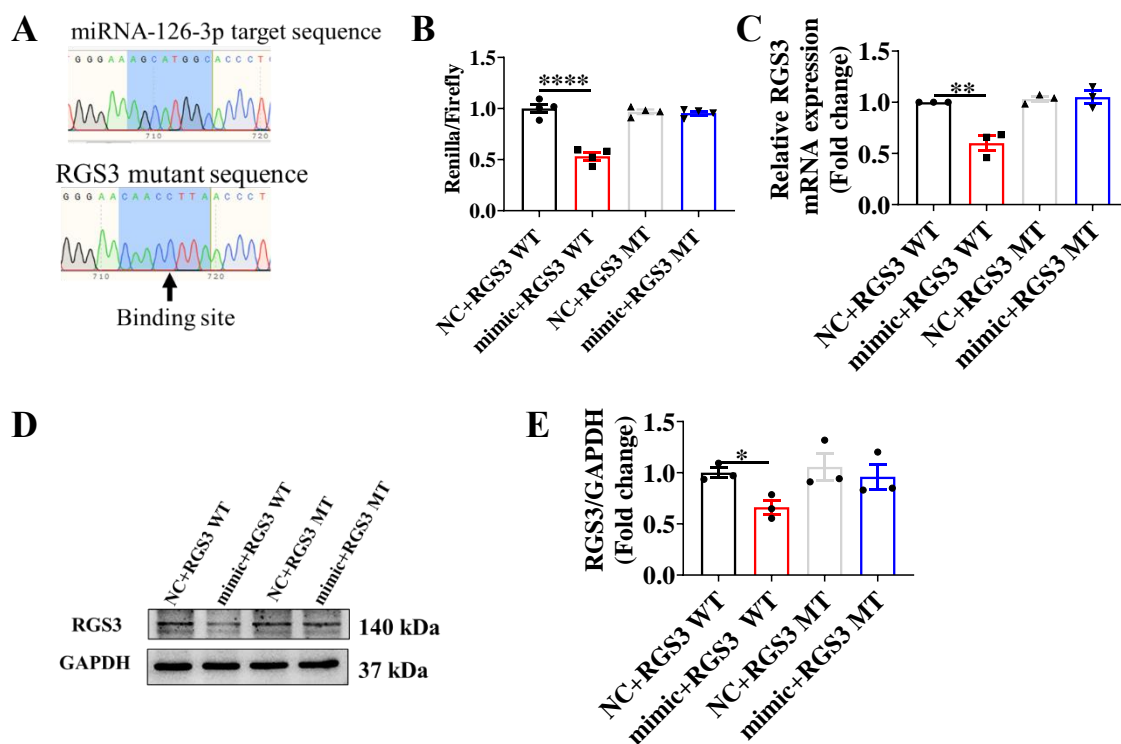


Figure 29. miR-126-3p targeted RGS3 in HEK293T cells. (A) Predicted miR-126-3p target

sequence in RGS3-3' UTRs by TargetScan and miRDB (https://www.targetscan.org/vert_80/ and <https://mirdb.org/>). Predicted target sequences of RGS3-3'UTRs were mutated for examining the change of binding to miR-126-3p. **(B)** Luciferase reporter assay of HEK293T cells transfected with RGS3-3' UTR-WT (RGS3 WT) or RGS3-3' UTR-mutant (RGS3 MT) together with miR-126-3p NC or miR-126-3p mimic. **(C)** The real time qPCR analysis of HEK293T cells transfected with RGS3 WT or RGS3 MT together with miR-126-3p NC or miR-126-3p mimic. **(D)-(E)** Representative (D) and mean values (E) of western blot analyses of RGS3 protein level in HEK293T cells transfected with RGS3WT or RGS3 MT together with miR-126-3p NC or miR-126-3p mimic. Results are presented as means \pm SD (n=4 in each group in B, n=3 in each group in C and E). * $P < 0.05$, ** $P < 0.01$, **** $P < 0.0001$ determined by one-way ANOVA with Holm-Sidak post-hoc test.

Next, qPCR and western blot analysis were employed to determine effects of miR126-3p on the mRNA and protein expression of RGS3 in HCMECs and hiPSC-CMs. The expression of RGS3 gene was decreased when HCMECs were treated with miR-126-3p mimic, whereas the mRNA level in HCMECs treated with miR-126-3p inhibitor was upregulated (**Figure 30A**). hiPSC-CMs treated with exosomes derived from HCMECs transfected with miR-126-3p mimic showed also a decrease in RGS3 gene expression (**Figure 30B**). The mRNA level of RGS3 was significantly increased in hiPSC-CMs treated with exosomes derived from HCMECs transfected with miR-126-3p inhibitor (**Figure 30B**).

At the protein level, miR-126-3p mimic downregulated RGS3 expression in HCMECs, whereas the miR-126-3p inhibitor upregulated it (**Figure 30C**). hiPSC-CMs treated with exosomes derived from HCMECs transfected with miR-126-3p mimic showed a decrease in RGS3 protein expression compared with that of Exo-NC group and Exo-ctr (**Figure 30D**). All the data confirmed that RGS3 is the target of miR-126-3p. However, Exo-mimic or Exo-inhibitor did not affect Gs (GNAS) protein expression (**Figure 30E**).

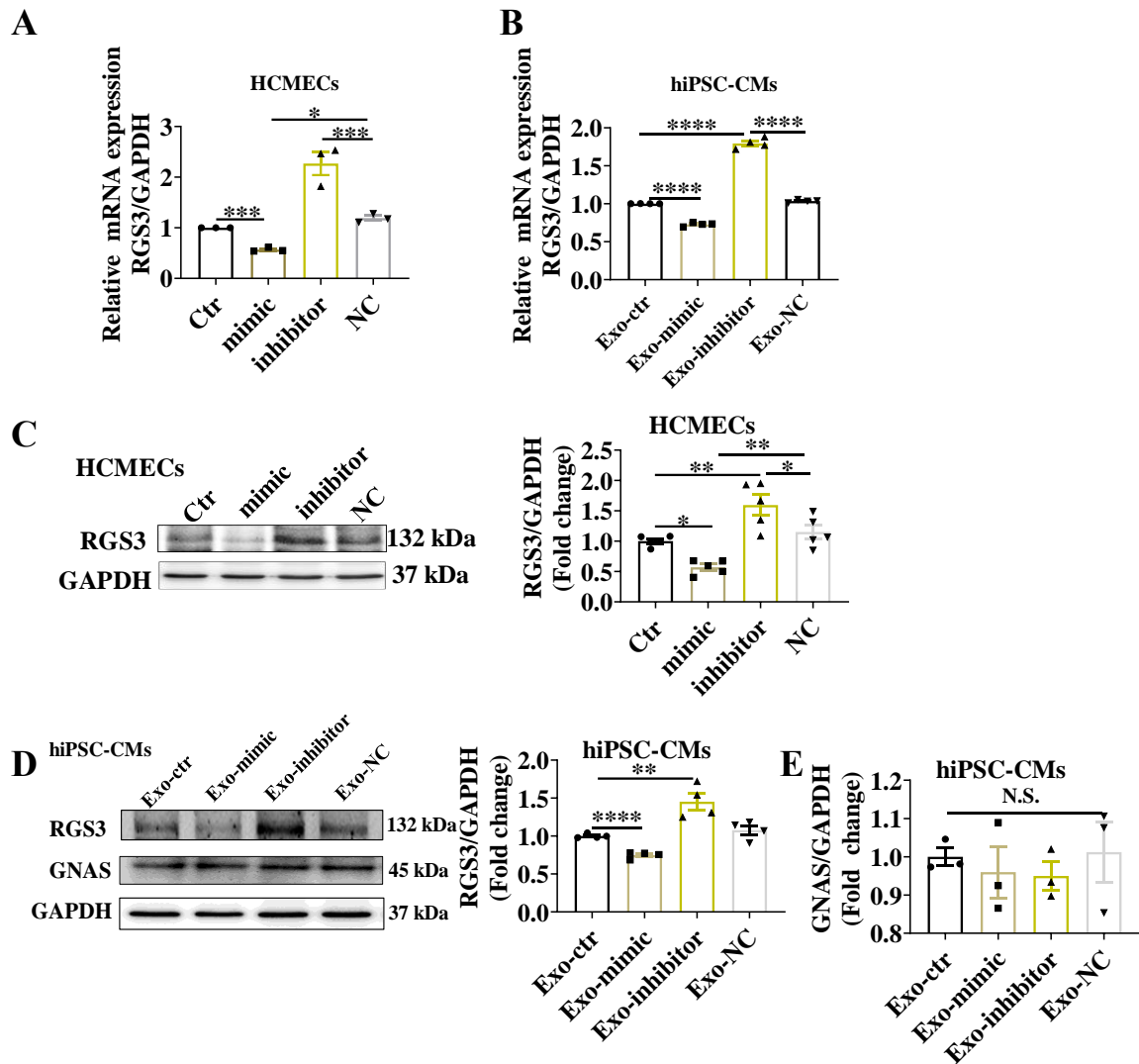


Figure 30. miR-126-3p targeted RGS3 in HCMECs and hiPSC-CMs. HCMECs were transfected with vehicle (Ctr), or miR-126-3p mimic (mimic), or miR-126-3p inhibitor (inhibitor), or miR-126-3p negative control (NC), respectively. hiPSC-CMs were treated for 48 h with exosomes from HCMECs transfected with vehicle (Exo-ctr) or miR-126-3p mimic (Exo-mimic) or miR-126-3p inhibitor (Exo-inhibitor) or miR-126-3p negative control (Exo-NC), respectively. The RGS3 or Gs expression was measured. **(A)** The relative mRNA expression of RGS3 detected by qPCR in HCMECs transfected with vehicle or miR-126-3p mimic or miR-126-3p inhibitor or miR-126-3p NC. **(B)** qPCR analysis of RGS3 mRNA level in hiPSC-CMs treated with Exo-ctr, Exo-mimic or Exo-inhibitor or Exo-NC. **(C)** Representative bands (left panel) and mean values (right panel) of western blot analyzed RGS3 protein levels in HCMECs treated with miR-126-3p mimic or miR-126-3p inhibitor or miR-126-3p NC. **(D)** Representative bands (left panel) and mean values (right panel) of RGS3 protein expression in hiPSC-CMs treated with Exo-ctr, Exo-mimic or Exo-

inhibitor or Exo-NC measured by Western blot. **(E)** Gs (GNAS) protein expression in hiPSC-CMs treated with Exo-ctr, Exo-mimic or Exo-inhibitor or Exo-NC measured by Western blot. Results are presented as means \pm SD. Scatter plots show the value of every experiment. $*P < 0.05$, $**P < 0.01$, $***P < 0.001$, $****P < 0.0001$ determined by one-way ANOVA with Holm-Sidak post-hoc test. N.S., no significance.

5 DISCUSSION

5.1 Novelty of the study

To date, no study has investigated the roles of Ang II in the pathogenesis of TTS. Our study demonstrates for the first time that catecholamine induced Ang II production in HCMECs, which contributed to endothelial dysfunction by regulating SK4 channel and ROS production. The novel findings in present study are: (1) Epi facilitated Ang II release in HCMECs, (2) Ang II elevated ET-1 production and reduced NO generation via inhibiting SK4 channel current, (3) Ang II suppressed SK4 channel current through down-regulating PKA and increasing ROS, (4) SK4 inhibition contributed to endothelial dysfunction caused by Epi/Ang II. Given that endothelial dysfunction is a well-known feature in TTS, this study has provided experimental evidences showing that Ang II signaling can contribute to pathogenesis of TTS.

In addition, to our knowledge, this is the first study to use HCMECs and hiPSC-CMs to demonstrate the roles and mechanisms of exosomal miRNAs for the ion channel dysfunction in TTS. The second part of novel findings in this study contains: (1) Exosomes secreted by endothelial cells could be taken up by hiPSC-CMs; (2) Exosomes secreted by endothelial cells could reverse APD prolonged by high concentration of catecholamines; (3) Exosomes secreted by endothelial cells could attenuate arrhythmias triggered by high concentration of catecholamines; (4) Exosomes derived from endothelial cells could attenuate ion channel dysfunction induced by high concentration of catecholamines. (5) Exosomes derived from dysfunctional (epinephrine-challenged) endothelial cells mimicked the effects of high concentration

of catecholamines on ion channels in cardiomyocytes. (6) Exosome secreted from endothelial cells regulated ion channels of cardiomyocytes by exosomal miR-126-3p. (7) miR-126-3p affected cardiac ion channel function by targeting RGS3. These results may provide novel insight into the connection between endothelial dysfunction and TTS pathogenesis.

5.2 Roles and mechanisms of Ang II/SK4 related endothelial dysfunction in the pathogenesis of TTS

Patients with TTS had a significant increase in endothelial dysfunction compared to matched controls [159]. Martin et al. found that patients diagnosed with TTS 6 months later had a worsening endothelial function in response to stress compared to post-myocardial infarction controls [55]. Endothelial dysfunction is characterized by an imbalance between vasoconstricting and vasodilating factors [160], which is considered one of the pathophysiological mechanisms of some cardiac disorders. Furthermore, catecholamine-induced senescence of endothelial cells plays a pivotal role in the progression of heart failure [161]. Several methods have been applied to estimate endothelial function. One of them is to measure NO level and ET-1 level and observe changes of the vasodilation and vasoconstriction following a stimulus [162,163]. When the ability of the endothelial cells to release NO is reduced, endothelial dysfunction ensues [164], and vasoconstriction can be facilitated. Our study revealed that high concentration Epi significantly stimulated ET-1 release and reduced NO level in the supernatant of HCMECs, indicating that high level catecholamine may cause endothelial dysfunction. It was shown that Ang II increased Epi level in perfused chromaffin cells [165]. However, few papers reported the effects of Epi on Ang II level in endothelial cells. We detected in the present study that Epi significantly elevated Ang II level in HCMECs, implying that Ang II may contribute to toxic effects of catecholamine excess.

Previous studies have demonstrated that Ang II decreased NO production in

endothelial cells, increased ET-1 level, and promoted the production of ROS by inducing multiple downstream pathways in endothelial cells [166-168], but the underlying mechanisms have not been clarified. The effects of Ang II leading to endothelial dysfunction are reported to be mediated by the AT1 receptor subtype [169,170]. We found that Ang II regulated ET-1 level by both AT1R and AT2R, and that Ang II decreased NO production by activating AT2R, suggesting that AT2R is also important for Ang II-induced endothelial dysfunction. More important and interesting findings in the present study are that NS309 reversed and Tram-34 mimicked Ang II-induced increase in ET-1 and decrease in NO generation in HCMECs, indicating that SK4 channel may exert a crucial role in endothelial dysfunction (the ET-1/NO imbalance) induced by Ang II.

Endothelial nitric oxide synthase (eNOS), also called nitric oxide synthase 3 (NOS3), is an enzyme encoded by the *NOS3* gene. Literature reports concerning the effect of Ang II on NOS3 expression in endothelial cells are controversial. Zheng et al. reported that Ang II increased eNOS protein expression but not NOS3 mRNA level in ovine fetoplacental artery endothelial (OFPAE) cells [171]. Some studies demonstrated that Ang II treatment could decrease eNOS activity and total level of NO in HUVECs [172]. The primary function of eNOS is NO production [172]. In our study, we demonstrated that Ang II decreased NO level by reducing NOS3 gene expression. Considering that the NO-reduction induced by Ang II contained SK4 channel effects, it could be possible that the SK4 channel inhibition, which may change cell membrane potential, changed the NOS3 expression level and hence reduced NO generation.

It was reported that Ang II increased apoptosis rate, reduced tube formation by Nox2/Nox4 upregulation elevating ROS production, and impaired mitochondrial function [173,174]. In our study, we observed similar results. However, the study added new data showing that the Ang II-induced apoptosis and tube formation involved roles of SK4 channels. Here a question is how SK4 channel can contribute to endothelial tube formation and apoptosis. Ang II inhibited I_{SK4} and led to a depolarization of cell

membrane potential. Therefore, we checked whether a depolarization can contribute to the cell apoptosis caused by Ang II. Indeed, a depolarizing high concentration (10 mM) of KCl in culture medium increased cell apoptosis, similar to effect of Ang II. This may help us understand how SK4 inhibition by Ang II can contribute to endothelial dysfunction, including ET-1/NO imbalance, abnormal tube formation and abnormal ATP level as well as apoptosis. It is well-known that membrane potential is important for maintaining cell functions. Any change in membrane potential may change cell functions. For example, a depolarization of endothelial cells can reduce the driving force for influx of positively charged ions like Na^+ , Ca^{2+} , etc., which may be important for some intracellular signaling, and hence can influence cell functions. For clarifying more exactly the mechanism for alterations in HCMECs caused by the depolarization, further studies are required.

The abundant formation of ROS within the vascular wall is a key determinant in endothelial dysfunction [64,175]. Ang II can increase the production of ROS by regulating the activity of nicotinamide adenine dinucleotide phosphate oxidase (NOX) [172,176,177]. We observed also an increase in ROS production of HCMECs stimulated by Ang II and proved that Ang II-induced ROS can participate in the inhibition of SK4 current. Consistent with previous studies which showed that Ang II can reduce MMP in ECs [178], our data confirmed that Ang II can decrease MMP and inhibit ATP production. Given that damages of the mitochondria can lead to cell apoptosis [179], we tested the effects of Ang II on Bcl2, Bax, cleaved caspase 3, and BAD expression and observed changes, which are consistent with enhancement of apoptosis. Importantly, our data displayed that the change of SK channel function and cell membrane depolarization were involved in Ang II-induced apoptosis in HCMECs.

Previous studies demonstrated that the increased stress hormone release, formation of oxidative stress, and activation of inflammatory pathways subsequently led to vascular/endothelial dysfunction [180]. Previous studies also reported that Ang II induced CRP generation in human aortic endothelial cells (HAECs), increased TNF- α

secretions in HAECs [181,182]. Our results confirmed that the Ang II can increase CRP and TNF- α expression, which can be prevented by Los. In addition, we also demonstrated that both Los and PD reduced Ang II-induced CCL2 gene expression, implying that both ATR1 and ATR2 blockers may be helpful for relieving Ang II-induced inflammation reaction. Whether SK4 channel is important for Ang II-induced inflammatory reaction needs to be explored in future studies. Another mechanism for Ang II-induced inhibition of SK4 is the downregulation of PKA. It was shown that SK4 channel could be activated by PKA [183], in agreement with the result from this study, showing an enhancement of I_{SK4} by a PKA activator (Sp-8-Br-cAMPS). Ang II can reduce PKA expression and hence reduce I_{SK4} . The mechanism by which Ang II reduces PKA expression remains to be clarified in the future.

The inhibition of I_{SK4} can cause a depolarization of membrane potential in endothelial. The depolarization in endothelial cell can be transmitted to smooth muscle through myoendothelial gap junctions connecting the endothelial and smooth muscle cells [126,184]. It implies that the depolarization in endothelial cells can lead to a depolarization of smooth muscle cells via gap junctions. The depolarization in smooth muscle cells can activate L-type calcium channels, increase the inward calcium current and increase calcium release through calcium-induced calcium release mechanism, and in turn cause contraction of smooth muscle cells. Taking this together with the results showing the involvements of I_{SK4} in the generation of ET-1 and NO, we can expect that the inhibition of SK4 channel can contribute to catecholamine induced blood vessel contraction through at least two mechanisms, i.e., a depolarization of smooth muscle and an ET-1/NO imbalance. The contraction of coronary artery can reduce blood flow and cause ischemic changes in cardiomyocytes and ECG, which are usually detected in TTS patients. In addition, SK4 channels can also contribute to other process of endothelial dysfunction like apoptosis or inflammatory process or energy metabolism (ATP production), which may also influence the blood vessel contraction.

Given that the area of dysfunctional cardiomyocytes in TTS is usually beyond the area covered by a single coronary artery, it is possible that the endothelial dysfunction can exert effects on cardiomyocytes through a mechanism other than reduction of blood flow, for example through endothelial secretions, which can affect cardiomyocytes.

5.3 Roles and mechanism of endothelial exosomes in the pathogenesis of TTS

TTS is characterized by acute myocardial dysfunction of the left and/or right ventricle. The common complications of TTS include heart failure, rupture of the left ventricular free wall and fatal arrhythmias. The incidence of life-threatening arrhythmias in TTS patients was 6.29% [185,186]. Ventricular arrhythmias (VA) in TTS patients, which has largely been underestimated for many years, are an important contributor to increased morbidity and mortality and are currently a treatment challenge [187,188]. TTS cases are often associated with cardiac arrhythmias such as ventricular tachycardia, ventricular fibrillation, and atrioventricular nodal block [187,189]. Catecholamines released by adrenal medullary chromaffin cells surge during the acute phase of TTS, leading to myocardial injury through multiple mechanisms. So far, the exact mechanism has not been fully elucidated. In our study, high concentrations of Epi induced arrhythmia-like events in single cardiomyocytes, which is consistent with the important clinical feature of TTS. Cardiac arrhythmias are often linked to dysfunction of the cardiac ion channels. Thus, we observed that high concentrations of Epi lead to changes in AP by affecting ion channel currents, such as I_{Ca-L} , I_{Na} , I_{Na-L} , I_{NCX} , I_{Kr} , and I_{to} .

The cross-talk between cardiomyocytes and endothelial cells is essential for maintaining the normal development and function of the heart. Mechanisms regulating endothelial cell-cardiomyocyte crosstalk, especially during acute stress situations, are poorly understood. Exosomes, which can be generated by different kinds of cells, can mediate cross-talk between different cells. Exosomes may play an important role in

mediating cell-to-cell communication in the heart by regulating the activity and functions of target cells under physiological and pathological conditions. Importantly, cardiac-specific exosomal miRNAs can regulate the expression of sarcomeric genes, autophagy, ion channel genes, anti-apoptotic and anti-fibrotic activities, and angiogenesis [190]. Exosomes derived from adipose-derived mesenchymal stem cells (MSC) suppressed cardiac apoptosis, cardiac dysfunction, inflammatory responses, and cardiac fibrosis by activating S1P/SK1/S1PR1 signaling and inducing macrophage M2 polarization [191]. Exosomes can transmit signals to target cells through direct binding of their transmembrane ligands, fusion with target cells, or endocytosis by receptor cells [192-195]. Currently, it was shown that exosomes derived from MSCs increased contractility in human engineered cardiac tissue (hECT) comprised of human embryonic stem cell-derived cardiomyocytes [196]. In addition, hMSC paracrine signaling can modulate ion channel/pump activity of cardiomyocytes, enhance excitation-contraction coupling and reduce cardiac fibrosis [197-199]. In our study, exosomes derived from non-Epi-challenged HCMECs reversed Epi-induced cardiac ion channel dysfunction and arrhythmias by affecting ion channel activity, suggesting that exosomes secreted from endothelial cells contributes to modulation of cardiac ion channel functions.

Endothelial cells can maintain the cardiac homeostasis by secreting a variety of biologically active substances, and play an important role in maintaining normal heart function and repairing injury. Although clinical features in TTS patients are transient, the endothelial stimulation persists even in an apparent quiescent phase of TTS [35,57,61,200]. However, the exact mechanism of how cardiomyocyte function is affected by endothelial dysfunction remains obscure. Our study demonstrated that exosomes derived from dysfunctional (Epi-challenged) endothelial cells mimicked or further aggravated Epi-induced ion channel dysfunction and arrhythmias of cardiomyocytes by affecting expression and currents of ion channels on the cell membrane of cardiomyocytes. The normal rhythm of the heart is maintained by normal electrophysiological properties of different transmembrane ion channels in

cardiomyocytes [201]. Exosomes can exert the function of cellular communication via three mechanisms such as internalization by cells, direct fusion to the cell membrane, and receptor-ligand interactions. In this study, exosomes derived from HCMECs could be taken up by hiPSC-CMs. Therefore, it is possible to apply exosomes isolated from HCMECs to hiPSC-CMs for elucidating how endothelial cell-derived exosomes can regulate the ion channel function in cardiomyocytes in the setting of TTS.

Cardiac exosomes can transmit proteins, mRNA, and miRNAs to other cells under both physiological and pathological conditions. Cardiac-specific exosome miRNAs can regulate the expression of ion channel genes and transfer genetic information between cells. It was demonstrated that miRNAs, which are 22 to 25 nucleotides in length, suppressed and degraded mRNAs, or alternatively stimulated translation of mRNAs by binding to the 3'-UTR of their target mRNAs [103,202]. miRNAs have been extensively studied in the pathogenesis of cardiovascular disease. miR-133a-3p induced repolarization abnormalities and significantly increased I_{Ca-L} in atrial cardiomyocytes [203]. In addition, miR-1 affected both repolarization and depolarization phases of the cardiac action potential by inhibiting the expression of the KCNJ2 gene and modulating the expression of CaV1.2 (CACNA1C) gene which is involved in myocardial depolarization, action potential duration and excitation-contraction coupling [204-208]. Of note, circulating miRNAs, such as miR-1, miR-133a, miR-16, and miR-26a, are used to diagnose acute TTS and even distinguish TTS from acute MI [65]. Moreover, miR-16 and miR-26a reduced calcium transient amplitude, and decreased I_{Ca-L} at the apex of cardiomyocytes [157]. In our study, the expression of miR-16, miR-26a, miR-133a, miR-126-3p in exosomes derived from HCMEC treated by Epi was higher than that in exosomes from normal (non-Epi-challenged) HCMECs, suggesting that these miRNAs may mediate the observed exosome effects and may play a crucial role in the process of TTS. Given that miR-16, miR-26a and miR-133a but not miR-126-3p have been shown to be related to TTS, we focused on miR126-3p in the current study.

Exosomes derived from HCMECs overexpressing miR-126-3p (Exo-mimic)

displayed effects on APs similar to Epi effects, showing that Exo-mimic reduced V_{max} and prolonged APD, as Epi did. Moreover, Exo-mimic promotes arrhythmic events, suggesting that miR-126-3p may play a role in arrhythmogenesis in TTS. Exo-mimic simulated Epi effects on the gene expression of CACNA1C, SCN10A, SLC8A1, SCN5A, KCND3, KCNH2, and KCNQ1. These data indicate that miR-126-3p is involved in catecholamine induced ion channel dysfunction and arrhythmias.

miR-126 is highly expressed in endothelial cells [209]. miR-126-3p was correlated with AF, heart failure and childhood dilated cardiomyopathy (CDCM) [210,211]. So far, how miR-126-3p regulate the contractile function and electrophysiological properties of cardiomyocytes is poorly understood. Overexpressing miR-126-3p in the human saphenous vein endothelial cells led to increased migration and proliferation by silencing SPRED1 and PIK3R2 [212]. Moreover, miR-126-3p inhibited the proliferation, migration, invasion, and angiogenesis of triple-negative breast cancer cells by targeting RGS3 [213]. RGS3, a GTPase-activating protein, is a negative regulator of G protein-mediated signaling. Upregulation of RGS3 inhibits maladaptive hypertrophy and fibrosis to improve cardiac function by blocking MEK-ERK1/2 signaling [214]. An alternatively spliced short RGS3 isoform (RGS3s) significantly reduced the maximal ACh-evoked G protein-gated inwardly rectifying K^+ (GIRK) channel current amplitude [215]. In this study, our results demonstrated that miR-126-3p regulates the electrophysiological properties of cardiomyocytes by directly binding RGS3 gene and inhibiting RGS3 expression. The downregulation of RGS3 by miR-126-3p could enhance the activity of Gs-protein although miR-126-3p did not change the expression level of Gs. Hence, miR-126-3p could mimic or enhance Epi effects on cardiac ion channels via suppressing RGS3 expression.

Another interesting finding in this study is that exosomes from HCMECs with and without Epi-challenge exerted differential effects on hiPSC-CMs. Exosomes from HCMECs without Epi-challenge (Wt-exo) attenuated Epi-effects on ion channel currents, APs and beating rhythm of hiPSC-CMs, whereas exosomes from Epi-

challenged HCMECs (Epi-exo) mimicked or even further enhanced Epi-effects. The former suggests a protective effect of exosomes against toxic effects of catecholamine excess, and the later suggests an aggravating effect of exosomes in catecholamine excess. Since Epi increased the expression level of miR-126-3p in HCMECs and exosomes from HCMECs, and more importantly, exosomes overexpressing miR-126-3p (by transfecting HCMECs with miR-126-3p-mimic) could mimic Epi-effects, miR-126-3p should be at least one of factors responsible for the aggravating effects of exosomes from Epi-challenged HCMECs on ion channel function and arrhythmic events in the presence of Epi. Therefore, we can understand it as that under physiological conditions, exosomes from endothelial cells may exert effects on cardiomyocytes to participate in maintaining normal cardiac function by attenuating detrimental effects of catecholamine excess, while under stress miR-126-3p in endothelial cells and also in endothelial exosomes is upregulated, and then exerts effects mimicking or enhancing toxic effects of catecholamine, contributing to the pathogenesis of TTS. Here, which factor is responsible for the beneficial effects of exosome from non-Epi-challenged HCMECs is still an open question. Previous studies reported protective effects of exosomes or miRNAs in cardiomyocytes [216-218]. In this study, the expression of miR-16, miR-26a, miR-133a in HCMECs and exosomes derived from HCMECs was also increased by Epi, suggesting that miR-16, miR-26a and miR-133a may also contribute to Epi-exo effects and are unlikely the factors responsible for the protective effects of Wt-exo. Further studies are needed to explore the effects of other factors on endothelial exosomes.

Taking all together, this study has for the first time investigated and elucidated the effects of endothelial cell secretion on cardiac ion channel functions and electrophysiological properties as well as underlying mechanisms using HCMECs and hiPSC-CMs in the setting of TTS. Our data showed that high concentration of catecholamine can increase Ang II release to cause endothelial dysfunction via inhibiting SK4 channels. The endothelial dysfunction including ET-1/NO imbalance, cell membrane depolarization, inflammatory action, abnormal energy metabolism and

apoptosis may cause coronary spasm, leading to cardiomyocyte dysfunction. Besides Ang II, endothelial cells can secrete exosomes, which can through unknown mechanism exert protective effects against catecholamine excess. However, exosomes from dysfunctional endothelial cells (in the setting of catecholamine excess) could induce ion channel dysfunction in cardiomyocytes, which may contribute to the occurrence of arrhythmias in the presence of catecholamine excess. The effects of endothelial exosomes may result from the upregulation of exosomal miR-126-3p, which targets RGS3 signaling in cardiomyocytes (Figure 31).

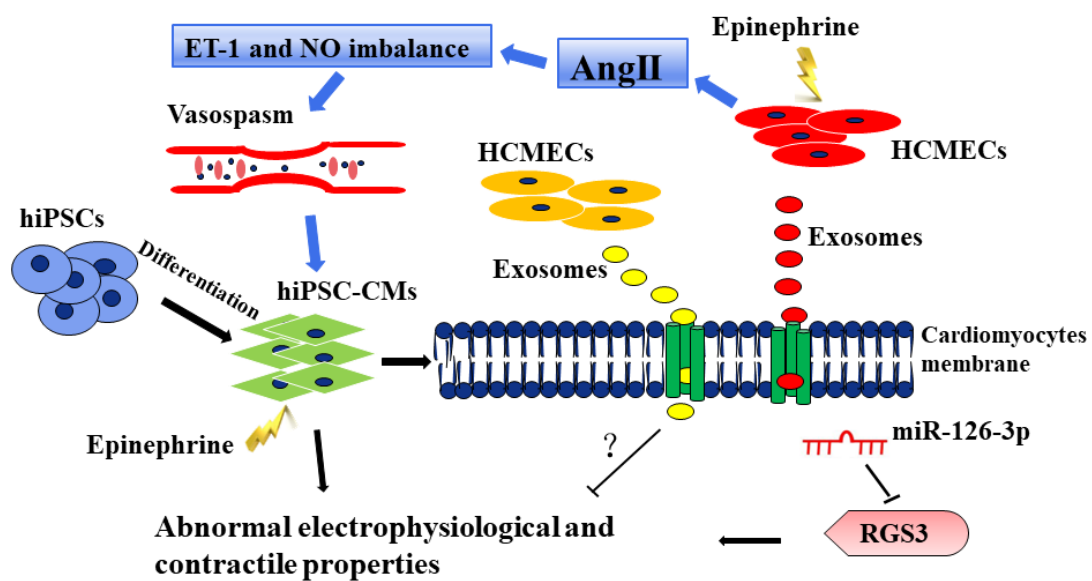


Figure 31. Schematic diagram showing possible mechanisms by which catecholamine excess causes endothelial dysfunction and endothelial cell secretion modulates electrophysiological properties of hiPSC-CMs in the setting of TTS. Epi triggers Ang II release and in turn leads endothelial dysfunction (ET-1/NO imbalance), leading to vasospasm and then cardiomyocyte dysfunction. On the other hand, Epi can upregulate miR-126-3p in endothelial cells and endothelial exosomes, which can be delivered to cardiomyocytes and affect cardiac channel function via inhibiting RGS3 signaling. Exosomes derived from normal endothelial cells may exert protective effect against catecholamine excess.

5.4 Study limitations

There are multiple limitations which need to be considered. First, how Epi can increase Ang II release from HCMECs and how Epi can upregulate miR126-3p in HCMECs have not been clarified. Epi is a non-specific adrenoceptor agonist. Every adrenoceptor signaling could be potential candidate for Epi effects, which needs to be clarified in future studies. Further investigations are needed to clarify how RGS3 regulates ion channel function in the setting of TTS. In addition, miR-126-3p may have other binding targets affecting electrophysiological properties of hiPSC-CMs. Besides, intracellular signaling pathways in immature hiPSC-CMs may be different from that in adult human cardiomyocytes. However, due to easy access to large numbers of cells and genetic modification to simulate pathological conditions, hiPSC-CMs become the most common sources of human cardiomyocytes which were used in vitro studies. Finally, whether hiPSC-CMs from TTS patients display results different from that obtained in hiPSC-CMs from healthy donors treated with Epi remains unknown.

5.5 Conclusions

From this study, it can be concluded that endothelial dysfunction may play important roles in the pathogenesis of TTS. Catecholamine excess can cause endothelial dysfunction through Ang II/ROS/PKA/SK4 signaling. Catecholamine can upregulate miR-126-3p in endothelial cells and endothelial exosomes, which can contribute to cardiomyocyte dysfunctions in catecholamine excess.

6 SUMMARY

Typical ST-segment changes in ECG of patients with Takotsubo syndrome (TTS) suggest coronary spasm and endothelial dysfunction. Although several studies have detected endothelial dysfunction in TTS patients, the exact cellular mechanism of endothelial dysfunction in the setting of TTS has not been completely elucidated. Since the area of dysfunctional cardiomyocytes is usually beyond the area covered by a single coronary artery, it is possible that the endothelial dysfunction can exert effects on cardiomyocytes through a mechanism other than reduction of blood flow. Therefore, we hypothesize that high concentration catecholamine may cause endothelial dysfunction and change endothelial secretions, which can contribute to the pathogenesis of TTS. To test the hypothesis, the present study was designed to investigate the catecholamine excess induced endothelial dysfunction and roles and mechanisms of the endothelial dysfunction in cardiomyocyte dysfunction in the setting of catecholamine excess.

Epinephrine was applied to human cardiac microvascular endothelial cells (HCMECs) or to human induced pluripotent stem cell derived cardiomyocytes (hiPSC-CMs) to mimic the setting of catecholamine excess. Endothelial dysfunction was detected by measurements of levels of nitric oxide (NO) and endothelin -1(ET-1), tube formation, inflammatory factors, mitochondrial function and cell apoptosis in HCMECs. Secretions from HCMECs including Ang II and exosomes were measured and isolated, and their effects and mechanisms underlying effects were assessed in HCMECs and hiPSC-CMs, respectively. Multiple techniques including ELISA, flow cytometry, qPCR, patch-clamp, dual luciferase reporter assay and western blotting were performed for the study.

Epi increased ET-1 and decreased NO generation in HCMECs. The Epi effects could be attenuated by Ang II subtype-1 receptor (AT1R) antagonist losartan (Los) and subtype-2 receptor (AT2R) antagonist PD123319 (PD). Epi increased Ang II secretion

by HCMECs and Ang II mimicked Epi effects on ET-1 and NO generation, indicating that Epi can cause endothelial dysfunction through enhancing Ang II signaling. Ang II effects on ET-1/NO generation, tube formation, and apoptosis could be mimicked by an SK4 channel blocker Tram-34 and attenuated by an SK4 channel activator NS309, suggesting an involvement of SK4 channel function. Patch clamp results showed that SK4 channel current was inhibited by Ang II and ROS, but enhanced by PKA activator. Ang II could increase ROS generation and suppress PKA expression, which can explain the inhibitory effect of Ang II on SK4 channels.

High-concentration Epi suppressed the maximal depolarization velocity (V_{max}) of action potential, prolonged the action potential duration at 10% repolarization (APD10), the action potential duration at 50% repolarization (APD50), and the action potential duration at 90% repolarization (APD90), and induced arrhythmic events in hiPSC-CMs. Exosomes derived from HCMECs without Epi-treatment (Wt-exo) reversed the effects of Epi on action potentials and ion channel currents including L-type calcium channel current (I_{Ca-L}), peak sodium current (I_{Na}), the transient outward current (I_{to}), late sodium current (I_{Na-L}), the slowly activating delayed rectifier K^+ current (I_{Ks}) and the rapidly activating delayed rectifier K^+ current (I_{Kr}) and gene expression of these ion channels in hiPSC-CMs. Exosomes derived from HCMECs treated with epinephrine (Epi-exo) mimicked or further enhanced Epi effects. Epi could increase the level of miR-126-3p in HCMECs and exosomes from HCMECs, suggesting a contribution of miR-126-3p to Epi-exo effects in hiPSC-CMs. HCMECs transfected with miR-126-3p mimic secreted exosome with overexpression (increased level) of miR-126-3p. The exosome with overexpression of miR-126-3p mimicked the effects of Epi-exo, confirming key roles of miR-126-3p in Epi-exo effects. Dual luciferase reporter assay with gene mutation techniques proved a targeting site of miRNA-126-3p in G-protein signaling 3 (RGS3) gene. Western blot and qPCR analyses displayed that miR-126-3p mimic could reduce RGS3 expression level in both HCMECs and hiPSC-CMs, confirming that miR-126-3p can exert effects by inhibiting RGS3 signaling.

The study demonstrated that high level catecholamine can increase Ang II release in endothelial cells, and Ang II can cause endothelial dysfunction by inhibiting SK4 channel current via increasing ROS generation and reducing PKA expression. Exosomes derived from dysfunctional HCMECs (affected by high level of catecholamine) can exert effects on cardiomyocytes and induce cardiac ion channel dysfunctions, which may contribute to the occurrence of arrhythmias in presence of catecholamine excess. The exosomal miR-126-3p can mediate the endothelial exosome effects via targeting RGS3 signaling in cardiomyocytes. This study may provide new insights into pathogenesis of TTS. AT1R and AT2R signaling, SK4 channel and miR-126-3p may be potential targets for preventing or treating TTS.

7 References

1. Cramer, M.J.; De Boeck, B.; Melman, P.G.; Sieswerda, G.J. The 'broken heart' syndrome: What can be learned from the tears and distress? *Neth Heart J* **2007**, *15*, 283-285.
2. Sharkey, S.W.; Windenburg, D.C.; Lesser, J.R.; Maron, M.S.; Hauser, R.G.; Lesser, J.N.; Haas, T.S.; Hodges, J.S.; Maron, B.J. Natural history and expansive clinical profile of stress (tako-tsubo) cardiomyopathy. *J Am Coll Cardiol* **2010**, *55*, 333-341.
3. Topal, Y.; Topal, H.; Dogan, C.; Tiryaki, S.B.; Biteker, M. Takotsubo (stress) cardiomyopathy in childhood. *Eur J Pediatr* **2020**, *179*, 619-625.
4. Dote, K.; Sato, H.; Tateishi, H.; Uchida, T.; Ishihara, M. [myocardial stunning due to simultaneous multivessel coronary spasms: A review of 5 cases]. *J Cardiol* **1991**, *21*, 203-214.
5. Lyon, A.R.; Bossone, E.; Schneider, B.; Sechtem, U.; Citro, R.; Underwood, S.R.; Sheppard, M.N.; Figtree, G.A.; Parodi, G.; Akashi, Y.J., *et al.* Current state of knowledge on takotsubo syndrome: A position statement from the taskforce on takotsubo syndrome of the heart failure association of the european society of cardiology. *Eur J Heart Fail* **2016**, *18*, 8-27.
6. Prasad, A.; Lerman, A.; Rihal, C.S. Apical ballooning syndrome (tako-tsubo or stress cardiomyopathy): A mimic of acute myocardial infarction. *Am Heart J* **2008**, *155*, 408-417.
7. Orphanou, N.; Eftychiou, C.; Papasavvas, E.; Ioannides, M.; Avraamides, P. Syncope in a hypertrophic heart at a wedding party: Can happiness break a thick heart? Takotsubo cardiomyopathy complicated with left ventricular outflow tract obstruction in a hypertrophic heart. *Oxf Med Case Reports* **2020**, *2020*, omaa036.
8. Ancona, F.; Bertoldi, L.F.; Ruggieri, F.; Cerri, M.; Magnoni, M.; Beretta, L.; Cianflone, D.; Camici, P.G. Takotsubo cardiomyopathy and neurogenic stunned myocardium: Similar albeit different. *Eur Heart J* **2016**, *37*, 2830-2832.
9. Madias, J.E. "Neurogenic stress cardiomyopathy in heart donors" is a form of takotsubo syndrome. *Int J Cardiol* **2015**, *184*, 612-613.
10. Mohamedali, B.; Bhat, G.; Zelinger, A. Frequency and pattern of left ventricular dysfunction in potential heart donors: Implications regarding use of dysfunctional hearts for successful transplantation. *J Am Coll Cardiol* **2012**, *60*, 235-236.
11. Akashi, Y.J.; Nef, H.M.; Lyon, A.R. Epidemiology and pathophysiology of takotsubo syndrome. *Nat Rev Cardiol* **2015**, *12*, 387-397.
12. Moussouttas, M.; Mearns, E.; Walters, A.; DeCaro, M. Plasma catecholamine profile of subarachnoid hemorrhage patients with neurogenic cardiomyopathy. *Cerebrovasc Dis Extra* **2015**, *5*, 57-67.
13. Kow, K.; Watson, T.J.; Foo, D.; Ho, H.H. Clinical characteristics and outcomes of south-east asian patients with takotsubo (stress-induced) cardiomyopathy. *Int J Cardiol Heart Vasc* **2018**, *21*, 29-31.
14. Templin, C.; Ghadri, J.R.; Diekmann, J.; Napp, L.C.; Bataiosu, D.R.; Jaguszewski, M.; Cammann, V.L.; Sarcon, A.; Geyer, V.; Neumann, C.A., *et al.* Clinical features and outcomes of takotsubo (stress) cardiomyopathy. *N Engl J Med* **2015**, *373*, 929-938.
15. Doyen, D.; Moschietto, S.; Squara, F.; Moceri, P.; Hyvernats, H.; Ferrari, E.; Dellamonica, J.; Bernardin, G. Incidence, clinical features and outcome of takotsubo syndrome in the intensive care unit. *Arch Cardiovasc Dis* **2020**, *113*, 176-188.
16. Minhas, A.S.; Hughey, A.B.; Koliass, T.J. Nationwide trends in reported incidence of takotsubo

- cardiomyopathy from 2006 to 2012. *Am J Cardiol* **2015**, *116*, 1128-1131.
17. Ghadri, J.R.; Wittstein, I.S.; Prasad, A.; Sharkey, S.; Dote, K.; Akashi, Y.J.; Cammann, V.L.; Crea, F.; Galiuto, L.; Desmet, W., *et al.* International expert consensus document on takotsubo syndrome (part i): Clinical characteristics, diagnostic criteria, and pathophysiology. *Eur Heart J* **2018**, *39*, 2032-2046.
 18. Budnik, M.; Nowak, R.; Fijalkowski, M.; Kochanowski, J.; Nargiello, E.; Piatkowski, R.; Peller, M.; Kucharz, J.; Jaguszewski, M.; Gruchala, M., *et al.* Sex-dependent differences in clinical characteristics and in-hospital outcomes in patients with takotsubo syndrome. *Pol Arch Intern Med* **2020**, *130*, 25-30.
 19. Park, J.H.; Kang, S.J.; Song, J.K.; Kim, H.K.; Lim, C.M.; Kang, D.H.; Koh, Y. Left ventricular apical ballooning due to severe physical stress in patients admitted to the medical icu. *Chest* **2005**, *128*, 296-302.
 20. Rozema, T.; Klein, L.R. Takotsubo cardiomyopathy: A case report and literature review. *Cardiol Young* **2016**, *26*, 406-409.
 21. Chinali, M.; Formigari, R.; Grutter, G. Takotsubo cardiomyopathy in a young adult with transplanted heart: What happened to denervation? *ESC Heart Fail* **2018**, *5*, 197-200.
 22. Cammann, V.L.; Szawan, K.A.; Stahli, B.E.; Kato, K.; Budnik, M.; Wischnewsky, M.; Dreiding, S.; Levinson, R.A.; Di Vece, D.; Gili, S., *et al.* Age-related variations in takotsubo syndrome. *J Am Coll Cardiol* **2020**, *75*, 1869-1877.
 23. Deshmukh, A.; Kumar, G.; Pant, S.; Rihal, C.; Murugiah, K.; Mehta, J.L. Prevalence of takotsubo cardiomyopathy in the united states. *Am Heart J* **2012**, *164*, 66-71 e61.
 24. Desai, A.; Noor, A.; Joshi, S.; Kim, A.S. Takotsubo cardiomyopathy in cancer patients. *Cardiooncology* **2019**, *5*, 7.
 25. Giza, D.E.; Lopez-Mattei, J.; Vejpongsa, P.; Munoz, E.; Iliescu, G.; Kitkungvan, D.; Hassan, S.A.; Kim, P.; Ewer, M.S.; Iliescu, C. Stress-induced cardiomyopathy in cancer patients. *Am J Cardiol* **2017**, *120*, 2284-2288.
 26. Cammann, V.L.; Sarcon, A.; Ding, K.J.; Seifert, B.; Kato, K.; Di Vece, D.; Szawan, K.A.; Gili, S.; Jurisic, S.; Bacchi, B., *et al.* Clinical features and outcomes of patients with malignancy and takotsubo syndrome: Observations from the international takotsubo registry. *J Am Heart Assoc* **2019**, *8*, e010881.
 27. Joy, P.S.; Guddati, A.K.; Shapira, I. Outcomes of takotsubo cardiomyopathy in hospitalized cancer patients. *J Cancer Res Clin Oncol* **2018**, *144*, 1539-1545.
 28. Sattler, K.; El-Battrawy, I.; Lang, S.; Zhou, X.; Schramm, K.; Tulumen, E.; Kronbach, F.; Roger, S.; Behnes, M.; Kuschyk, J., *et al.* Prevalence of cancer in takotsubo cardiomyopathy: Short and long-term outcome. *Int J Cardiol* **2017**, *238*, 159-165.
 29. El-Battrawy, I.; Santoro, F.; Stiermaier, T.; Moller, C.; Guastafierro, F.; Novo, G.; Novo, S.; Santangelo, A.; Mariano, E.; Romeo, F., *et al.* Prevalence, management, and outcome of adverse rhythm disorders in takotsubo syndrome: Insights from the international multicenter geist registry. *Heart Fail Rev* **2020**, *25*, 505-511.
 30. Di Vece, D.; Silverio, A.; Bellino, M.; Galasso, G.; Vecchione, C.; La Canna, G.; Citro, R. Dynamic left intraventricular obstruction phenotype in takotsubo syndrome. *J Clin Med* **2021**, *10*.
 31. Conradi, P.M.; van Loon, R.B.; Handoko, M.L. Dynamic left ventricular outflow tract obstruction in takotsubo cardiomyopathy resulting in cardiogenic shock. *BMJ Case Rep* **2021**, *14*.
 32. Redfors, B.; Jha, S.; Thorleifsson, S.; Jernberg, T.; Angeras, O.; Frobert, O.; Petursson, P.; Tornvall,

- P.; Sarno, G.; Ekenback, C., *et al.* Short- and long-term clinical outcomes for patients with takotsubo syndrome and patients with myocardial infarction: A report from the swedish coronary angiography and angioplasty registry. *J Am Heart Assoc* **2021**, *10*, e017290.
33. Bonacchi, M.; Vannini, A.; Harmelin, G.; Batacchi, S.; Bugetti, M.; Sani, G.; Peris, A. Inverted-takotsubo cardiomyopathy: Severe refractory heart failure in poly-trauma patients saved by emergency extracorporeal life support. *Interact Cardiovasc Thorac Surg* **2015**, *20*, 365-371.
 34. Aweimer, A.; El-Battrawy, I.; Akin, I.; Borggrefe, M.; Mugge, A.; Patsalis, P.C.; Urban, A.; Kummer, M.; Vasileva, S.; Stachon, A., *et al.* Abnormal thyroid function is common in takotsubo syndrome and depends on two distinct mechanisms: Results of a multicentre observational study. *J Intern Med* **2021**, *289*, 675-687.
 35. Naegele, M.; Flammer, A.J.; Enseleit, F.; Roas, S.; Frank, M.; Hirt, A.; Kaiser, P.; Cantatore, S.; Templin, C.; Frohlich, G., *et al.* Endothelial function and sympathetic nervous system activity in patients with takotsubo syndrome. *Int J Cardiol* **2016**, *224*, 226-230.
 36. El-Battrawy, I.; Zhao, Z.; Lan, H.; Schunemann, J.D.; Sattler, K.; Buljubasic, F.; Patocskai, B.; Li, X.; Yucel, G.; Lang, S., *et al.* Estradiol protection against toxic effects of catecholamine on electrical properties in human-induced pluripotent stem cell derived cardiomyocytes. *Int J Cardiol* **2018**, *254*, 195-202.
 37. Scally, C.; Abbas, H.; Ahearn, T.; Srinivasan, J.; Mezincescu, A.; Rudd, A.; Spath, N.; Yucel-Finn, A.; Yucel, R.; Oldroyd, K., *et al.* Myocardial and systemic inflammation in acute stress-induced (takotsubo) cardiomyopathy. *Circulation* **2019**, *139*, 1581-1592.
 38. Paur, H.; Wright, P.T.; Sikkil, M.B.; Tranter, M.H.; Mansfield, C.; O'Gara, P.; Stuckey, D.J.; Nikolaev, V.O.; Diakonov, I.; Pannell, L., *et al.* High levels of circulating epinephrine trigger apical cardiodepression in a beta2-adrenergic receptor/gi-dependent manner: A new model of takotsubo cardiomyopathy. *Circulation* **2012**, *126*, 697-706.
 39. Fan, X.; Yang, G.; Kowitz, J.; Akin, I.; Zhou, X.; El-Battrawy, I. Takotsubo syndrome: Translational implications and pathomechanisms. *Int J Mol Sci* **2022**, *23*.
 40. D'Aloia, A.; Caretta, G.; Vizzardi, E.; Zanini, G.; Bugatti, S.; Bonadei, I.; Dei Cas, L. Heart failure syndrome due to dobutamine stress echocardiography: Tako-tsubo induced-cardiomyopathy. *Panminerva Med* **2012**, *54*, 53-55.
 41. Abraham, J.; Mudd, J.O.; Kapur, N.K.; Klein, K.; Champion, H.C.; Wittstein, I.S. Stress cardiomyopathy after intravenous administration of catecholamines and beta-receptor agonists. *J Am Coll Cardiol* **2009**, *53*, 1320-1325.
 42. Kido, K.; Guglin, M. Drug-induced takotsubo cardiomyopathy. *J Cardiovasc Pharmacol Ther* **2017**, *22*, 552-563.
 43. Wittstein, I.S.; Thiemann, D.R.; Lima, J.A.; Baughman, K.L.; Schulman, S.P.; Gerstenblith, G.; Wu, K.C.; Rade, J.J.; Bivalacqua, T.J.; Champion, H.C. Neurohumoral features of myocardial stunning due to sudden emotional stress. *N Engl J Med* **2005**, *352*, 539-548.
 44. Mori, H.; Ishikawa, S.; Kojima, S.; Hayashi, J.; Watanabe, Y.; Hoffman, J.I.; Okino, H. Increased responsiveness of left ventricular apical myocardium to adrenergic stimuli. *Cardiovasc Res* **1993**, *27*, 192-198.
 45. Redfors, B.; Ali, A.; Shao, Y.; Lundgren, J.; Gan, L.M.; Omerovic, E. Different catecholamines induce different patterns of takotsubo-like cardiac dysfunction in an apparently afterload dependent manner. *Int J Cardiol* **2014**, *174*, 330-336.
 46. Lyon, A.R.; Rees, P.S.; Prasad, S.; Poole-Wilson, P.A.; Harding, S.E. Stress (takotsubo)

- cardiomyopathy--a novel pathophysiological hypothesis to explain catecholamine-induced acute myocardial stunning. *Nat Clin Pract Cardiovasc Med* **2008**, *5*, 22-29.
47. Huang, M.; Fan, X.; Yang, Z.; Cyganek, L.; Li, X.; Yucel, G.; Lan, H.; Li, Y.; Wendel, A.; Lang, S., *et al.* Alpha 1-adrenoceptor signalling contributes to toxic effects of catecholamine on electrical properties in cardiomyocytes. *Europace* **2021**, *23*, 1137-1148.
 48. Huang, M.; Yang, Z.; Li, Y.; Lan, H.; Cyganek, L.; Yucel, G.; Lang, S.; Bieback, K.; El-Battrawy, I.; Zhou, X., *et al.* Dopamine d1/d5 receptor signaling is involved in arrhythmogenesis in the setting of takotsubo cardiomyopathy. *Front Cardiovasc Med* **2021**, *8*, 777463.
 49. Sumpio, B.E.; Riley, J.T.; Dardik, A. Cells in focus: Endothelial cell. *Int J Biochem Cell Biol* **2002**, *34*, 1508-1512.
 50. Sorriento, D.; Santulli, G.; Del Giudice, C.; Anastasio, A.; Trimarco, B.; Iaccarino, G. Endothelial cells are able to synthesize and release catecholamines both in vitro and in vivo. *Hypertension* **2012**, *60*, 129-136.
 51. Flammer, A.J.; Luscher, T.F. Human endothelial dysfunction: Edrfs. *Pflugers Arch* **2010**, *459*, 1005-1013.
 52. Munzel, T.; Gori, T.; Bruno, R.M.; Taddei, S. Is oxidative stress a therapeutic target in cardiovascular disease? *Eur Heart J* **2010**, *31*, 2741-2748.
 53. Gori, T.; Munzel, T. Oxidative stress and endothelial dysfunction: Therapeutic implications. *Ann Med* **2011**, *43*, 259-272.
 54. Patel, S.M.; Lerman, A.; Lennon, R.J.; Prasad, A. Impaired coronary microvascular reactivity in women with apical ballooning syndrome (takotsubo/stress cardiomyopathy). *Eur Heart J Acute Cardiovasc Care* **2013**, *2*, 147-152.
 55. Martin, E.A.; Prasad, A.; Rihal, C.S.; Lerman, L.O.; Lerman, A. Endothelial function and vascular response to mental stress are impaired in patients with apical ballooning syndrome. *J Am Coll Cardiol* **2010**, *56*, 1840-1846.
 56. Spieker, L.E.; Hurlimann, D.; Ruschitzka, F.; Corti, R.; Enseleit, F.; Shaw, S.; Hayoz, D.; Deanfield, J.E.; Luscher, T.F.; Noll, G. Mental stress induces prolonged endothelial dysfunction via endothelin-a receptors. *Circulation* **2002**, *105*, 2817-2820.
 57. Cecchi, E.; Parodi, G.; Fatucchi, S.; Angelotti, P.; Giglioli, C.; Gori, A.M.; Bandinelli, B.; Bellandi, B.; Sticchi, E.; Romagnuolo, I., *et al.* Prevalence of thrombophilic disorders in takotsubo patients: The (thrombophilia in takotsubo cardiomyopathy) trota study. *Clin Res Cardiol* **2016**, *105*, 717-726.
 58. Wilson, H.M.; Cheyne, L.; Brown, P.A.J.; Kerr, K.; Hannah, A.; Srinivasan, J.; Duniak, N.; Horgan, G.; Dawson, D.K. Characterization of the myocardial inflammatory response in acute stress-induced (takotsubo) cardiomyopathy. *JACC Basic Transl Sci* **2018**, *3*, 766-778.
 59. Parkkonen, O.; Mustonen, P.; Puurunen, M.; Valkonen, K.; Nieminen, M.; Sinisalo, J. Coagulation changes in takotsubo cardiomyopathy support acute phase reaction and catecholamine excess, but not thrombus production. *Int J Cardiol* **2014**, *177*, 1063-1065.
 60. Eitel, I.; Stiermaier, T.; Graf, T.; Moller, C.; Rommel, K.P.; Eitel, C.; Schuler, G.; Thiele, H.; Desch, S. Optical coherence tomography to evaluate plaque burden and morphology in patients with takotsubo syndrome. *J Am Heart Assoc* **2016**, *5*.
 61. Marcucci, R.; Mannini, L.; Andrei, V.; Bandinelli, B.; Gori, A.M.; Fatucchi, S.; Giglioli, C.; Romano, S.M.; Piazzai, C.; Marchionni, N., *et al.* Transient stress-related hyperviscosity and endothelial dysfunction in takotsubo syndrome: A time course study. *Heart Vessels* **2022**, *37*, 1776-1784.

62. Wang, Y.; Ma, X. Healthy coronary endothelial cells, happy cardiomyocytes. *Circulation* **2021**, *143*, 581-582.
63. Yaribeygi, H.; Atkin, S.L.; Sahebkar, A. A review of the molecular mechanisms of hyperglycemia-induced free radical generation leading to oxidative stress. *J Cell Physiol* **2019**, *234*, 1300-1312.
64. Munzel, T.; Templin, C.; Cammann, V.L.; Hahad, O. Takotsubo syndrome: Impact of endothelial dysfunction and oxidative stress. *Free Radic Biol Med* **2021**, *169*, 216-223.
65. Jaguszewski, M.; Osipova, J.; Ghadri, J.R.; Napp, L.C.; Widera, C.; Franke, J.; Fijalkowski, M.; Nowak, R.; Fijalkowska, M.; Volkmann, I., *et al.* A signature of circulating micrnas differentiates takotsubo cardiomyopathy from acute myocardial infarction. *Eur Heart J* **2014**, *35*, 999-1006.
66. Amadio, P.; Porro, B.; Cavalca, V.; Barbieri, S.S.; Eligini, S.; Fiorelli, S.; Di Minno, A.; Gorini, A.; Giuliani, M.; Werba, J.P., *et al.* Persistent long-term platelet activation and endothelial perturbation in women with takotsubo syndrome. *Biomed Pharmacother* **2021**, *136*, 111259.
67. Li, R.; Mi, X.; Yang, S.; Yang, Y.; Zhang, S.; Hui, R.; Chen, Y.; Zhang, W. Long-term stimulation of angiotensin ii induced endothelial senescence and dysfunction. *Exp Gerontol* **2019**, *119*, 212-220.
68. Klingbeil, A.U.; John, S.; Schneider, M.P.; Jacobi, J.; Handrock, R.; Schmieder, R.E. Effect of at1 receptor blockade on endothelial function in essential hypertension. *Am J Hypertens* **2003**, *16*, 123-128.
69. Mennuni, S.; Rubattu, S.; Pierelli, G.; Tocci, G.; Fofi, C.; Volpe, M. Hypertension and kidneys: Unraveling complex molecular mechanisms underlying hypertensive renal damage. *J Hum Hypertens* **2014**, *28*, 74-79.
70. Sun, L.; Zhang, J.; Li, Y. Chronic central mir-29b antagonism alleviates angiotensin ii-induced hypertension and vascular endothelial dysfunction. *Life Sci* **2019**, *235*, 116862.
71. Wei, X.; Zhu, X.; Hu, N.; Zhang, X.; Sun, T.; Xu, J.; Bian, X. Baicalin attenuates angiotensin ii-induced endothelial dysfunction. *Biochem Biophys Res Commun* **2015**, *465*, 101-107.
72. Ding, J.; Yu, M.; Jiang, J.; Luo, Y.; Zhang, Q.; Wang, S.; Yang, F.; Wang, A.; Wang, L.; Zhuang, M., *et al.* Angiotensin ii decreases endothelial nitric oxide synthase phosphorylation via at1r nox/ros/pp2a pathway. *Front Physiol* **2020**, *11*, 566410.
73. Lee, S.H.; Fujioka, S.; Takahashi, R.; Oe, T. Angiotensin ii-induced oxidative stress in human endothelial cells: Modification of cellular molecules through lipid peroxidation. *Chem Res Toxicol* **2019**, *32*, 1412-1422.
74. Talman, V.; Kivela, R. Cardiomyocyte-endothelial cell interactions in cardiac remodeling and regeneration. *Front Cardiovasc Med* **2018**, *5*, 101.
75. Colliva, A.; Braga, L.; Giacca, M.; Zacchigna, S. Endothelial cell-cardiomyocyte crosstalk in heart development and disease. *J Physiol* **2020**, *598*, 2923-2939.
76. Giordano, F.J.; Gerber, H.P.; Williams, S.P.; VanBruggen, N.; Bunting, S.; Ruiz-Lozano, P.; Gu, Y.; Nath, A.K.; Huang, Y.; Hickey, R., *et al.* A cardiac myocyte vascular endothelial growth factor paracrine pathway is required to maintain cardiac function. *Proc Natl Acad Sci U S A* **2001**, *98*, 5780-5785.
77. Brutsaert, D.L. Cardiac endothelial-myocardial signaling: Its role in cardiac growth, contractile performance, and rhythmicity. *Physiol Rev* **2003**, *83*, 59-115.
78. Higashikuni, Y.; Sainz, J.; Nakamura, K.; Takaoka, M.; Enomoto, S.; Iwata, H.; Tanaka, K.; Sahara, M.; Hirata, Y.; Nagai, R., *et al.* The atp-binding cassette transporter abcg2 protects against

- pressure overload-induced cardiac hypertrophy and heart failure by promoting angiogenesis and antioxidant response. *Arterioscler Thromb Vasc Biol* **2012**, *32*, 654-661.
79. Kuramochi, Y.; Cote, G.M.; Guo, X.; Lebrasseur, N.K.; Cui, L.; Liao, R.; Sawyer, D.B. Cardiac endothelial cells regulate reactive oxygen species-induced cardiomyocyte apoptosis through neuregulin-1beta/erb4 signaling. *J Biol Chem* **2004**, *279*, 51141-51147.
 80. Leucker, T.M.; Ge, Z.D.; Procknow, J.; Liu, Y.; Shi, Y.; Bienengraeber, M.; Warltier, D.C.; Kersten, J.R. Impairment of endothelial-myocardial interaction increases the susceptibility of cardiomyocytes to ischemia/reperfusion injury. *PLoS One* **2013**, *8*, e70088.
 81. Subramani, J.; Kundumani-Sridharan, V.; Hilgers, R.H.; Owens, C.; Das, K.C. Thioredoxin uses a gsh-independent route to deglutathionylate endothelial nitric-oxide synthase and protect against myocardial infarction. *J Biol Chem* **2016**, *291*, 23374-23389.
 82. Niwa, Y.; Nagata, N.; Oka, M.; Toyoshima, T.; Akiyoshi, H.; Wada, T.; Nakaya, Y. Production of nitric oxide from endothelial cells by 31-amino-acid-length endothelin-1, a novel vasoconstrictive product by human chymase. *Life Sci* **2000**, *67*, 1103-1109.
 83. Garcia, N.A.; Moncayo-Arlandi, J.; Sepulveda, P.; Diez-Juan, A. Cardiomyocyte exosomes regulate glycolytic flux in endothelium by direct transfer of glut transporters and glycolytic enzymes. *Cardiovasc Res* **2016**, *109*, 397-408.
 84. Fernandez-Llama, P.; Khositseth, S.; Gonzales, P.A.; Star, R.A.; Pisitkun, T.; Knepper, M.A. Tamm-horsfall protein and urinary exosome isolation. *Kidney Int* **2010**, *77*, 736-742.
 85. Schageman, J.; Zeringer, E.; Li, M.; Barta, T.; Lea, K.; Gu, J.; Magdaleno, S.; Setterquist, R.; Vlassov, A.V. The complete exosome workflow solution: From isolation to characterization of rna cargo. *Biomed Res Int* **2013**, *2013*, 253957.
 86. Turner, A.; Aggarwal, P.; Matter, A.; Olson, B.; Gu, C.C.; Hunt, S.C.; Lewis, C.E.; Arnett, D.K.; Lorier, R.; Broeckel, U. Donor-specific phenotypic variation in hipsc cardiomyocyte-derived exosomes impacts endothelial cell function. *Am J Physiol Heart Circ Physiol* **2021**, *320*, H954-H968.
 87. Shang, A.; Gu, C.; Wang, W.; Wang, X.; Sun, J.; Zeng, B.; Chen, C.; Chang, W.; Ping, Y.; Ji, P., *et al.* Exosomal circpacrgl promotes progression of colorectal cancer via the mir-142-3p/mir-506-3p-tgf-beta1 axis. *Mol Cancer* **2020**, *19*, 117.
 88. Hannafon, B.N.; Trigoso, Y.D.; Calloway, C.L.; Zhao, Y.D.; Lum, D.H.; Welm, A.L.; Zhao, Z.J.; Blick, K.E.; Dooley, W.C.; Ding, W.Q. Plasma exosome micrnas are indicative of breast cancer. *Breast Cancer Res* **2016**, *18*, 90.
 89. Lotvall, J.; Hill, A.F.; Hochberg, F.; Buzas, E.I.; Di Vizio, D.; Gardiner, C.; Gho, Y.S.; Kurochkin, I.V.; Mathivanan, S.; Quesenberry, P., *et al.* Minimal experimental requirements for definition of extracellular vesicles and their functions: A position statement from the international society for extracellular vesicles. *J Extracell Vesicles* **2014**, *3*, 26913.
 90. van der Pol, E.; Coumans, F.A.; Grootemaat, A.E.; Gardiner, C.; Sargent, I.L.; Harrison, P.; Sturk, A.; van Leeuwen, T.G.; Nieuwland, R. Particle size distribution of exosomes and microvesicles determined by transmission electron microscopy, flow cytometry, nanoparticle tracking analysis, and resistive pulse sensing. *J Thromb Haemost* **2014**, *12*, 1182-1192.
 91. Bang, C.; Batkai, S.; Dangwal, S.; Gupta, S.K.; Foinquinos, A.; Holzmann, A.; Just, A.; Remke, J.; Zimmer, K.; Zeug, A., *et al.* Cardiac fibroblast-derived micrna passenger strand-enriched exosomes mediate cardiomyocyte hypertrophy. *J Clin Invest* **2014**, *124*, 2136-2146.
 92. Zheng, B.; Yin, W.N.; Suzuki, T.; Zhang, X.H.; Zhang, Y.; Song, L.L.; Jin, L.S.; Zhan, H.; Zhang, H.; Li, J.S., *et al.* Exosome-mediated mir-155 transfer from smooth muscle cells to endothelial cells

- induces endothelial injury and promotes atherosclerosis. *Mol Ther* **2017**, *25*, 1279-1294.
93. Stamatikos, A.; Knight, E.; Vojtech, L.; Bi, L.; Wacker, B.K.; Tang, C.; Dichek, D.A. Exosome-mediated transfer of anti-mir-33a-5p from transduced endothelial cells enhances macrophage and vascular smooth muscle cell cholesterol efflux. *Hum Gene Ther* **2020**, *31*, 219-232.
 94. Colombo, M.; Raposo, G.; Thery, C. Biogenesis, secretion, and intercellular interactions of exosomes and other extracellular vesicles. *Annu Rev Cell Dev Biol* **2014**, *30*, 255-289.
 95. French, K.C.; Antonyak, M.A.; Cerione, R.A. Extracellular vesicle docking at the cellular port: Extracellular vesicle binding and uptake. *Semin Cell Dev Biol* **2017**, *67*, 48-55.
 96. Rana, S.; Yue, S.; Stadel, D.; Zoller, M. Toward tailored exosomes: The exosomal tetraspanin web contributes to target cell selection. *Int J Biochem Cell Biol* **2012**, *44*, 1574-1584.
 97. Gao, L.; Wang, L.; Wei, Y.; Krishnamurthy, P.; Walcott, G.P.; Menasche, P.; Zhang, J. Exosomes secreted by hipsc-derived cardiac cells improve recovery from myocardial infarction in swine. *Sci Transl Med* **2020**, *12*.
 98. Garcia, N.A.; Ontoria-Oviedo, I.; Gonzalez-King, H.; Diez-Juan, A.; Sepulveda, P. Glucose starvation in cardiomyocytes enhances exosome secretion and promotes angiogenesis in endothelial cells. *PLoS One* **2015**, *10*, e0138849.
 99. Li, G.; Qiu, Z.; Li, C.; Zhao, R.; Zhang, Y.; Shen, C.; Liu, W.; Long, X.; Zhuang, S.; Wang, Y., *et al.* Exosomal mir-29a in cardiomyocytes induced by angiotensin ii regulates cardiac microvascular endothelial cell proliferation, migration and angiogenesis by targeting vegfa. *Curr Gene Ther* **2022**, *22*, 331-341.
 100. Hu, J.; Wang, S.; Xiong, Z.; Cheng, Z.; Yang, Z.; Lin, J.; Wang, T.; Feng, X.; Gao, E.; Wang, H., *et al.* Exosomal mst1 transfer from cardiac microvascular endothelial cells to cardiomyocytes deteriorates diabetic cardiomyopathy. *Biochim Biophys Acta Mol Basis Dis* **2018**, *1864*, 3639-3649.
 101. Ye, M.; Ni, Q.; Qi, H.; Qian, X.; Chen, J.; Guo, X.; Li, M.; Zhao, Y.; Xue, G.; Deng, H., *et al.* Exosomes derived from human induced pluripotent stem cells-endothelia cells promotes postnatal angiogenesis in mice bearing ischemic limbs. *Int J Biol Sci* **2019**, *15*, 158-168.
 102. Cao, Y.; Wang, Y.; Xiao, L.; Xu, J.Y.; Liu, Y.; Jiang, R.; Li, T.; Jiang, J. Endothelial-derived exosomes induced by lipopolysaccharide alleviate rat cardiomyocytes injury and apoptosis. *Am J Transl Res* **2021**, *13*, 1432-1444.
 103. Yates, L.A.; Norbury, C.J.; Gilbert, R.J. The long and short of microrna. *Cell* **2013**, *153*, 516-519.
 104. Friedman, R.C.; Farh, K.K.; Burge, C.B.; Bartel, D.P. Most mammalian mrnas are conserved targets of micrnas. *Genome Res* **2009**, *19*, 92-105.
 105. Zhao, J.; Li, X.; Hu, J.; Chen, F.; Qiao, S.; Sun, X.; Gao, L.; Xie, J.; Xu, B. Mesenchymal stromal cell-derived exosomes attenuate myocardial ischaemia-reperfusion injury through mir-182-regulated macrophage polarization. *Cardiovasc Res* **2019**, *115*, 1205-1216.
 106. Wang, B.; Zhang, A.; Wang, H.; Klein, J.D.; Tan, L.; Wang, Z.M.; Du, J.; Naqvi, N.; Liu, B.C.; Wang, X.H. Mir-26a limits muscle wasting and cardiac fibrosis through exosome-mediated microrna transfer in chronic kidney disease. *Theranostics* **2019**, *9*, 1864-1877.
 107. Hedley, P.L.; Carlsen, A.L.; Christiansen, K.M.; Kanters, J.K.; Behr, E.R.; Corfield, V.A.; Christiansen, M. Micrnas in cardiac arrhythmia: DNA sequence variation of mir-1 and mir-133a in long qt syndrome. *Scand J Clin Lab Invest* **2014**, *74*, 485-491.
 108. Myers, R.; Timofeyev, V.; Li, N.; Kim, C.; Ledford, H.A.; Sirish, P.; Lau, V.; Zhang, Y.; Fayyaz, K.; Singapuri, A., *et al.* Feedback mechanisms for cardiac-specific micrnas and camp signaling in

- electrical remodeling. *Circ Arrhythm Electrophysiol* **2015**, *8*, 942-950.
109. Besser, J.; Malan, D.; Wystub, K.; Bachmann, A.; Wietelmann, A.; Sasse, P.; Fleischmann, B.K.; Braun, T.; Boettger, T. Mirna-1/133a clusters regulate adrenergic control of cardiac repolarization. *PLoS One* **2014**, *9*, e113449.
 110. Orr-Burks, N.; Murray, J.; Todd, K.V.; Bakre, A.; Tripp, R.A. Micrnas affect gpcr and ion channel genes needed for influenza replication. *J Gen Virol* **2021**, *102*.
 111. Briasoulis, A.; Sharma, S.; Telila, T.; Mallikethi-Reddy, S.; Papageorgiou, N.; Oikonomou, E.; Tousoulis, D. Micrnas in atrial fibrillation. *Curr Med Chem* **2019**, *26*, 855-863.
 112. Luo, X.; Pan, Z.; Shan, H.; Xiao, J.; Sun, X.; Wang, N.; Lin, H.; Xiao, L.; Maguy, A.; Qi, X.Y., *et al.* Microrna-26 governs profibrillatory inward-rectifier potassium current changes in atrial fibrillation. *J Clin Invest* **2013**, *123*, 1939-1951.
 113. Lu, Y.; Zhang, Y.; Wang, N.; Pan, Z.; Gao, X.; Zhang, F.; Zhang, Y.; Shan, H.; Luo, X.; Bai, Y., *et al.* Microrna-328 contributes to adverse electrical remodeling in atrial fibrillation. *Circulation* **2010**, *122*, 2378-2387.
 114. Yang, D.; Wan, X.; Dennis, A.T.; Bektik, E.; Wang, Z.; Costa, M.G.S.; Fagnen, C.; Venien-Bryan, C.; Xu, X.; Gratz, D.H., *et al.* Microrna biophysically modulates cardiac action potential by direct binding to ion channel. *Circulation* **2021**, *143*, 1597-1613.
 115. Binas, S.; Knyrim, M.; Hupfeld, J.; Kloeckner, U.; Rabe, S.; Mildenerberger, S.; Quarch, K.; Stratz, N.; Misiak, D.; Gekle, M., *et al.* Mir-221 and -222 target cacna1c and kcnj5 leading to altered cardiac ion channel expression and current density. *Cell Mol Life Sci* **2020**, *77*, 903-918.
 116. Wang, S.; Aurora, A.B.; Johnson, B.A.; Qi, X.; McAnally, J.; Hill, J.A.; Richardson, J.A.; Bassel-Duby, R.; Olson, E.N. The endothelial-specific microrna mir-126 governs vascular integrity and angiogenesis. *Dev Cell* **2008**, *15*, 261-271.
 117. Fish, J.E.; Santoro, M.M.; Morton, S.U.; Yu, S.; Yeh, R.F.; Wythe, J.D.; Ivey, K.N.; Bruneau, B.G.; Stainier, D.Y.; Srivastava, D. Mir-126 regulates angiogenic signaling and vascular integrity. *Dev Cell* **2008**, *15*, 272-284.
 118. Liu, R.; Zhang, Y.S.; Zhang, S.; Cheng, Z.M.; Yu, J.L.; Zhou, S.; Song, J. Mir-126-3p suppresses the growth, migration and invasion of nslc via targeting ccr1. *Eur Rev Med Pharmacol Sci* **2019**, *23*, 679-689.
 119. Soliman, S.E.; Abdelaleem, A.H.; Alhanafy, A.M.; Ibrahim, R.A.L.; Elhaded, A.S.A.; Assar, M.F.A. Circulating mir-21-5p and mir-126-3p: Diagnostic, prognostic value, and multivariate analysis in non-small-cell lung cancer. *Mol Biol Rep* **2021**, *48*, 2543-2552.
 120. Xiang, G.; Cheng, Y. Mir-126-3p inhibits ovarian cancer proliferation and invasion via targeting plxn2. *Reprod Biol* **2018**, *18*, 218-224.
 121. Verdelli, C.; Forno, I.; Morotti, A.; Maggiore, R.; Mari, G.; Vicentini, L.; Ferrero, S.; Kuhn, E.; Vaira, V.; Corbetta, S. Mir-126-3p contributes to parathyroid tumor angiogenesis. *Endocr Relat Cancer* **2021**, *28*, 53-63.
 122. Potus, F.; Ruffenach, G.; Dahou, A.; Thebault, C.; Breuils-Bonnet, S.; Tremblay, E.; Nadeau, V.; Paradis, R.; Graydon, C.; Wong, R., *et al.* Downregulation of microrna-126 contributes to the failing right ventricle in pulmonary arterial hypertension. *Circulation* **2015**, *132*, 932-943.
 123. Li, H.; Liu, Q.; Wang, N.; Xu, Y.; Kang, L.; Ren, Y.; Zhu, G. Transplantation of endothelial progenitor cells overexpressing mir-126-3p improves heart function in ischemic cardiomyopathy. *Circ J* **2018**, *82*, 2332-2341.
 124. Hsu, A.; Chen, S.J.; Chang, Y.S.; Chen, H.C.; Chu, P.H. Systemic approach to identify serum

- micrnas as potential biomarkers for acute myocardial infarction. *Biomed Res Int* **2014**, *2014*, 418628.
125. Goodwill, A.G.; Dick, G.M.; Kiel, A.M.; Tune, J.D. Regulation of coronary blood flow. *Compr Physiol* **2017**, *7*, 321-382.
 126. Grgic, I.; Kaistha, B.P.; Hoyer, J.; Kohler, R. Endothelial ca⁺-activated k⁺ channels in normal and impaired edhf-dilator responses--relevance to cardiovascular pathologies and drug discovery. *Br J Pharmacol* **2009**, *157*, 509-526.
 127. Kefaloyianni, E.; Coetzee, W.A. Transcriptional remodeling of ion channel subunits by flow adaptation in human coronary artery endothelial cells. *J Vasc Res* **2011**, *48*, 357-367.
 128. Millar, I.D.; Wang, S.; Brown, P.D.; Barrand, M.A.; Hladky, S.B. Kv1 and kir2 potassium channels are expressed in rat brain endothelial cells. *Pflugers Arch* **2008**, *456*, 379-391.
 129. Jackson, W.F. Boosting the signal: Endothelial inward rectifier k(+) channels. *Microcirculation* **2017**, *24*.
 130. Aziz, Q.; Li, Y.; Anderson, N.; Ojake, L.; Tsisanova, E.; Tinker, A. Molecular and functional characterization of the endothelial atp-sensitive potassium channel. *J Biol Chem* **2017**, *292*, 17587-17597.
 131. Thuesen, A.D.; Lyngso, K.S.; Rasmussen, L.; Stubbe, J.; Skott, O.; Poulsen, F.R.; Pedersen, C.B.; Rasmussen, L.M.; Hansen, P.B. P/q-type and t-type voltage-gated calcium channels are involved in the contraction of mammary and brain blood vessels from hypertensive patients. *Acta Physiol (Oxf)* **2017**, *219*, 640-651.
 132. Gilbert, G.; Courtois, A.; Dubois, M.; Cussac, L.A.; Ducret, T.; Lory, P.; Marthan, R.; Savineau, J.P.; Quignard, J.F. T-type voltage gated calcium channels are involved in endothelium-dependent relaxation of mice pulmonary artery. *Biochem Pharmacol* **2017**, *138*, 61-72.
 133. Earley, S.; Brayden, J.E. Transient receptor potential channels in the vasculature. *Physiol Rev* **2015**, *95*, 645-690.
 134. Smani, T.; Gomez, L.J.; Regodon, S.; Woodard, G.E.; Siegfried, G.; Khatib, A.M.; Rosado, J.A. Trp channels in angiogenesis and other endothelial functions. *Front Physiol* **2018**, *9*, 1731.
 135. Gauthier, K.M.; Liu, C.; Popovic, A.; Albarwani, S.; Rusch, N.J. Freshly isolated bovine coronary endothelial cells do not express the bk ca channel gene. *J Physiol* **2002**, *545*, 829-836.
 136. Feletou, M. Calcium-activated potassium channels and endothelial dysfunction: Therapeutic options? *Br J Pharmacol* **2009**, *156*, 545-562.
 137. Feletou, M.; Vanhoutte, P.M. Endothelium-dependent hyperpolarizations: Past beliefs and present facts. *Ann Med* **2007**, *39*, 495-516.
 138. Bers, D.M. Cardiac excitation-contraction coupling. *Nature* **2002**, *415*, 198-205.
 139. Bartos, D.C.; Grandi, E.; Ripplinger, C.M. Ion channels in the heart. *Compr Physiol* **2015**, *5*, 1423-1464.
 140. Schmitt, N.; Grunnet, M.; Olesen, S.P. Cardiac potassium channel subtypes: New roles in repolarization and arrhythmia. *Physiol Rev* **2014**, *94*, 609-653.
 141. Varro, A.; Tomek, J.; Nagy, N.; Virag, L.; Passini, E.; Rodriguez, B.; Baczko, I. Cardiac transmembrane ion channels and action potentials: Cellular physiology and arrhythmogenic behavior. *Physiol Rev* **2021**, *101*, 1083-1176.
 142. Grant, A.O. Cardiac ion channels. *Circ Arrhythm Electrophysiol* **2009**, *2*, 185-194.
 143. El-Battrawy, I.; Zhao, Z.; Lan, H.; Cyganek, L.; Tombers, C.; Li, X.; Buljubasic, F.; Lang, S.; Tiburcy, M.; Zimmermann, W.H., *et al.* Electrical dysfunctions in human-induced pluripotent stem cell-

- derived cardiomyocytes from a patient with an arrhythmogenic right ventricular cardiomyopathy. *Europace* **2018**, *20*, f46-f56.
144. El-Battrawy, I.; Besler, J.; Ansari, U.; Liebe, V.; Schimpf, R.; Tulumen, E.; Rudic, B.; Lang, S.; Odening, K.; Cyganek, L., *et al.* Long-term follow-up of implantable cardioverter-defibrillators in short qt syndrome. *Clin Res Cardiol* **2019**, *108*, 1140-1146.
 145. El-Battrawy, I.; Albers, S.; Cyganek, L.; Zhao, Z.; Lan, H.; Li, X.; Xu, Q.; Kleinsorge, M.; Huang, M.; Liao, Z., *et al.* A cellular model of brugada syndrome with scn10a variants using human-induced pluripotent stem cell-derived cardiomyocytes. *Europace* **2019**, *21*, 1410-1421.
 146. El-Battrawy, I.; Muller, J.; Zhao, Z.; Cyganek, L.; Zhong, R.; Zhang, F.; Kleinsorge, M.; Lan, H.; Li, X.; Xu, Q., *et al.* Studying brugada syndrome with an scn1b variants in human-induced pluripotent stem cell-derived cardiomyocytes. *Front Cell Dev Biol* **2019**, *7*, 261.
 147. Lan, H.; Xu, Q.; El-Battrawy, I.; Zhong, R.; Li, X.; Lang, S.; Cyganek, L.; Borggreffe, M.; Zhou, X.; Akin, I. Ionic mechanisms of disopyramide prolonging action potential duration in human-induced pluripotent stem cell-derived cardiomyocytes from a patient with short qt syndrome type 1. *Front Pharmacol* **2020**, *11*, 554422.
 148. El-Battrawy, I.; Lan, H.; Cyganek, L.; Zhao, Z.; Li, X.; Buljubasic, F.; Lang, S.; Yucel, G.; Sattler, K.; Zimmermann, W.H., *et al.* Modeling short qt syndrome using human-induced pluripotent stem cell-derived cardiomyocytes. *J Am Heart Assoc* **2018**, *7*.
 149. Buljubasic, F.; El-Battrawy, I.; Lan, H.; Lomada, S.K.; Chatterjee, A.; Zhao, Z.; Li, X.; Zhong, R.; Xu, Q.; Huang, M., *et al.* Nucleoside diphosphate kinase b contributes to arrhythmogenesis in human-induced pluripotent stem cell-derived cardiomyocytes from a patient with arrhythmogenic right ventricular cardiomyopathy. *J Clin Med* **2020**, *9*.
 150. Zhao, Z.; Li, X.; El-Battrawy, I.; Lan, H.; Zhong, R.; Xu, Q.; Huang, M.; Liao, Z.; Lang, S.; Zimmermann, W.H., *et al.* Drug testing in human-induced pluripotent stem cell-derived cardiomyocytes from a patient with short qt syndrome type 1. *Clin Pharmacol Ther* **2019**, *106*, 642-651.
 151. Yucel, G.; Zhao, Z.; El-Battrawy, I.; Lan, H.; Lang, S.; Li, X.; Buljubasic, F.; Zimmermann, W.H.; Cyganek, L.; Utikal, J., *et al.* Lipopolysaccharides induced inflammatory responses and electrophysiological dysfunctions in human-induced pluripotent stem cell derived cardiomyocytes. *Sci Rep* **2017**, *7*, 2935.
 152. Fan, X.; Yang, G.; Kowitz, J.; Duru, F.; Saguner, A.M.; Akin, I.; Zhou, X.; El-Battrawy, I. Preclinical short qt syndrome models: Studying the phenotype and drug-screening. *Europace* **2022**, *24*, 481-493.
 153. Fu, L.; Zhang, H.; Ong'achwa Machuki, J.; Zhang, T.; Han, L.; Sang, L.; Wu, L.; Zhao, Z.; James Turley, M.; Hu, X., *et al.* Gper mediates estrogen cardioprotection against epinephrine-induced stress. *J Endocrinol* **2021**, *249*, 209-222.
 154. Borchert, T.; Hubscher, D.; Guessoum, C.I.; Lam, T.D.; Ghadri, J.R.; Schellinger, I.N.; Tiburcy, M.; Liaw, N.Y.; Li, Y.; Haas, J., *et al.* Catecholamine-dependent beta-adrenergic signaling in a pluripotent stem cell model of takotsubo cardiomyopathy. *J Am Coll Cardiol* **2017**, *70*, 975-991.
 155. El-Battrawy, I.; Lang, S.; Ansari, U.; Tulumen, E.; Schramm, K.; Fastner, C.; Zhou, X.; Hoffmann, U.; Borggreffe, M.; Akin, I. Prevalence of malignant arrhythmia and sudden cardiac death in takotsubo syndrome and its management. *Europace* **2018**, *20*, 843-850.
 156. Wang, Y.; Zhang, L.; Li, Y.; Chen, L.; Wang, X.; Guo, W.; Zhang, X.; Qin, G.; He, S.H.; Zimmerman, A., *et al.* Exosomes/microvesicles from induced pluripotent stem cells deliver cardioprotective

- mirnas and prevent cardiomyocyte apoptosis in the ischemic myocardium. *Int J Cardiol* **2015**, *192*, 61-69.
157. Couch, L.S.; Fiedler, J.; Chick, G.; Clayton, R.; Dries, E.; Wienecke, L.M.; Fu, L.; Fourre, J.; Pandey, P.; Derda, A.A., *et al.* Circulating micrnas predispose to takotsubo syndrome following high-dose adrenaline exposure. *Cardiovasc Res* **2022**, *118*, 1758-1770.
158. Peng, L.; Chun-guang, Q.; Bei-fang, L.; Xue-zhi, D.; Zi-hao, W.; Yun-fu, L.; Yan-ping, D.; Yang-gui, L.; Wei-guo, L.; Tian-yong, H., *et al.* Clinical impact of circulating mir-133, mir-1291 and mir-663b in plasma of patients with acute myocardial infarction. *Diagn Pathol* **2014**, *9*, 89.
159. Naegele, M.; Flammer, A.J.; Enseleit, F.; Roas, S.; Frank, M.; Hirt, A.; Kaiser, P.; Cantatore, S.; Templin, C.; Fröhlich, G., *et al.* Endothelial function and sympathetic nervous system activity in patients with takotsubo syndrome. *International journal of cardiology* **2016**, *224*, 226-230.
160. Flammer, A.J.; Lüscher, T.F. Human endothelial dysfunction: Edrfs. *Pflugers Archiv : European journal of physiology* **2010**, *459*, 1005-1013.
161. Katsuumi, G.; Shimizu, I.; Yoshida, Y.; Hayashi, Y.; Ikegami, R.; Suda, M.; Wakasugi, T.; Nakao, M.; Minamino, T. Catecholamine-induced senescence of endothelial cells and bone marrow cells promotes cardiac dysfunction in mice. *Int Heart J* **2018**, *59*, 837-844.
162. Flammer, A.J.; Anderson, T.; Celermajer, D.S.; Creager, M.A.; Deanfield, J.; Ganz, P.; Hamburg, N.M.; Luscher, T.F.; Shechter, M.; Taddei, S., *et al.* The assessment of endothelial function: From research into clinical practice. *Circulation* **2012**, *126*, 753-767.
163. De Mey, J.G.; Claeys, M.; Vanhoutte, P.M. Endothelium-dependent inhibitory effects of acetylcholine, adenosine triphosphate, thrombin and arachidonic acid in the canine femoral artery. *J Pharmacol Exp Ther* **1982**, *222*, 166-173.
164. Vanhoutte, P.M.; Shimokawa, H.; Feletou, M.; Tang, E.H. Endothelial dysfunction and vascular disease - a 30th anniversary update. *Acta Physiol (Oxf)* **2017**, *219*, 22-96.
165. Cavadas, C.; Grand, D.; Mosimann, F.; Cotrim, M.D.; Fontes Ribeiro, C.A.; Brunner, H.R.; Grouzmann, E. Angiotensin ii mediates catecholamine and neuropeptide y secretion in human adrenal chromaffin cells through the at1 receptor. *Regul Pept* **2003**, *111*, 61-65.
166. Sata, M.; Fukuda, D. Crucial role of renin-angiotensin system in the pathogenesis of atherosclerosis. *J Med Invest* **2010**, *57*, 12-25.
167. Shatanawi, A.; Romero, M.J.; Iddings, J.A.; Chandra, S.; Umapathy, N.S.; Verin, A.D.; Caldwell, R.B.; Caldwell, R.W. Angiotensin ii-induced vascular endothelial dysfunction through rhoa/rho kinase/p38 mitogen-activated protein kinase/arginase pathway. *Am J Physiol Cell Physiol* **2011**, *300*, C1181-1192.
168. Wang, X.; Zhang, H.; Ge, Y.; Liu, J.; Rong, D.; Cao, L.; He, Y.; Sun, G.; Jia, S.; Guo, W. Angiotensin type 1 receptor regulates yes-associated protein in vascular endothelial cells. *Exp Ther Med* **2020**, *19*, 748-754.
169. Ghiadoni, L.; Virdis, A.; Magagna, A.; Taddei, S.; Salvetti, A. Effect of the angiotensin ii type 1 receptor blocker candesartan on endothelial function in patients with essential hypertension. *Hypertension* **2000**, *35*, 501-506.
170. Szabo, C.; Pacher, P.; Zsengeller, Z.; Vaslin, A.; Komjati, K.; Benko, R.; Chen, M.; Mabley, J.G.; Kollai, M. Angiotensin ii-mediated endothelial dysfunction: Role of poly(adp-ribose) polymerase activation. *Mol Med* **2004**, *10*, 28-35.
171. Zheng, J.; Wen, Y.; Chen, D.B.; Bird, I.M.; Magness, R.R. Angiotensin ii elevates nitric oxide synthase 3 expression and nitric oxide production via a mitogen-activated protein kinase

- cascade in ovine fetoplacental artery endothelial cells. *Biol Reprod* **2005**, *72*, 1421-1428.
172. Liu, H.; Chen, T.; Li, N.; Wang, S.; Bu, P. Role of sirt3 in angiotensin ii-induced human umbilical vein endothelial cells dysfunction. *BMC Cardiovasc Disord* **2015**, *15*, 81.
173. Wang, J.; Chen, S.; Bihl, J. Exosome-mediated transfer of ace2 (angiotensin-converting enzyme 2) from endothelial progenitor cells promotes survival and function of endothelial cell. *Oxid Med Cell Longev* **2020**, *2020*, 4213541.
174. Li, G.; Wang, M.; Hao, L.; Loo, W.T.; Jin, L.; Cheung, M.N.; Chow, L.W.; Ng, E.L. Angiotensin ii induces mitochondrial dysfunction and promotes apoptosis via jnk signalling pathway in primary mouse calvaria osteoblast. *Arch Oral Biol* **2014**, *59*, 513-523.
175. Cai, H.; Harrison, D.G. Endothelial dysfunction in cardiovascular diseases: The role of oxidant stress. *Circ Res* **2000**, *87*, 840-844.
176. Touyz, R.M. Reactive oxygen species and angiotensin ii signaling in vascular cells -- implications in cardiovascular disease. *Braz J Med Biol Res* **2004**, *37*, 1263-1273.
177. Meza, C.A.; La Favor, J.D.; Kim, D.H.; Hickner, R.C. Endothelial dysfunction: Is there a hyperglycemia-induced imbalance of nox and nos? *Int J Mol Sci* **2019**, *20*.
178. Zhang, Y.; Zou, C.; Yang, S.; Fu, J. P120 catenin attenuates the angiotensin ii-induced apoptosis of human umbilical vein endothelial cells by suppressing the mitochondrial pathway. *Int J Mol Med* **2016**, *37*, 623-630.
179. Jeong, S.Y.; Seol, D.W. The role of mitochondria in apoptosis. *BMB Rep* **2008**, *41*, 11-22.
180. Hahad, O.; Prochaska, J.H.; Daiber, A.; Muenzel, T. Environmental noise-induced effects on stress hormones, oxidative stress, and vascular dysfunction: Key factors in the relationship between cerebrocardiovascular and psychological disorders. *Oxid Med Cell Longev* **2019**, *2019*, 4623109.
181. Han, C.J.; Liu, J.T.; Li, M.; Cui, M.; Pang, X.M.; Mao, J.J.; Liu, X.F. Rosiglitazone inhibits angiotensin ii-induced c-reactive protein production in human aortic endothelial cells through regulating at(1)-ros-mapk signal pathway. *Inflamm Res* **2012**, *61*, 1031-1037.
182. Liang, E.S.; Bai, W.W.; Wang, H.; Zhang, J.N.; Zhang, F.; Ma, Y.; Jiang, F.; Yin, M.; Zhang, M.X.; Chen, X.M., *et al.* Parp-1 (poly[adp-ribose] polymerase 1) inhibition protects from ang ii (angiotensin ii)-induced abdominal aortic aneurysm in mice. *Hypertension* **2018**, *72*, 1189-1199.
183. Gerlach, A.C.; Gangopadhyay, N.N.; Devor, D.C. Kinase-dependent regulation of the intermediate conductance, calcium-dependent potassium channel, hik1. *The Journal of biological chemistry* **2000**, *275*, 585-598.
184. Kohler, R.; Ruth, P. Endothelial dysfunction and blood pressure alterations in k⁺-channel transgenic mice. *Pflugers Arch* **2010**, *459*, 969-976.
185. Rathore, S.S.; Iqbal, K.; Shafqat, S.; Tariq, E.; Tousif, S.; UIHaq, Z.G.; Fernandez-Sanchez, D.; Hernandez-Woodbine, M.J.; Granados-Mendoza, S.C.; Lacouture-Cardenas, N.A., *et al.* Meta-analysis of incidence and outcomes of life-threatening arrhythmias in takotsubo cardiomyopathy. *Indian Heart J* **2022**, *74*, 110-119.
186. Jesel, L.; Berthon, C.; Messas, N.; Lim, H.S.; Girardey, M.; Marzak, H.; Marchandot, B.; Trinh, A.; Ohlmann, P.; Morel, O. Atrial arrhythmias in takotsubo cardiomyopathy: Incidence, predictive factors, and prognosis. *Europace* **2019**, *21*, 298-305.
187. Stiermaier, T.; Eitel, C.; Deneff, S.; Desch, S.; Schuler, G.; Thiele, H.; Eitel, I. Prevalence and clinical significance of life-threatening arrhythmias in takotsubo cardiomyopathy. *J Am Coll Cardiol*

- 2015**, 65, 2148-2150.
188. Stiermaier, T.; Rommel, K.P.; Eitel, C.; Moller, C.; Graf, T.; Desch, S.; Thiele, H.; Eitel, I. Management of arrhythmias in patients with takotsubo cardiomyopathy: Is the implantation of permanent devices necessary? *Heart Rhythm* **2016**, 13, 1979-1986.
 189. Madias, C.; Fitzgibbons, T.P.; Alsheikh-Ali, A.A.; Bouchard, J.L.; Kalsmith, B.; Garlitski, A.C.; Tighe, D.A.; Estes, N.A., 3rd; Aurigemma, G.P.; Link, M.S. Acquired long qt syndrome from stress cardiomyopathy is associated with ventricular arrhythmias and torsades de pointes. *Heart Rhythm* **2011**, 8, 555-561.
 190. Stastna, M.; Chimenti, I.; Marban, E.; Van Eyk, J.E. Identification and functionality of proteomes secreted by rat cardiac stem cells and neonatal cardiomyocytes. *Proteomics* **2010**, 10, 245-253.
 191. Deng, S.; Zhou, X.; Ge, Z.; Song, Y.; Wang, H.; Liu, X.; Zhang, D. Exosomes from adipose-derived mesenchymal stem cells ameliorate cardiac damage after myocardial infarction by activating s1p/sk1/s1pr1 signaling and promoting macrophage m2 polarization. *Int J Biochem Cell Biol* **2019**, 114, 105564.
 192. Yuan, Y.; Du, W.; Liu, J.; Ma, W.; Zhang, L.; Du, Z.; Cai, B. Stem cell-derived exosome in cardiovascular diseases: Macro roles of micro particles. *Front Pharmacol* **2018**, 9, 547.
 193. Zhao, W.; Zheng, X.L.; Zhao, S.P. Exosome and its roles in cardiovascular diseases. *Heart Fail Rev* **2015**, 20, 337-348.
 194. Mulcahy, L.A.; Pink, R.C.; Carter, D.R. Routes and mechanisms of extracellular vesicle uptake. *J Extracell Vesicles* **2014**, 3.
 195. Bang, C.; Thum, T. Exosomes: New players in cell-cell communication. *Int J Biochem Cell Biol* **2012**, 44, 2060-2064.
 196. Mayourian, J.; Cashman, T.J.; Ceholski, D.K.; Johnson, B.V.; Sachs, D.; Kaji, D.A.; Sahoo, S.; Hare, J.M.; Hajjar, R.J.; Sobie, E.A., *et al.* Experimental and computational insight into human mesenchymal stem cell paracrine signaling and heterocellular coupling effects on cardiac contractility and arrhythmogenicity. *Circ Res* **2017**, 121, 411-423.
 197. Molina, E.J.; Palma, J.; Gupta, D.; Torres, D.; Gaughan, J.P.; Houser, S.; Macha, M. Reverse remodeling is associated with changes in extracellular matrix proteases and tissue inhibitors after mesenchymal stem cell (msc) treatment of pressure overload hypertrophy. *J Tissue Eng Regen Med* **2009**, 3, 85-91.
 198. Askar, S.F.; Ramkisoensing, A.A.; Atsma, D.E.; Schaliq, M.J.; de Vries, A.A.; Pijnappels, D.A. Engraftment patterns of human adult mesenchymal stem cells expose electrotonic and paracrine proarrhythmic mechanisms in myocardial cell cultures. *Circ Arrhythm Electrophysiol* **2013**, 6, 380-391.
 199. DeSantiago, J.; Bare, D.J.; Semenov, I.; Minshall, R.D.; Geenen, D.L.; Wolska, B.M.; Banach, K. Excitation-contraction coupling in ventricular myocytes is enhanced by paracrine signaling from mesenchymal stem cells. *J Mol Cell Cardiol* **2012**, 52, 1249-1256.
 200. Zilberman, L.; Zalik, A.; Fugenfirov, I.; Shimoni, S.; George, J.; Goland, S. Residual alterations of cardiac and endothelial function in patients who recovered from takotsubo cardiomyopathy. *Clin Cardiol* **2021**, 44, 797-804.
 201. Garcia-Elias, A.; Benito, B. Ion channel disorders and sudden cardiac death. *Int J Mol Sci* **2018**, 19.
 202. Henning, R.J. Cardiovascular exosomes and micrnas in cardiovascular physiology and pathophysiology. *J Cardiovasc Transl Res* **2021**, 14, 195-212.

203. Kuzmin, V.S.; Ivanova, A.D.; Filatova, T.S.; Pustovit, K.B.; Kobylina, A.A.; Atkinson, A.J.; Petkova, M.; Voronkov, Y.I.; Abramochkin, D.V.; Dobrzynski, H. Micro-rna 133a-3p induces repolarization abnormalities in atrial myocardium and modulates ventricular electrophysiology affecting i(ca,l) and ito currents. *Eur J Pharmacol* **2021**, *908*, 174369.
204. Turner, C.; Hilton-Jones, D. Myotonic dystrophy: Diagnosis, management and new therapies. *Curr Opin Neurol* **2014**, *27*, 599-606.
205. Klugbauer, N.; Welling, A.; Specht, V.; Seisenberger, C.; Hofmann, F. L-type ca²⁺ channels of the embryonic mouse heart. *Eur J Pharmacol* **2002**, *447*, 279-284.
206. Zhao, Y.; Ransom, J.F.; Li, A.; Vedantham, V.; von Drehle, M.; Muth, A.N.; Tsuchihashi, T.; McManus, M.T.; Schwartz, R.J.; Srivastava, D. Dysregulation of cardiogenesis, cardiac conduction, and cell cycle in mice lacking mirna-1-2. *Cell* **2007**, *129*, 303-317.
207. Yang, B.; Lin, H.; Xiao, J.; Lu, Y.; Luo, X.; Li, B.; Zhang, Y.; Xu, C.; Bai, Y.; Wang, H., *et al.* The muscle-specific microRNA mir-1 regulates cardiac arrhythmogenic potential by targeting gja1 and kcnj2. *Nat Med* **2007**, *13*, 486-491.
208. Suffredini, S.; Stillitano, F.; Comini, L.; Bouly, M.; Brogioni, S.; Ceconi, C.; Ferrari, R.; Mugelli, A.; Cerbai, E. Long-term treatment with ivabradine in post-myocardial infarcted rats counteracts f-channel overexpression. *Br J Pharmacol* **2012**, *165*, 1457-1466.
209. Cavarretta, E.; Chiariello, G.A.; Condorelli, G. Platelets, endothelium, and circulating microRNA-126 as a prognostic biomarker in cardiovascular diseases: Per aspirin ad astra. *Eur Heart J* **2013**, *34*, 3400-3402.
210. Jiao, M.; You, H.Z.; Yang, X.Y.; Yuan, H.; Li, Y.L.; Liu, W.X.; Jin, M.; Du, J. Circulating microRNA signature for the diagnosis of childhood dilated cardiomyopathy. *Sci Rep* **2018**, *8*, 724.
211. Wei, X.J.; Han, M.; Yang, F.Y.; Wei, G.C.; Liang, Z.G.; Yao, H.; Ji, C.W.; Xie, R.S.; Gong, C.L.; Tian, Y. Biological significance of mir-126 expression in atrial fibrillation and heart failure. *Braz J Med Biol Res* **2015**, *48*, 983-989.
212. Qu, Q.; Bing, W.; Meng, X.; Xi, J.; Bai, X.; Liu, Q.; Guo, Y.; Zhao, X.; Bi, Y. Upregulation of mir-126-3p promotes human saphenous vein endothelial cell proliferation in vitro and prevents vein graft neointimal formation ex vivo and in vivo. *Oncotarget* **2017**, *8*, 106790-106806.
213. Hong, Z.; Hong, C.; Ma, B.; Wang, Q.; Zhang, X.; Li, L.; Wang, C.; Chen, D. MicroRNA -126-3p inhibits the proliferation, migration, invasion, and angiogenesis of triple - negative breast cancer cells by targeting rgs3. *Oncol Rep* **2019**, *42*, 1569-1579.
214. Liu, Y.; Huang, H.; Zhang, Y.; Zhu, X.Y.; Zhang, R.; Guan, L.H.; Tang, Q.; Jiang, H.; Huang, C. Regulator of G protein signaling 3 protects against cardiac hypertrophy in mice. *J Cell Biochem* **2014**, *115*, 977-986.
215. Jaen, C.; Doupnik, C.A. Neuronal kir3.1/kir3.2a channels coupled to serotonin 1a and muscarinic m2 receptors are differentially modulated by the "short" rgs3 isoform. *Neuropharmacology* **2005**, *49*, 465-476.
216. Dai, Y.; Wang, S.; Chang, S.; Ren, D.; Shali, S.; Li, C.; Yang, H.; Huang, Z.; Ge, J. M2 macrophage-derived exosomes carry microRNA-148a to alleviate myocardial ischemia/reperfusion injury via inhibiting txnip and the tlr4/nf-kappab/nlrp3 inflammasome signaling pathway. *J Mol Cell Cardiol* **2020**, *142*, 65-79.
217. Nasser, M.I.; Masood, M.; Adlat, S.; Gang, D.; Zhu, S.; Li, G.; Li, N.; Chen, J.; Zhu, P. Mesenchymal stem cell-derived exosome microRNA as therapy for cardiac ischemic injury. *Biomed Pharmacother* **2021**, *143*, 112118.

218. Barile, L.; Moccetti, T.; Marban, E.; Vassalli, G. Roles of exosomes in cardioprotection. *Eur Heart J* **2017**, *38*, 1372-1379.

8 LIST OF FIGURES AND TABLES

8.1 List of figures

- Figure 1 The possible mechanisms related to TTS.
- Figure 2 Analysis of action potential parameters in hiPSC-CMs.
- Figure 3 Study design.
- Figure 4 Schematic representation of differentiating hiPSCs into cardiomyocytes in this study.
- Figure 5 Ang II and SK4 channel contributed to epinephrine-induced endothelial dysfunction.
- Figure 6 SK4 channel activator rescued and SK4 channel blocker mimicked Ang II effect on tube formation.
- Figure 7 The effects of Ang II on inflammation-related factors, mitochondrial membrane potential ($\Delta\psi_m$), ATP production and apoptosis.
- Figure 8 NS309 restored and Tram-34 mimicked Ang II-effects on apoptosis in HCMECs.
- Figure 9 KCl depolarized cell membrane potential and increased cell apoptosis.
- Figure 10 Ang II reduced RP and inhibited SK4 channel currents in HCMECs via PD-sensitive AT2R and Los-sensitive AT1R signaling.
- Figure 11 Ang II reduced SK4 channel current by increasing ROS production.
- Figure 12 Ang II reduced SK4 channel current by inhibiting PKA expression.
- Figure 13 Isolation and characterization of exosomes from HCMEC culture supernatant.
- Figure 14 Exosomes secreted by endothelial cells can be taken up by hiPSC-CMs.
- Figure 15 Exosome effects on arrhythmia events in hiPSC-CMs.
- Figure 16 Exosomes derived from HCMECs contributed to action potential changes induced by Epi.
- Figure 17 Ion channel gene expression of hiPSC-CMs was affected by exosomes derived from HCMECs.
- Figure 18 Effects of exosomes derived from HCMECs on the L-type calcium

current (I_{Ca-L}) in hiPSC-CMs in the presence of Epi.

- Figure 19 Exosome effects on biophysical properties of sodium channels.
- Figure 20 Effects of epinephrine and exosomes on I_{NCX} in hiPSC-CMs.
- Figure 21 Effects of epinephrine and exosomes on I_{Kr} of hiPSC-CMs.
- Figure 22 Measurements of I_{to} in hiPSC-CMs treated with epinephrine or exosomes.
- Figure 23 Measurements of I_{Ks} in hiPSC-CMs treated with epinephrine or exosomes.
- Figure 24 Changes of miRNAs in HCMECs or hiPSC-CMs treated with epinephrine, miR-126-3p activator and inhibitor.
- Figure 25 Exosomes secreted by endothelial cells overexpressing miR-126-3p mimicked the effects of epinephrine on action potential of hiPSC-CMs.
- Figure 26 Exosomes derived from HCMECs could induce arrhythmia events of hiPSC-CMs via miR-126-3p.
- Figure 27 Effects of exosomes overexpressing miR-126-3p on single cell contractions of hiPSC-CMs.
- Figure 28 Effects of exosomes derived from HCMECs transfected with miR-126-3p on ion channel expression in hiPSC-CMs.
- Figure 29 miR-126-3p targeted RGS3 in HEK293T cells.
- Figure 30 miR-126-3p targeted RGS3 in HCMECs and hiPSC-CMs.
- Figure 31 Schematic diagram showing possible mechanisms by which catecholamine excess causes endothelial dysfunction and endothelial cell secretion modulates electrophysiological properties of hiPSC-CMs in the setting of TTS.

8.2 List of tables

- Table 1 Clinical and experimental features between TTS and NSM
- Table 2 Cell culture reagents in this study
- Table 3 Drugs and chemicals used in this study
- Table 4 Kits and chemicals

Table 5	Primary antibodies for experiments
Table 6	Secondary antibodies used in this study
Table 7	Primers for real-time polymerase chain reaction (qPCR)
Table 8	Primer sequence for qPCR
Table 9	Disposable items
Table 10	The main instruments used in this study
Table 11	Components for RT-PCR
Table 12	Components for qPCR
Table 13	Plasmid digestion reaction
Table 14	Ligation

9 CURRICULUM VITAE

Personal details:

First name and family name: Xuehui Fan
Date of birth: 27.11.1985
Nationality: Chinese
Marital state: Married
Email: Xuehui.Fan@medma.uni-heidelberg.de

Education:

11.2019-present Ph.D. student (Dr. sc. hum.)
First Department of Medicine, Medical Faculty Mannheim,
University of Heidelberg
09.2011-07.2014 Master of Science
Southwest Medical University
09.2009-07.2011 Bachelor of Medicine
Binzhou Medical University
09.2006-07.2009 Heze Medical College

Work Experience:

10.2019- Assistant Professor, Southwest Medical University
Key Laboratory of Medical Electrophysiology, Ministry of
Education and Medical Electrophysiological Key Laboratory of
Sichuan Province, Collaborative Innovation Center for
Prevention of Cardiovascular Diseases, Institute of
Cardiovascular Research
10.2017-10.2019 Research associate (Lecturer), Southwest Medical University
Key Laboratory of Medical Electrophysiology, Ministry of
Education and Medical Electrophysiological Key Laboratory of

Sichuan Province, Collaborative Innovation Center for Prevention of Cardiovascular Diseases, Institute of Cardiovascular Research

07.2014-10.2017 Research assistant, Southwest Medical University
Key Laboratory of Medical Electrophysiology, Ministry of Education and Medical Electrophysiological Key Laboratory of Sichuan Province, Collaborative Innovation Center for Prevention of Cardiovascular Diseases, Institute of Cardiovascular Research

Publications (2019-2022):

1. **Fan X**, Cyganek L, Nitschke K, Uhlig S, Nuhn P, Bieback K, et al. Functional Characterization of Human Induced Pluripotent Stem Cell-Derived Endothelial Cells. *Int. J. Mol. Sci.* 2022, 23(15), 8507; <https://doi.org/10.3390/ijms23158507>
2. **Fan X**, Yang G, Kowitz J, Akin I, Zhou X, El-Battrawy I. Takotsubo Syndrome: Translational Implications and Pathomechanisms. *Int J Mol Sci* 2022; 23 (4):1951.
3. **Fan X**, Yang G, Kowitz J, Duru F, Saguner AM, Akin I, et al. Preclinical short QT syndrome models: studying the phenotype and drug-screening. *Europace* 2022; 24: 481-493.
4. Qiao L, **Fan X**, Yang Z, El-Battrawy I, Zhou X, Akin I. Glucose Counteracts Isoprenaline Effects on Ion Channel Functions in Human-Induced Pluripotent Stem Cell-Derived Cardiomyocytes. *J Cardiovasc Dev Dis* 2022; 9.
5. Liao Z, Li Y, **Fan X**, Yang Z, El-Battrawy I, Zhou X, et al. Lipopolysaccharide Modifies Sodium Current Kinetics through ROS and PKC Signalling in Induced Pluripotent Stem-Derived Cardiomyocytes from Brugada Syndrome Patient. *J Cardiovasc Dev Dis* 2022; 9.
6. Huang M, **Fan X**, Yang Z, Cyganek L, Li X, Yucel G, et al. Alpha 1-adrenoceptor signalling contributes to toxic effects of catecholamine on electrical properties in cardiomyocytes. *Europace* 2021; 23: 1137-1148.

7. Huang M, Liao Z, Li X, Yang Z, **Fan X**, Li Y, et al. Effects of Antiarrhythmic Drugs on hERG Gating in Human-Induced Pluripotent Stem Cell-Derived Cardiomyocytes from a Patient with Short QT Syndrome Type 1. *Front Pharmacol* 2021; 12: 675003.

Conference posters

1. 88. Jahrestagung der Deutschen Gesellschaft für Kardiologie - Herz- und Kreislaufforschung e.V (Mannheim, Germany)
Poster presentation: Functional characterization of human induced pluripotent stem cell-derived endothelial cells. **Xuehui Fan** et al.
2. Cardiovascular bioengineering (CVBE) Symposium 2022 (Gottingen, Germany)
Poster presentation: Angiotensin II contributes to catecholamine-induced endothelial dysfunction via reducing SK channel currents and increasing ROS production. **Xuehui Fan** et al.
3. Retreat DZHK Heidelberg/Mannheim 2022 (Heidelberg, Germany)
Poster presentation: Endothelial cells-derived exosomal miRNA-126-3p modulates cardiac ion channel function by targeting RGS3. **Xuehui Fan** et al.

10 ACKNOWLEDGEMENT

I would like to express my sincere thanks to everyone who gave me care and support during my study in the First Department of Medicine, Faculty of Medicine, University Medical Centre Mannheim (UMM), University of Heidelberg.

First of all, I would like to express my heartfelt thanks to my Doktorvater Prof. Dr. Ibrahim Akin who gave me the opportunity to study at Mannheim Medical Faculty of Heidelberg University as a doctoral student. I am also very grateful to him for his valuable instructions and constant support during the whole study.

Second, I would like to express my sincere gratitude to my first supervisor, Dr. Xiaobo Zhou and his wife Mrs. Shan, who helped me a lot in my study as well as my daily life. He gave me great guidance and encouragement in selecting research topics, doing research, writing papers and correcting papers, which has provided help for my work and benefits for all my life.

Furthermore, I would like to express my particular heartfelt gratitude to Prof. Dr. Gergana Dobрева, Yinuo Wang, Haojie Shi. They kindly and warmly helped me a lot in molecular biology experiment and provided a lot of constructive suggestions.

Besides, I would like to thank Dr. Ibrahim El-Battrawy, who gave valuable suggestions for my study, and also express my gratitude to Dr. Siegfried Lang and Dr. Katherine Sattler, who helped me for my research.

I wish to acknowledge my colleagues and friends, Zhenxing Liao, Qiang Xu, Mengying Huang, Rujia Zhong, Lin Qiao, Zhen Yang, Feng Zhang, Yingrui Li, Zenghui Meng, Chen Yan, Miaoling Li, Xinhao Lei, Emine Yellice, Alyssa Hohn, Timo Prädell, who shared their study experience with me and helped me a lot during my research.

Particularly, I am sincerely grateful to the Chinese Scholarship Council for financial support during my PhD study in Germany.

Finally, I would like to express my deepest gratefulness to my parents, my brother, my husband and my daughter for supporting me all the time.